

**FAA-77-9.I**

REPORT NO. FAA-RD-77-48, I

REFERENCE USE ONLY

# MOBILE LASER DOPPLER SYSTEM CHECKOUT AND CALIBRATION

## Volume I: Text

M.R. Brashears  
T.R. Lawrence  
A.D. Zalay

Lockheed Missiles & Space Company, Inc.  
Huntsville Research & Engineering Center  
4800 Bradford Drive  
Huntsville AL 35807



JUNE 1977

FINAL REPORT

DOCUMENT IS AVAILABLE TO THE U.S. PUBLIC  
THROUGH THE NATIONAL TECHNICAL  
INFORMATION SERVICE, SPRINGFIELD,  
VIRGINIA 22161

Prepared for  
U.S. DEPARTMENT OF TRANSPORTATION  
FEDERAL AVIATION ADMINISTRATION  
Systems Research and Development Service  
Washington DC 20591

NOTICE

This document is disseminated under the sponsorship of the Department of Transportation in the interest of information exchange. The United States Government assumes no liability for its contents or use thereof.

NOTICE

The United States Government does not endorse products or manufacturers. Trade or manufacturers' names appear herein solely because they are considered essential to the object of this report.

1. Report No. FAA-RD-77-48, I		2. Government Accession No.		3. Recipient's Catalog No.	
4. Title and Subtitle MOBILE LASER DOPPLER SYSTEM CHECKOUT AND CALIBRATION  Volume I: Text				5. Report Date June 1977	
				6. Performing Organization Code	
7. Author(s) M.R. Brashears, T.R. Lawrence, A.D. Zalay				8. Performing Organization Report No. LMSC-HREC TR D497036 -1 DOT-TSC-FAA-77-9, I	
9. Performing Organization Name and Address Lockheed Missiles & Space Company Inc.* Huntsville Research & Engineering Center 4800 Bradford Drive Huntsville AL 35807				10. Work Unit No. (TRAIS) FA705/R7126	
				11. Contract or Grant No. DOT-TSC-1098-1	
12. Sponsoring Agency Name and Address U.S. Department of Transportation Federal Aviation Administration Systems Research and Development Service Washington DC 20591				13. Type of Report and Period Covered Final Report July 1975 - September 1976	
				14. Sponsoring Agency Code	
15. Supplementary Notes *Under Contract to: U.S. Department of Transportation Transportation Systems Center Kendall Square Cambridge MA 02142					
16. Abstract  A program has been carried out to make modifications to the Lockheed-Huntsville Mobile Laser Doppler Velocimeter (LDV) system; to calibrate and operate the system at the John F. Kennedy (JFK) Airport; to obtain a data base of wind, wind shear, and wake vortex measurements; and to assess the basic operational capabilities of the system based on these measurements. The basic operational capabilities, resolution, and integrity of a scanning LDV for the remote sensing of winds, wind shear, and wake vortices at terminal areas have been established.  Volume II, 342 pages, contains appendixes.					
17. Key Words Wind Shear Aircraft Wakes Wake Vortices Atmospheric Effects Trailing Vortex  Laser Doppler Velocimetry				18. Distribution Statement  DOCUMENT IS AVAILABLE TO THE U.S. PUBLIC THROUGH THE NATIONAL TECHNICAL INFORMATION SERVICE, SPRINGFIELD, VIRGINIA 22161	
19. Security Classif. (of this report) Unclassified		20. Security Classif. (of this page) Unclassified		21. No. of Pages 150	22. Price

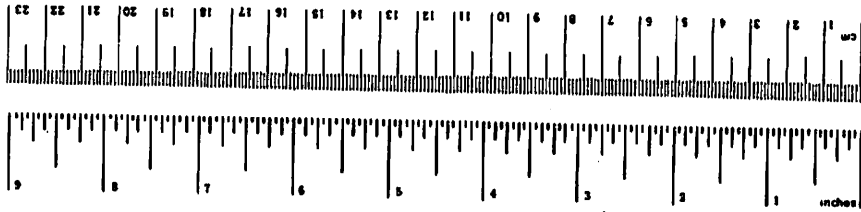
## PREFACE

This final report presents the results of work performed by the Lockheed Missiles & Space Company, Inc., Huntsville Research & Engineering Center, under Contract DOT-TSC-1098 for the Department of Transportation Systems Center, Cambridge, Mass. The objective of the contract was to modify, calibrate, and deploy a mobile laser Doppler velocimeter system for the measurement of wake vortices and winds at terminal areas. The period of performance for this study was from July 1975 through June 1976. Lockheed-Huntsville personnel contributing to this effort were E. W. Coffey, C. E. Craven, B. B. Edwards, E. W. Feese, E. J. Gorzynski, J. L. Jetton, A. J. Jordan, M. C. Krause, G. M. Miller and K. R. Shrider. The Contracting Officer's Representative for this work was Dr. J. N. Hallock.

# METRIC CONVERSION FACTORS

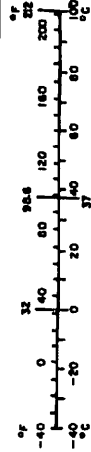
## Approximate Conversions to Metric Measures

Symbol	What You Know	Multiply by	To Find	Symbol
<b>LENGTH</b>				
in	inches	2.5	centimeters	cm
ft	feet	30	meters	m
yd	yards	0.9	kilometers	km
mi	miles	1.6		
<b>AREA</b>				
in <sup>2</sup>	square inches	6.5	square centimeters	cm <sup>2</sup>
ft <sup>2</sup>	square feet	0.09	square meters	m <sup>2</sup>
yd <sup>2</sup>	square yards	0.8	square meters	m <sup>2</sup>
mi <sup>2</sup>	square miles	2.5	square kilometers	km <sup>2</sup>
	acres	0.4	hectares	ha
<b>MASS (weight)</b>				
oz	ounces	28	grams	g
lb	pounds	0.45	kilograms	kg
	short tons (2000 lb)	0.9	tonnes	t
<b>VOLUME</b>				
teaspoon	teaspoons	5	milliliters	ml
Tablespoon	tablespoons	15	milliliters	ml
fluid ounce	fluid ounces	30	milliliters	ml
cup	cups	0.24	liters	l
pint	pints	0.47	liters	l
quart	quarts	0.96	liters	l
gallon	gallons	3.8	liters	l
cubic foot	cubic feet	0.03	cubic meters	m <sup>3</sup>
cubic yard	cubic yards	0.76	cubic meters	m <sup>3</sup>
<b>TEMPERATURE (exact)</b>				
°F	Fahrenheit temperature	5/9 (after subtracting 32)	Celsius temperature	°C



## Approximate Conversions from Metric Measures

Symbol	What You Know	Multiply by	To Find	Symbol
<b>LENGTH</b>				
mm	millimeters	0.04	inches	in
cm	centimeters	0.4	inches	in
m	meters	3.3	feet	ft
km	kilometers	0.6	miles	mi
<b>AREA</b>				
cm <sup>2</sup>	square centimeters	0.16	square inches	in <sup>2</sup>
m <sup>2</sup>	square meters	1.2	square yards	yd <sup>2</sup>
km <sup>2</sup>	square kilometers	0.4	square miles	mi <sup>2</sup>
ha	hectares (10,000 m <sup>2</sup> )	2.5	acres	
<b>MASS (weight)</b>				
g	grams	0.035	ounces	oz
kg	kilograms	2.2	pounds	lb
t	tonnes (1000 kg)	1.1	short tons	
<b>VOLUME</b>				
ml	milliliters	0.03	fluid ounces	fl oz
l	liters	2.1	pints	pt
l	liters	1.06	quarts	qt
m <sup>3</sup>	cubic meters	0.26	gallons	gal
m <sup>3</sup>	cubic meters	35	cubic feet	ft <sup>3</sup>
m <sup>3</sup>	cubic meters	1.3	cubic yards	yd <sup>3</sup>
<b>TEMPERATURE (exact)</b>				
°C	Celsius temperature	9/5 (then add 32)	Fahrenheit temperature	°F



## CONTENTS

Section		Page
	VOLUME I	
1	INTRODUCTION AND SUMMARY	1-1
	1.1 Background	1-1
	1.2 Program Objectives	1-2
	1.3 Report Format	1-3
2	LASER DOPPLER SYSTEM DEVELOPMENT	2-1
	2.1 System Description	2-1
	2.1.1 Laser Doppler Principle	2-1
	2.1.2 Optical System	2-3
	2.1.3 Optical Scanning System	2-5
	2.1.4 Signal Processing System	2-7
	2.1.5 Data Recording and Display	2-14
	2.2 System Specifications	2-15
	2.3 Modes of System Operation	2-15
	2.3.1 Winds Aloft Sensing	2-15
	2.3.2 Coordinated Range and Elevation Scanning and the Point Sensing Mode of Operation	2-23
	2.4 On-Line Data Manipulation	2-25
	2.5 Pertinent LDV Performance Parameters	2-29
	2.5.1 Theory	2-29
	2.5.2 Summary of Pertinent Performance Data	2-32
	2.6 Discussion of Limitations of Present System	2-36
3	COMPUTER SOFTWARE SYSTEM DEVELOPMENT	3-1
	3.1 Description of LDV Software System	3-1
	3.2 Operation of LDV Software System	3-14
	3.2.1 On-Line Data Processing	3-14
	3.2.2 Off-Line Data Processing	3-20

CONTENTS (Concluded)

Section		Page
4	FIELD TESTS OF LDV SYSTEM	4-1
5	RESULTS OF WAKE VORTEX MEASUREMENTS	5-1
6	RESULTS OF WIND MEASUREMENTS	6-1
7	CONCLUSIONS	7-1
8	REFERENCES	8-1
Appendixes	VOLUME II	
A	Data Report	A-1
B	Computer Program Documentation	B-1
C	LDV External Log Sheets	C-1
D	Report of Inventions	D-1

VOLUME I  
LIST OF TABLES

<u>Table</u>		<u>Page</u>
2-1	Scan Capability	2-9
2-2	Lockheed Detailed Component Specifications	2-20
3-1	Output from Data Logger Program	3-7
3-2	Input from SEL Computer	3-15
3-3	Summary of Off-Line Data Processing Technique	3-20
5-1	Summary of Wake Vortex Measurements Conducted at Kennedy International Airport with Lockheed-Huntsville LDV	5-2

LIST OF ILLUSTRATIONS

<u>Figure</u>		<u>Page</u>
2-1	System Configuration	2-2
2-2	Typical Optical Component Configuration of Lockheed LDV	2-4
2-3	Scan Equipment Added to LDV	2-6
2-4	Multimode Scanner	2-8
2-5	Scan Capabilities of LDV	2-10
2-6	LDV Signal Processing System	2-11
2-7	Typical LDV Wind Signature as Displayed by Spectrum Analyzer	2-12
2-8	Output of Signal Processor for FM Modulated Input	2-13
2-9	LDV Monitoring Wake Vortex Generated by L-1011 at Huntsville Airport	2-16
2-10	Interior View of LDV Looking Forward (Depicted in Foreground is Elevation Scanning Mirror on Left Hand and Laser on Right Hand.)	2-17
2-11	Interior View of LDV (Depicted in Background is Display and Scanner Controls in First Rack, Computer in Second Rack, Digital Tape Unit Aft, and Optics Package on Right Hand.)	2-18

LIST OF ILLUSTRATIONS (Continued)

<u>Figure</u>		<u>Page</u>
2-12	Computer Mainframe, Teletype, and LDV Electronics	2-19
2-13	VAD Principle of Operation	2-24
2-14	Azimuth Angle Dependence of Measured Velocity Component	2-25
2-15	Scan Configurations	2-26
2-16	SEL 810A Magnetic Tape Format (Peak Intensity Logger)	2-28
2-17	Typical Spatial Resolution Experiment Traces	2-33
2-18	Field Measurements of Coherent Spatial Resolution	2-34
2-19	Acoustic-Optic Modulator (Bragg Cell)	2-40
2-20	Optical Arrangement of LDV with Acoustic Modulator Included	2-41
2-21	Signal Budget for Various Bragg Cell Frequency Components	2-43
2-22	Frequency Translator Spectrum Analyzer Signatures (Spinning Disk as Target)	2-44
3-1	General Elements of LDV Data Acquisition and Processing System	3-2
3-2	Data Flow from Lockheed LDV	3-3
3-3	Data Logger Macro	3-4
3-4	Typical Vortex Spectrum	3-6
3-5	VAD and Vortex Track Program	3-13
3-6	Dump of Sample Output Tape from Data Logger with System Operating in Vortex Track Mode	3-17
3-7	Dump of Sample Output Tape from Data Logger with System Operating in VAD Mode	3-19
3-8	Input Parameters to VAD and Vortex Track Program	3-25
3-9	Sample of VAD and Vortex Track Program Operating in VAD Mode	3-28
3-10	Sample of VAD and Vortex Track Program Operating in VAD Mode	
	a. Basic Signal	3-30
	b. Twenty-One Point Average of Basic Signal	3-31
	c. Computed Flip of Basic Signal	3-32

LIST OF ILLUSTRATIONS (Concluded)

<u>Figure</u>		<u>Page</u>
3-11	Sample of VAD and Vortex Track Program Operating in Vortex Track Mode	3-35
4-1	Field Site Location for Huntsville Jetplex LDV Tests	4-2
4-2	Sample Wake Vortex Trajectory Measured by LDV at Huntsville Jetplex	4-3
4-3	Field Site Location for the JFK LDV Tests	4-5
5-1	Wake Vortex Trajectory of B-747 Aircraft - Date, 10/31/75; Time, 16:51:30	5-3
5-2	Wake Vortex Trajectory of B-747 Aircraft - Date, 10/31/75; Time, 17:15:00	5-4
5-3	Wake Vortex Trajectory of B-747 Aircraft - Date, 10/31/75; Time 17:27:00	5-5
5-4	Wake Vortex Trajectory of B-747 Aircraft - Date, 11/18/75; Time, 15:57:00	5-6
5-5	Wake Vortex Trajectory of B-747 Aircraft - Date, 11/18/75; Time, 17:2:00	5-7
5-6	Wake Vortex Trajectory of B-747 Aircraft - Date, 1/14/76; Time, 16:47:00	5-8
5-7	Wake Vortex Trajectory of B-747 Aircraft - Date, 1/15/76; Time, 14:41:00	5-9
5-8	Wake Vortex Trajectory of B-747 Aircraft - Date, 1/30/76; Time, 15:15:00	5-10
5-9	Wake Vortex Trajectory of B-747 Aircraft - Date, 1/30/76; Time, 16:10:00	5-11
5-10	Wake Vortex Trajectory of B-747 Aircraft - Date, 1/30/76; Time, 17:00:00	5-12
6-1	Wind Profile, JFK Runway 31R (10/30/75)	6-3
6-2	Wind Profile, JFK Runway 31R (10/30/75)	6-7
6-3	Comparison of Meteorological Tower Wind Speed Measurements with Lockheed-Huntsville LDV at JFK on 11/5/75 14:06-14:36	6-11
6-4	Comparison of Meteorological Tower Wind Direc- tion Measurements with Lockheed-Huntsville LDV at JFK on 11/5/75 14:06 - 14:36	6-12
6-5	Comparison of LDV Line of Sight and Corresponding Meteorological Tower Wind Speed Measurements	6-13

## 1. INTRODUCTION AND SUMMARY

### 1.1 BACKGROUND

Considerable effort is currently being devoted to the development of instrumentation to remotely sense atmospheric flow phenomena. Some of the avenues being pursued are both active and passive acoustic, optical, and radio methods. A useful survey of such methods is presented in Ref. 1. Two advantages of remote sensors are that flow conditions can be ascertained in regions of space where it would not be convenient to locate conventional instrumentation, and no modification of the flow at the point of interest is introduced by their use. The laser Doppler velocimeter (LDV) is a particularly attractive device for remote sensing of atmospheric phenomena. In the LDV system, laser radiation is backscattered from moving particulates in the atmosphere and is used to establish the velocity of the flow. Since optical tracking of the laser focal volume is possible, a scanning LDV system can rapidly determine the velocity field over a large region in space. A CO<sub>2</sub> laser Doppler velocimeter system possesses the following advantages over other remote sensing techniques: (1) the sensing volume can be varied with ease as only optic pointing and focusing operations are involved; (2) the ambient aerosol provides an adequate scattering target; and (3) the sensing mechanism is non-mechanical which results in the potential for a high frequency turbulence sensor.

The feasibility of utilizing a LDV system for the remote sensing of boundary layer winds and for the detection, tracking and measurement of aircraft wake vortices has been demonstrated (Refs. 2, 3 and 4). However, the development of an effective LDV system for monitoring wind, wind shear, and wake vortices at terminal areas required further refinement and application of this technology including the following tasks:

Design and fabrication of a compact, mobile, self-supporting LDV system.

Improvements to the automatic optical scanner, display, and software and accommodation of both wind and vortex tracking modes of operation.

Comprehensive field testing of the LDV system in both wind and vortex tracking modes to establish the basic operational capabilities, resolution, and integrity of the system.

This technical report deals with the above tasks and summarizes the efforts carried out by Lockheed-Huntsville to develop a wind, wind shear, and wake vortex remote sensor. Tasks 1 and 2 were undertaken by Lockheed-Huntsville using Company funds. A mobile self-supporting LDV system, the Lockheed-Huntsville LDV van, with automatic scanning capabilities for wind and wake vortex measurements was designed, fabricated, and field tested in 1975. Based on the successful demonstration of the LDV system, the Department of Transportation, Transportation Systems Center, contracted Lockheed-Huntsville to make further refinements to the mobile LDV system and to deploy it at the John F. Kennedy International Airport (JFK) and to evaluate its operational capabilities. The results of the research and development effort are the subject of this technical report.

## 1.2 PROGRAM OBJECTIVES

The research program focused on the evaluation of the Lockheed-Huntsville LDV for providing wind, wind shear, and wake vortex measurements in support of airport operations. The program encompassed the following tasks:

- Completion of minor modifications to the Lockheed-Huntsville LDV to enable tracking of vortices over a long period of time
- Calibration of the laser system in its various scanning modes
- Installation of displays to monitor the operation of the system on-line
- Collection of a data base of both wind and wake vortex measurements at JFK
- Establishment of the overall performance capabilities of the system for wind, wind shear, and wake vortex measurements based on the analysis of the above measurements.

To achieve these program objectives, the LDV system was deployed at two test sites: at the Huntsville Jetplex in Huntsville, Alabama, and at the John F. Kennedy (JFK) International Airport in New York. The purpose of the Huntsville Jetplex tests was to calibrate the system and to obtain sample wake vortex measurements. Following the successful demonstration of the system at the Jetplex, the LDV system was transported to JFK. During the JFK field tests, spanning 30 days, the LDV observed and recorded wake vortex trajectories during normal landing operations. In addition, wind field measurements were carried out with the LDV and compared with JFK meteorological tower measurements. The report discusses the check out, calibration, and operation of the mobile laser Doppler system during the two tests.

### 1.3 REPORT FORMAT

A discussion of the mobile laser Doppler system is presented in the following sections. The development of the LDV system is addressed first in Section 2 followed by a description of the computer software algorithms in Section 3. The field tests of the LDV are discussed in Section 4 and the wake vortex measurements are presented in Section 5. Wind and wind shear measurements are discussed in Section 6. A summary and overview of the program is given in Section 7.

## 2. LASER DOPPLER SYSTEM DEVELOPMENT

### 2.1 SYSTEM DESCRIPTION

A remote sensing system has been developed by Lockheed-Huntsville for tracking wake vortices and for measuring a three-dimensional wind profile. The basic hardware consists of a laser and associated optical systems, the scanning system, and the display/processing system as shown in Fig. 2-1. The apparatus is housed in a mobile van, sketched in the upper right-hand corner of Fig. 2-1. A description of the LDV system includes discussion of the laser Doppler principle, optical system, scanning system, signal processing system, and data recording and display system.

#### 2.1.1 Laser Doppler Principle

An LDV wind/vortex sensor involves measurement of the Doppler spectrum of laser radiation backscattered by atmospheric aerosols. The instrument must incorporate means to transmit the laser radiation to the region of interest, collect the radiation backscattered from the atmospheric aerosol, and to photomix on a photodetector the scattered radiation and a portion of the transmitted beam. A variable frequency component, at the Doppler shift frequency, is generated at the photodetector which is translatable into an along-optic-axis wind velocity component using appropriate electronics. The magnitude of the Doppler shift,  $\Delta f$ , is given by the equation

$$\Delta f = \frac{2}{\lambda} |\vec{V}| \cos\theta,$$

where

- $\vec{V}$  = velocity vector in the region being sensed
- $\lambda$  = the laser radiation wavelength (10.6 microns for the CO<sub>2</sub> laser), and
- $\theta$  = the angle subtended by the velocity vector and the optic system line of sight.

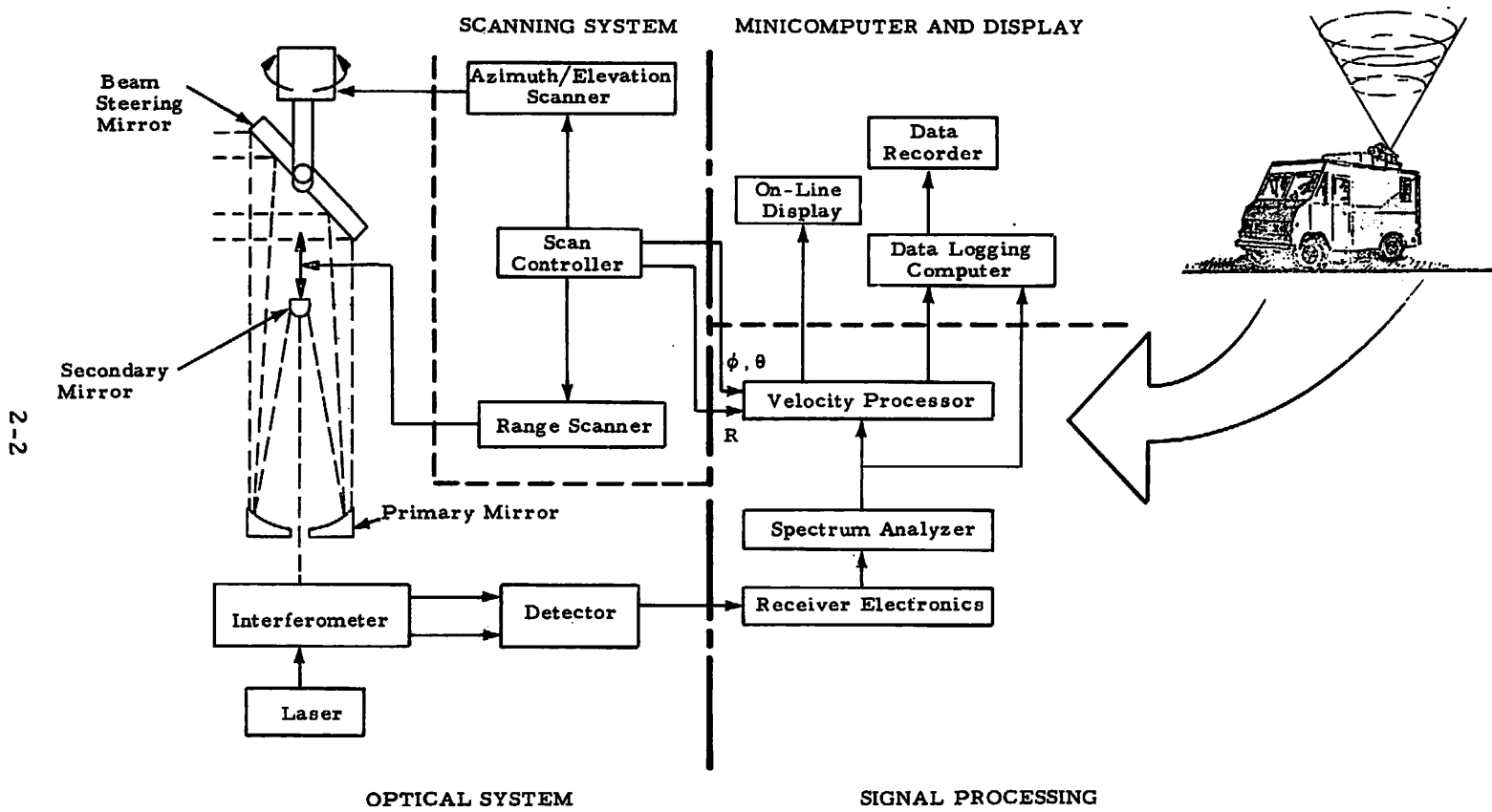


Fig. 2-1 - System Configuration

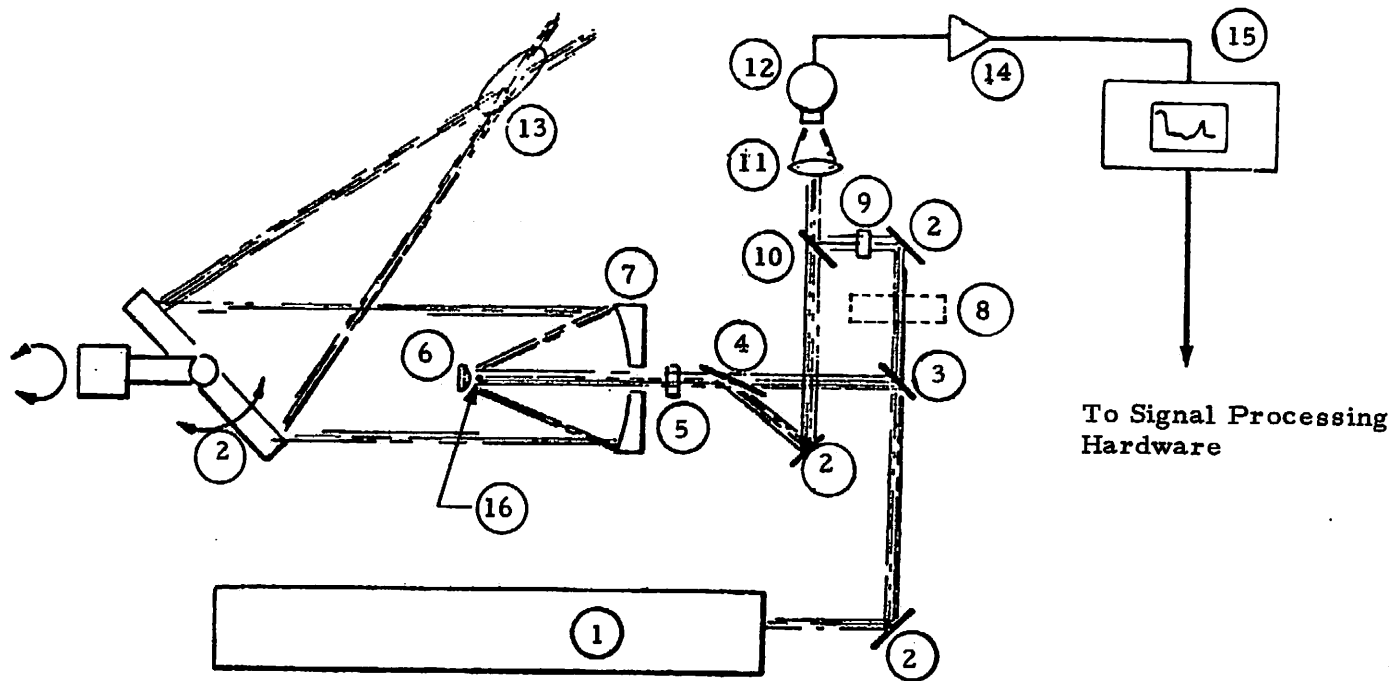
Using the CO<sub>2</sub> laser, 1 m/sec of line-of-sight velocity component yields a Doppler shift of 188 kHz. Thus, measurement of the Doppler shift frequency,  $\Delta f$ , yields directly the line-of-sight velocity component  $|\vec{V}| \cos\theta$ . Some advantages of the CO<sub>2</sub> laser Doppler method are: (1) the Doppler shift is a direct absolute measure of the velocity (for example, a hot wire yields velocity via a cooling effect on the wire), (2) the ease with which the sensing volume can be varied (optics pointing and focusing operations only being involved); (3) the ambient aerosols provide sufficient scattering, thus enabling operation in clear air conditions; and (4) the ambient aerosol tracer has a small inertia and responds quickly to variations in windspeed and could thus be a good turbulence indicator.

A useful instrument must incorporate means to scan the system's resolution volume in a prescribed manner and to effect the required signal processing, on-line read-out, and permanent recording requirements. The hardware implementation of the field laser Doppler unit used during the investigation is discussed in the following subsections.

### 2.1.2 Optical System

The optical system is of a monostatic design and uses a continuous wave laser. The system depends on focusing the transmitter telescope at the location of interest for its spatial resolution property. Details of the optical arrangement are shown in Fig. 2-2.

A horizontally-polarized, 15-watt, continuous wave CO<sub>2</sub> laser beam (10.6 micron wavelength) emerges from the laser (1) and is deflected 90 degrees first by a mirror (2) and then by a 90% reflecting beamsplitter (3). The approximately 0.23 in. diameter beam then passes through a Brewster window (4) and a CdS quarter waveplate (5) which converts the beam to circular polarization. The beam impinges on the secondary mirror (6) and is expanded and reflected into the primary mirror (1 ft diameter) (7) and then focused out into the atmosphere. A wire stop (16) eliminates most of the secondary mirror reflection of the outgoing beam. A small portion of



- |                         |                        |
|-------------------------|------------------------|
| ① CO <sub>2</sub> Laser | ⑨ Half Wave Plate      |
| ② Mirror                | ⑩ Beamsplitter (90% T) |
| ③ Beamsplitter (90% R)  | ⑪ Lens                 |
| ④ Brewster Window       | ⑫ Photodetector        |
| ⑤ Quarter Wave Plate    | ⑬ Focal Volume         |
| ⑥ Secondary Mirror      | ⑭ Preamplifier         |
| ⑦ Primary Mirror        | ⑮ Spectrum Analyzer    |
| ⑧ Optional Beam Stop    | ⑯ Wire Beam Stop       |

Fig. 2-2 - Typical Optical Component Configuration of Lockheed LDV

the original laser beam is transmitted through the beamsplitter (3) and is used as a local oscillator after being rotated to vertical polarization by a half waveplate (9). Energy scattered by aerosols, at the focal volume (13) is collected by the primary mirror (7), collimated by the secondary (6), and passed through the quarter waveplate (5). The quarter waveplate (5) changes the polarization of the aerosol backscattered radiation from circular to vertical linear polarization. The vertically polarized beam is approximately 78% reflected off the Brewster window (4) and directed via a mirror (2) through the beamsplitter (10) where it is combined with the local oscillator radiation. After passing through the collecting lens (11) the two beams are photomixed on the detector (12) in a heterodyne configuration. The electrical output of the detector (12) is amplified with a 5 MHz bandwidth, 20 dB gain low noise type preamplifier (14) and fed into a spectrum analyzer (15).

An alternative operating configuration consists of using the portion of the outgoing beam backscattered into the interferometer by the secondary mirror (6) as the local oscillator beam. This mode of operation is less susceptible to optical misalignment difficulties and was the technique used during most of this investigation. When incorporated, the optical leg (3)(2)(9) was deactivated by the beam stop (8) and the wire stop (16) removed.

### 2.1.3 Optical Scanning System

To give the flexibility needed to operate in various modes of operation (Section 2.3) the antenna arrangement shown in Fig. 2-3 is used. The mirror arrangement AB can be rotated about the vertical axis, thus producing the Velocity-Azimuth Display (VAD) or conical scan mode of operation. Mirror A is adjusted to deflect the beam into a plane normal to the plane of the paper and at a zenith angle corresponding to the required conical scan angle.

A plane or an arc in space can be interrogated by using the system's elevation scan capability which consists of rotating mirror A about a horizontal axis. The transfer of this capability from mirror C to mirror A and the increase of the elevation scan angle range from 60 to 180 degrees was one of

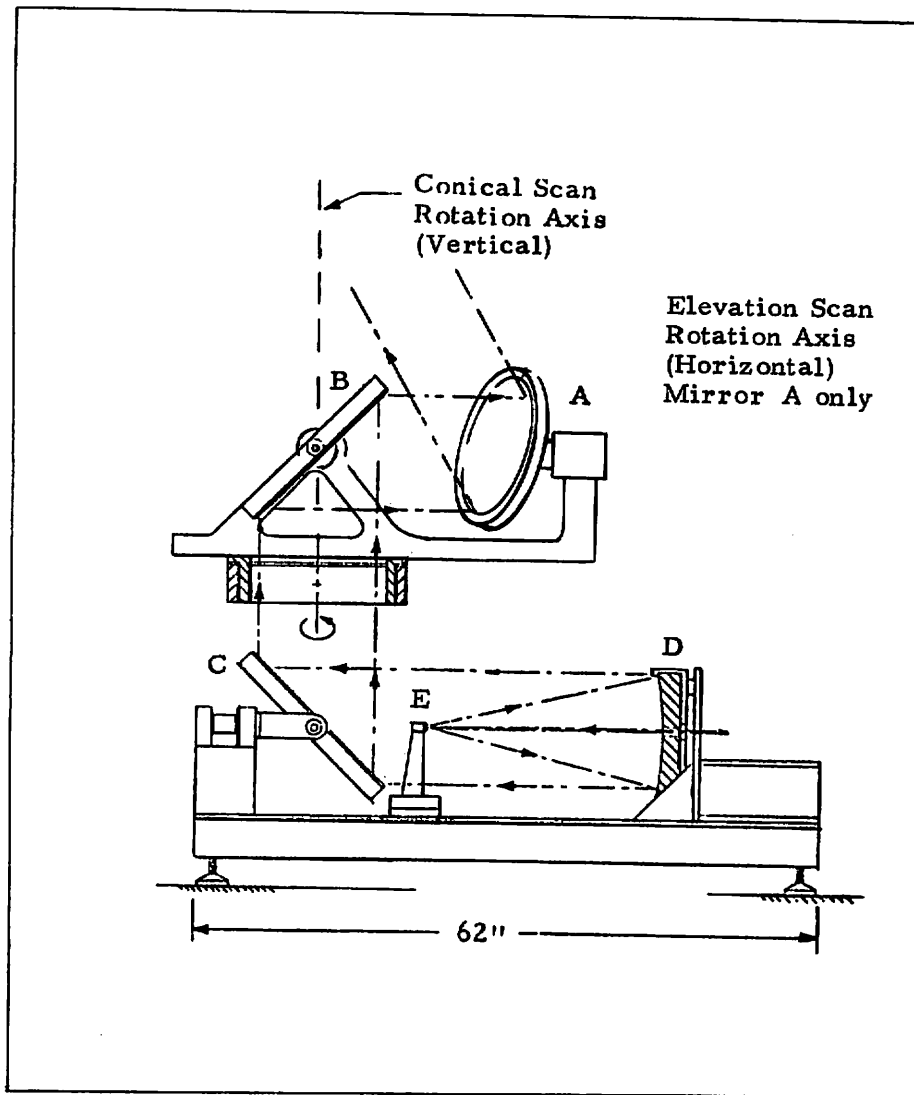


Fig. 2-3 - Scan Equipment Added to LDV

the tasks of this program. This added capability admitted considerable flexibility in the tracking of wake vortices. The scanning hardware is deployed on the mobile van as shown in Fig. 2-4.

The system's focal volume is range scanned by varying the separation of the telescope secondary mirror, E, and the primary mirror, D (Fig. 2-3). This is done by varying the position of the mirror, E, in a controlled manner by an electric motor/optical encoder combination. The scanning system is addressed by a control panel incorporating thumbswitch controls and LED monitors. The system's scan capabilities are summarized in Table 2-1 and Fig. 2-5.

#### 2.1.4 Signal Processing System

The LDV signal processing system consists of a detector, spectrum analyser, frequency voltage converter (tracker), input/output coupler, and peripheral hardware. A block diagram of the basic signal processing system is shown in Fig. 2-6. The heterodyned laser return is converted into an electrical signal by the detector and is amplified. The frequency content of the signal is determined by the spectrum analyzer. The resulting signal is displayed and its intensity and frequency ultimately recorded in digital form.

The Doppler content of the photodetector output is extracted through the use of a sampled spectrum analyzer which provides frequency spectra at a 70 Hz rate. A typical Doppler wind spectrum is shown in Fig. 2-7. To yield a line-of-sight velocity estimate, a voltage is generated which has the same time behavior as the Doppler shift,  $f_d$ , as given by the peak of the spectrum.

The implementation of this technique is, in essence, a recursive comparison method. The spectrum analyzer scan is driven by a sawtooth voltage derived from a D/A converter, the input to which is counter clocked at a constant rate, hence the digital number output of the counter represents frequency on a linear scale. At each new count, the spectrum analyzer output is converted to a digital representation by an A/D converter, and the binary number

Elevation -  $0^{\circ}$  To  $90^{\circ}$   
Azimuth -  $360^{\circ}$

2-8

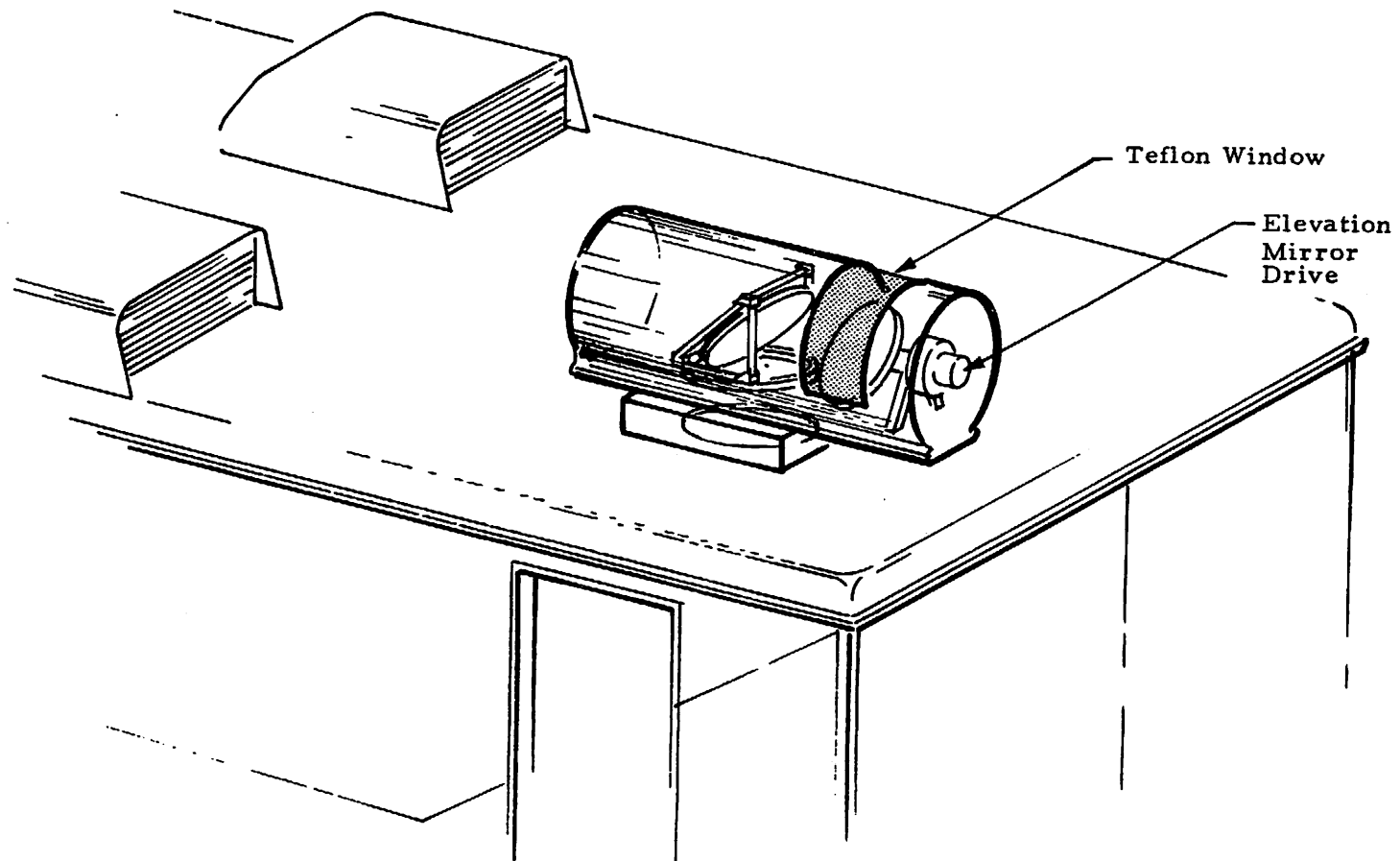
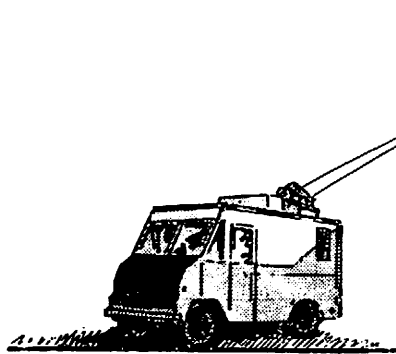


Fig. 2-4 - Multimode Scanner

Table 2-1  
SCAN CAPABILITY

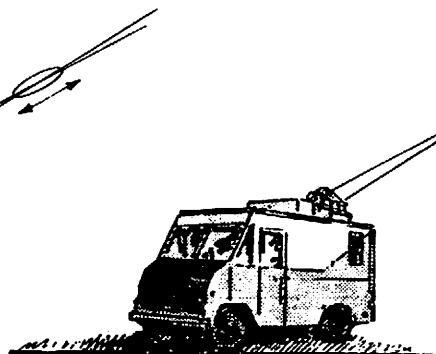
RANGE	Maximum Limit: 2600 ft Minimum Limit: 52 ft Scan Frequency: 0.1 to 6.9 Hz
ELEVATION	Maximum Limit: 90 deg Minimum Limit: 0 deg Hard Limit: 3 deg with Override Scan Frequency: 0.1 to 0.5 Hz
VAD MODE	Measurement Altitude: 33 to 2100 ft Measurement Time/Altitude: 5 sec Sample Rate: 1 to 7 Cycles Number of Altitudes: 8
MULTIMODE	Elevation Coverage: 3 to 90 deg Upwind and Downwind Scan Plane Azimuth: 360 deg Vertical Line Scan: 52 to 2100 ft Overhead Arc Scan: 90 deg Coverage Maximum
ACCURACY	Range: 1 ft at 98 ft, 98 ft at 984 ft Elevation: 0.25 deg



RANGE SCAN

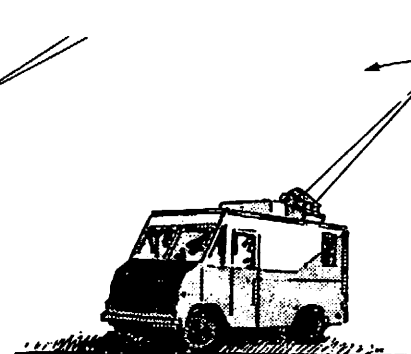
Limits		Rates
Max.	Min.	
328 to 2624 ft	52 to 2132 ft	0.1 to 6.9 Hz
3.28 ft increment		0.1 Hz increm.

Also can be stepped between 8 pre-selectable ranges.



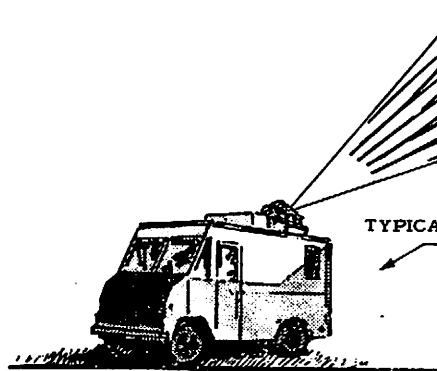
ELEVATION SCAN

Limits		Rates
Max.	Min.	
10 to 90°	0 to 90°	0.1 to 0.5 Hz
1 deg. increment		0.1 Hz increm.



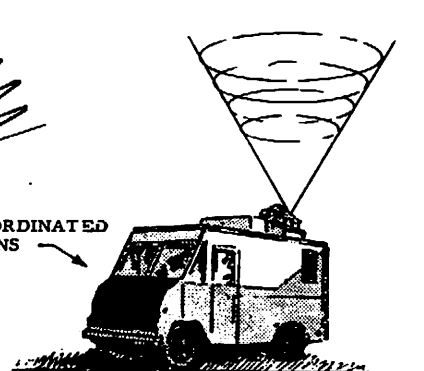
AZIMUTH SCAN

Currently 360° open loop operation. Can be modified for closed loop pointing and scanning.



Range - Elevation  
(for vortex tracks, plume tracks, etc.)

TYPICAL COORDINATED SCANS



Range - Azimuth  
(for wind shear, ballistic winds, etc.)

Notes:

- Maximum Sampling Rate:
  - Current Technique - 69 Hz
  - Advanced Technique - 1 kHz
- Focal Volume Varies with Square of Range and Output Optics Size, i.e.,

Range \ Optics Size	1 ft	1.5 ft
	98 ft	1 ft
984 ft	100 ft	43 ft

Fig.2-5 - Scan Capabilities of LDV

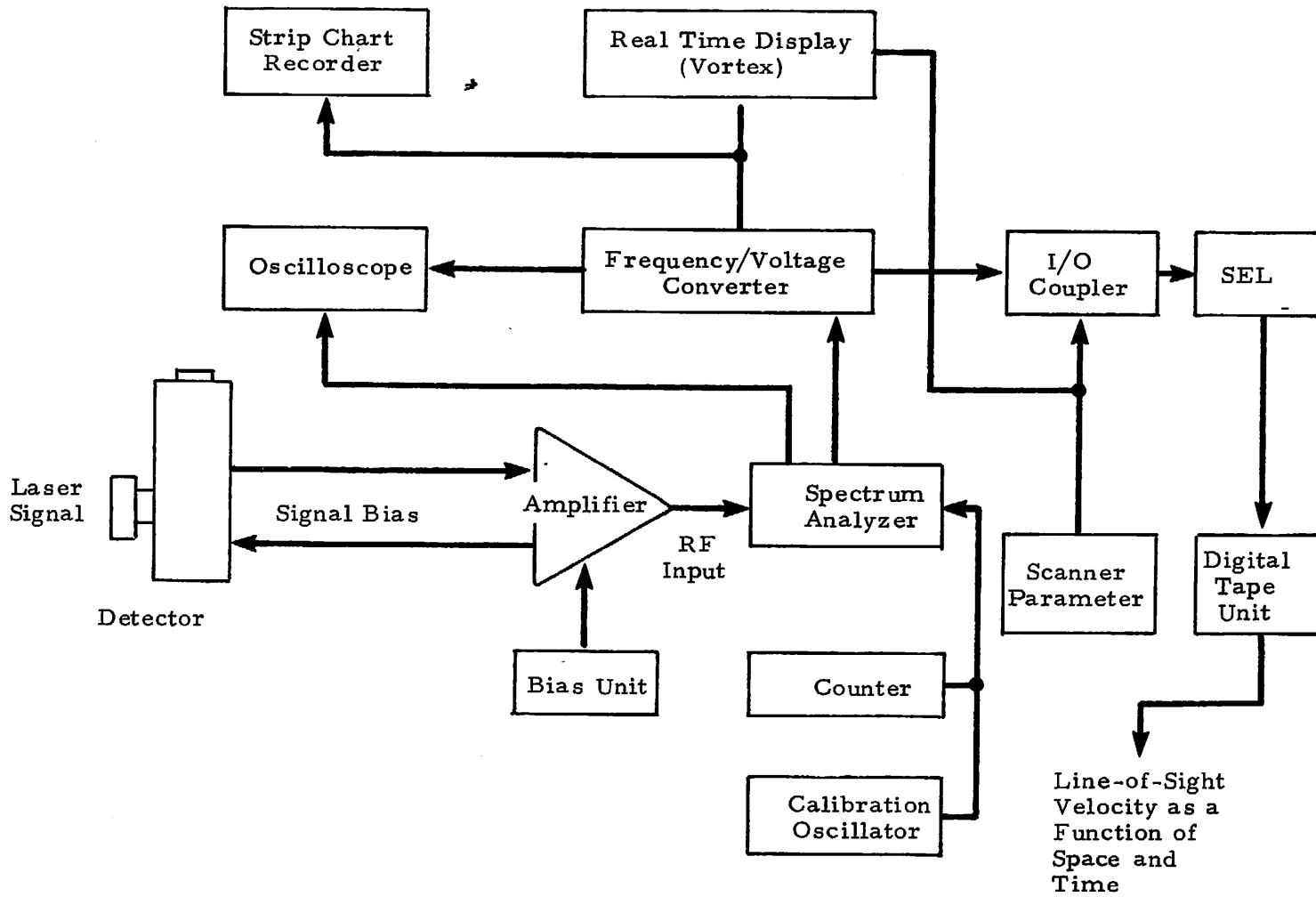


Fig. 2-6 - LDV Signal Processing System

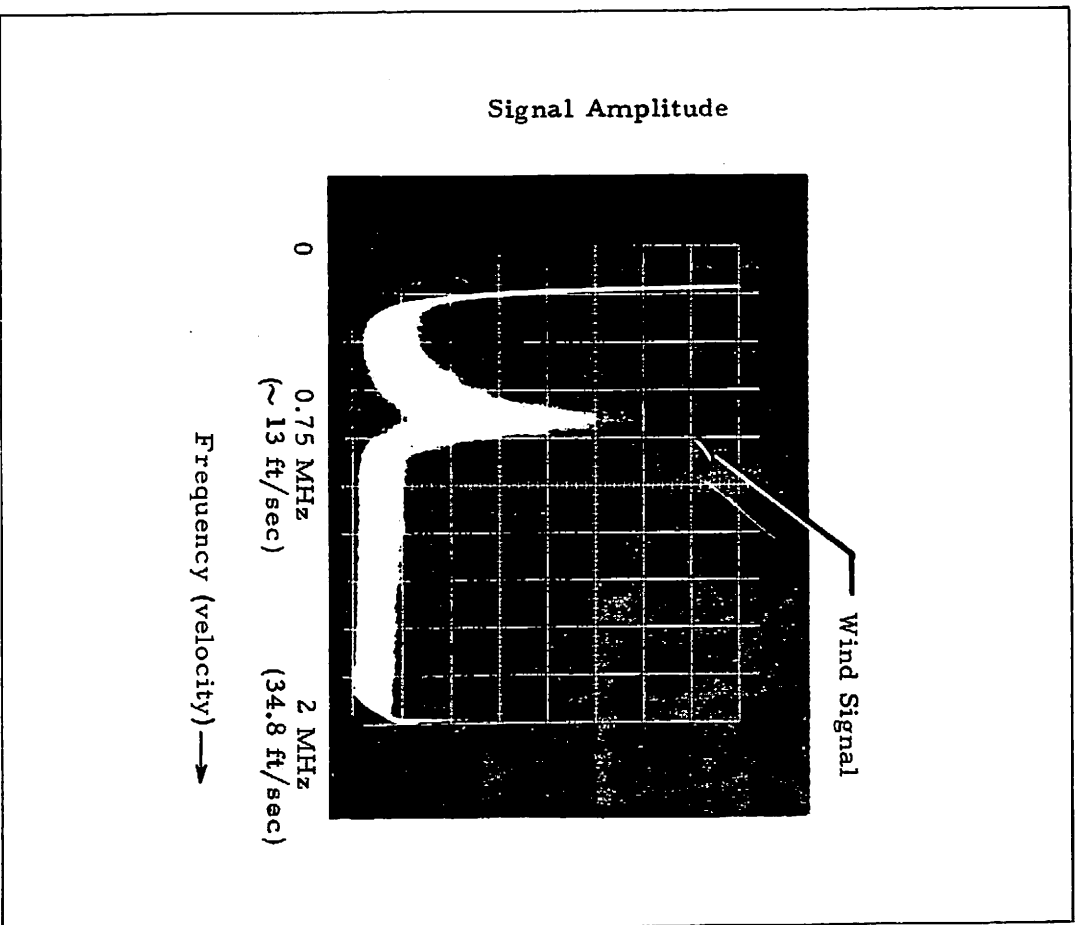
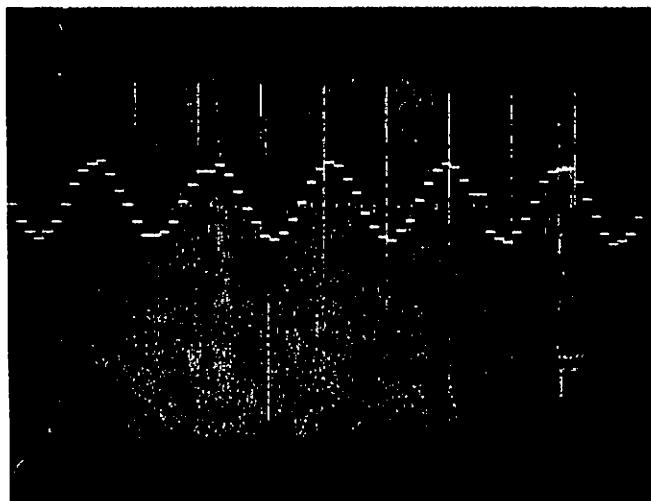


Fig. 2-7 - Typical LDV Wind Signature as Displayed by Spectrum Analyzer

representing the current sample is compared with that obtained on the previous count. If the current one is the larger of the two, it is saved by storing in a latch, along with the binary number representing its frequency; if it is smaller, the previous one is retained until the next comparison. This process is continued for the entire sweep. It is evident that the number remaining in the frequency store latch, when the sweep is completed, corresponds to the highest signal power observed, i.e., the peak of the spectrum. At the end of each sweep, the new peak frequency found replaces that obtained on the previous sweep. An example of the output is shown in Fig. 2-8 for the case of an FM signal of center frequency 2.0 MHz ( $f_o$ ) modulated to  $\pm 200$  kHz about  $f_o$  at a 5 Hz rate sinusoidally.



$f_m = 5$  Hz Sine Wave

Oscilloscope Data

Horiz. = 0.1 sec/div

Vert. = 1 V/div

Fig. 2-8 - Output of Signal Processor for FM Modulated Input

A provision is included for tracking single sideband-suppressed carrier signals, with an identification of upper or lower sideband such that if used in conjunction with an acousto-optic modulator the unit can discriminate the sign of the Doppler shift. The signal feedthrough at the translated frequency can also be discriminated against digitally, thus eliminating the need for a "notch filter."

The raw spectral information (output of the spectrum analyzer) is also made available to the Systems Engineering Laboratories (SEL) 810A data logging minicomputer which is programmed to generate its own estimate of the spectral peak and is discussed later in Section 3.

#### 2.1.5 Data Recording and Display

The primary data gathering function is performed by a SEL 810A general purpose minicomputer. Data acquired by the Mobile Atmospheric Unit is formatted by the computer software and stored on magnetic tape for subsequent processing. The SEL 7-track tape control and magnetic tape units allow digital recording of data at 800 bpi at 45 ips. The data logged by the computer includes:

- a. All scan volume location parameters
- b. "Mode of operation" identifier
- c. The instantaneous line-of-sight velocity information
- d. The Doppler spectrum peak strength
- e. Full spectrum intensity and frequency information (optical)
- f. A data quality identifier.

Properties of the Doppler spectrum, namely the amplitude and frequency corresponding to the spectral peak, are obtained as a result of on-line computer processing; the frequency is also obtained by the spectral peak locator (velocity processor) discussed previously. The latter allows some flexibility for on-line operator displays (see below).

The velocity processor estimate of the instantaneous line-of-sight velocity, updated at a 70-Hz rate, is available in analog format which can be recorded directly on a strip chart recorder (an option which is extremely useful during the VAD mode of operation for monitoring the characteristic profile). During vortex tracking operations the velocity processor's output is used to modulate the intensity of a CRT beam which is driven to trace on the tube face an exact replica of the scan pattern generated by the

scanning system. The display shows on-line the location of high velocity regions. For vortex tracking purposes, the display aids the operator in selecting the optimum scan adjustments so that the trajectory of the wake vortex can be recorded. The integration of such a vortex display into the system was a required task in the Scope of Work. The information in this subsection is supplemented by the discussion in Section 2.4 relating to data transfer and formatting.

Some overall views of the mobile unit hardware as used during the program are shown in Figs. 2-9 through 2-12.

## 2.2 SYSTEM SPECIFICATIONS

Specifications for the subsystems and components are as shown in Table 2-2.

## 2.3 MODES OF SYSTEM OPERATION

### 2.3.1 Winds Aloft Sensing

Using the basic system outlined previously it is possible, by scanning operations, to determine the three-component wind field at any specified altitude between 50 and 2000 feet. Since the LDV system measures the wind velocity at a given point in space along the optical system's line of sight, it is necessary to sample the line-of-sight velocity at different points in space to compute the full three-dimensional wind field. The scanning method employed is commonly referred to as the Velocity Azimuth Display\* (VAD) technique which was used by Lhermitte and Atlas in conjunction with a microwave radar (Ref. 5).

The telescope is focused at the altitude of interest, the beam being directed at a zenith angle,  $\alpha$ . The beam is then scanned in azimuth, thus tracing

---

\*Also known as conical scan technique because of beam scanning configuration.



Fig.2-9 - LDV Monitoring Wake Vortex Generated by L-1011 at Huntsville Airport

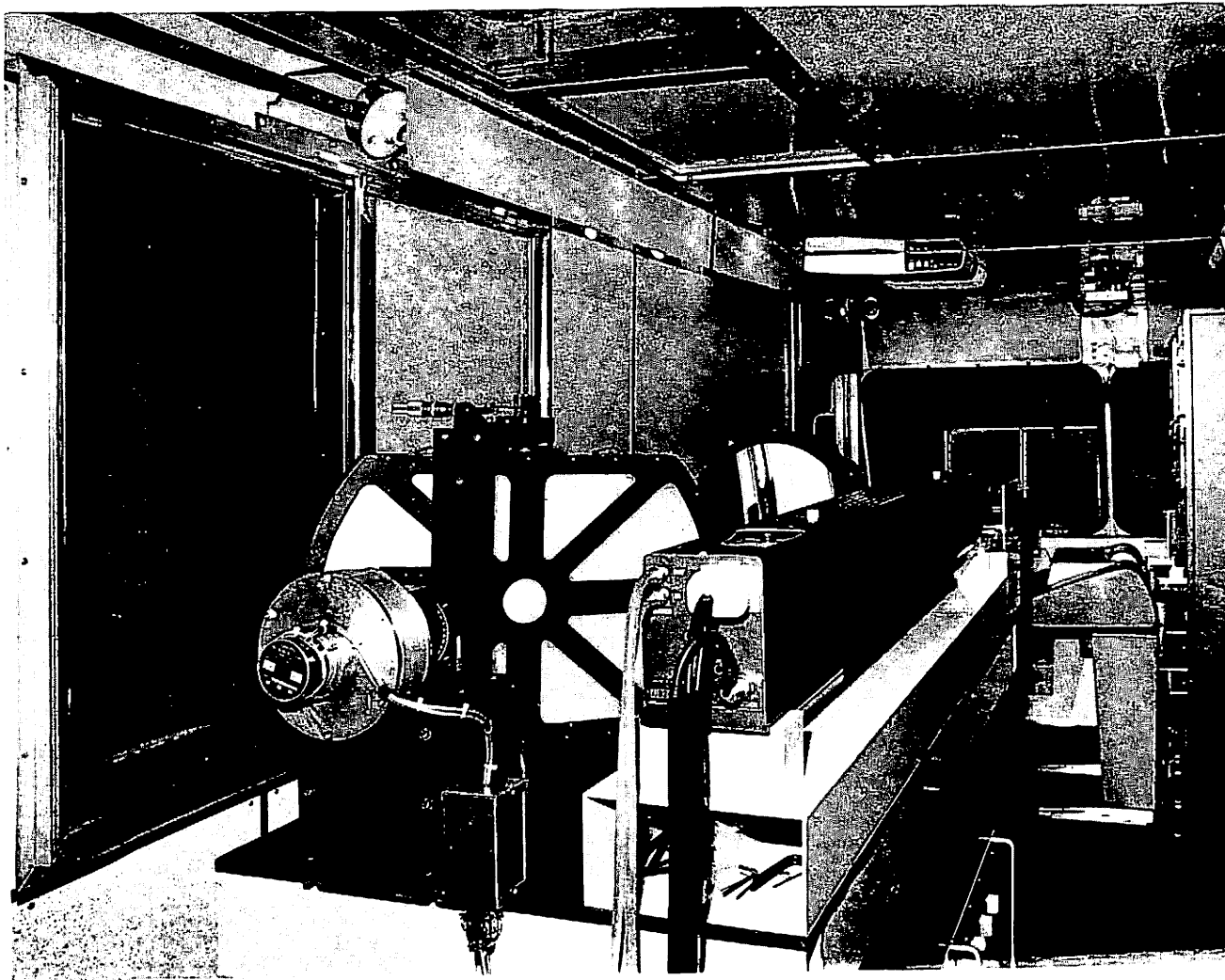


Fig. 2-10 - Interior View of LDV Looking Forward (Depicted in Foreground is Elevation Scanning Mirror on Left Hand and Laser on Right Hand.)

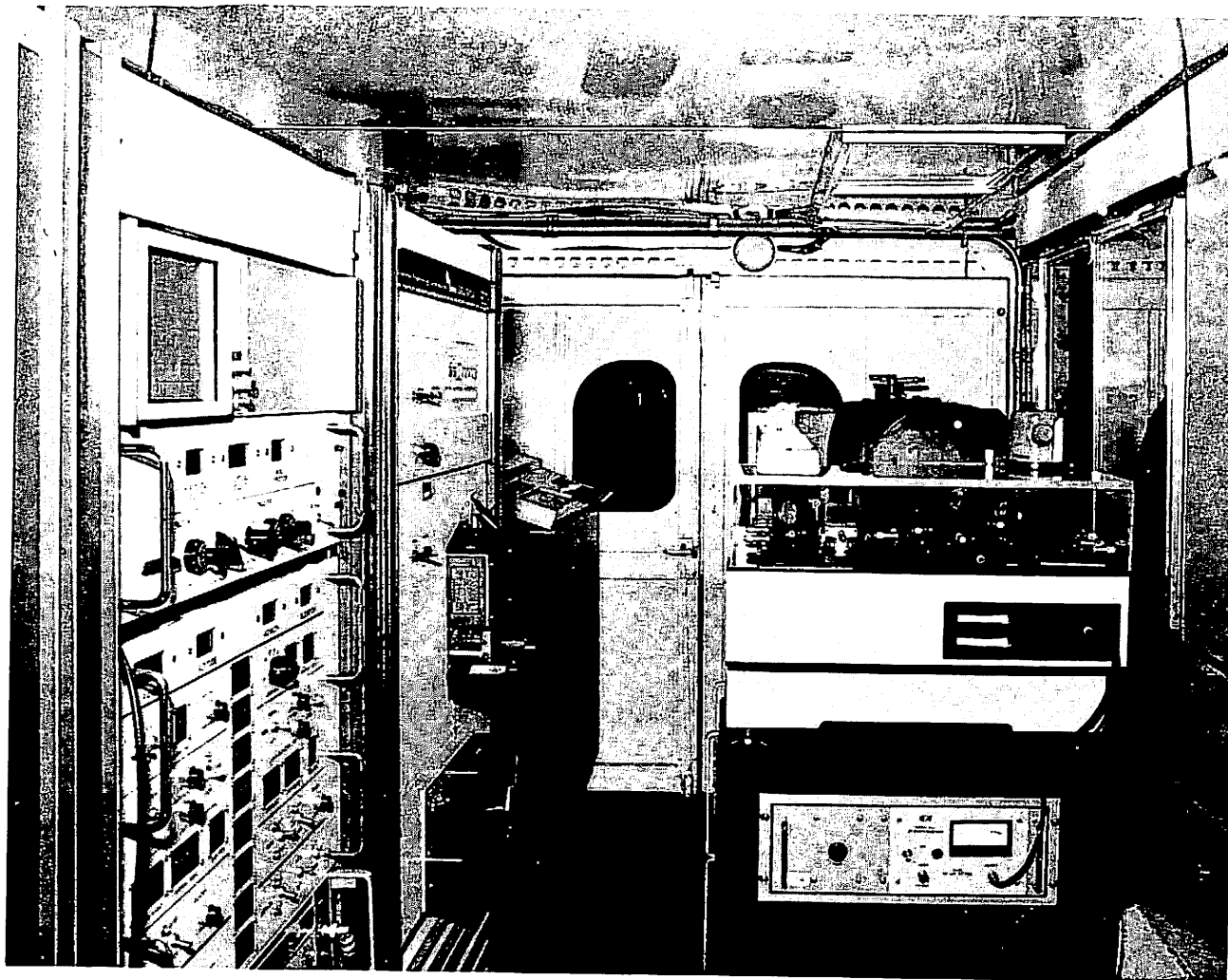


Fig. 2-11 - Interior View of LDV (Depicted in Background is Display and Scanner Controls in First Rack, Computer in Second Rack, Digital Tape Unit Aft, and Optics Package on Right Hand.)

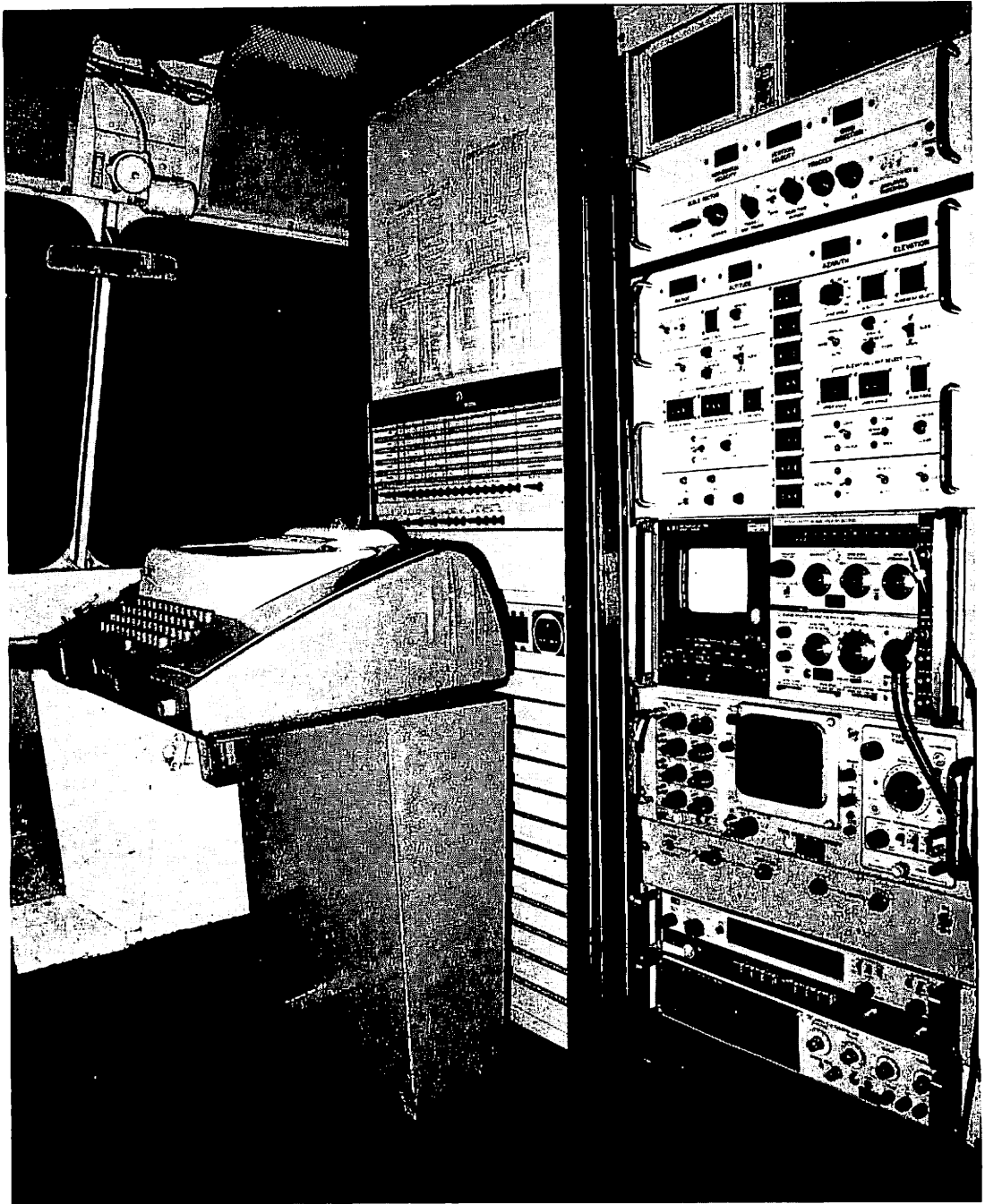


Fig.2-12 - Computer Mainframe, Teletype, and LDV Electronics

Table 2-2  
 LOCKHEED DETAILED COMPONENT SPECIFICATIONS

	<p>Overall Performance Specifications</p> <p>Range <math>\approx</math> 52 ft to 2600 ft Line of Sight          Velocity Measurement Threshold: <math>\approx</math> .7 ft/sec Line of Sight          Measurement Accuracy: Velocity <math>\approx</math> <math>\pm</math>1.64 ft/sec, Direction <math>\approx</math> <math>\pm</math>3 deg.</p>
<p>1. Laser</p>	<p>Type: Honeywell Model 9000 with Recharging Capability          Power: 15 W at P(20) (Nominal)          Mode: TEM<sub>00n</sub>, (Single Mode)          Stability: Long Term, +2%; Short Term, <math>\pm</math>0.5%          Beam Diameter: 0.0197 ft</p>
<p>2. Detector</p>	<p>Type: Rockwell, Pb-Sn-Te Photovoltaic          Quantum Efficiency <math>\geq</math> 40%          Freq. Response: <math>\geq</math> 50 MHz          Element Size: <math>\sim</math>.4 x 10<sup>-7</sup> ft<sup>2</sup>          Dynamic Impedance: &gt;200 <math>\Omega</math>          Number of Elements: 4</p>
<p>3. Telescope</p>	<p>Diameter: 12 in. Primary, 0.5 in. Secondary          Spatial Resolution: <math>\pm</math>125 ft at 1000 ft range at 50% power point</p>
<p>4. Interferometer</p>	<p>Type: Mach-Zehnder          Polarization Input: Horizontal          Polarization Output: Circular          Polarization Recombined: Vertical          Components: Mirrors (4)                            Half Wave Plate (1)                            Quarter Wave Plate (1)                            Brewster Window (1)                            Beamsplitter (2)                            Lens (1)                            Aperture (1)</p>

Table 2-2 (Continued)

<p>5</p>	<p><b>Range/Altitude Scan</b></p> <p>Excursion: 52 ft to 2600 ft          Rate (Auto): 0.1 to 6.9 Hz in 0.1 Hz Steps          Rate (Manual): Slew - 0.2 Hz                                            Step - 6.56 ft Increments          Accuracy: Static - 0.7% at 1148 ft Range                                            Dynamic - 0.5% at 561 ft Range</p> <p>Modes: Manual - Slew                    Manual - Single Increment                    Auto - Range                    Auto - Altitude</p> <p>Altitude Limits: 33 ft to 2100 ft          Altitude Steps: 8 maximum, Any Combination                                            Incremental Altitudes for 8 Equal Steps          Readout (LED): Range, Altitude, Azimuth Angle, Altitude Increment</p>
<p>6.</p>	<p><b>VAD Scan</b></p> <p>Measurement Time/Alt.: 5 sec          Frame Rate: 40 sec          Cone Angle: 0 to 60 deg, Manually Adjustable</p>
<p>7.</p>	<p><b>Processing System</b></p> <p>Signal Processor: HP Spectrum Analyzer, Velocity Processor (LMSC)          Sample Rate: 70 Hz          Modes: Translate or Non-Translate                    Velocity Peak or Velocity Max.          AGC: Auto Threshold          Output: 0 to 5 Vdc          Resolution: 0.328 ft/sec</p>
<p>8.</p>	<p><b>Minicomputer</b></p> <p>SEL 810 Data Logging System</p>



out a circle at the selected altitude (Fig.2-13). The instantaneous mean radial velocity within the sensing volume as measured by the radar,  $v_r$ , is given by

$$v_r = v_h \sin\alpha \cos(\theta - \theta_o) + w \cos\alpha,$$

$v_h$  and  $\theta_o$ , respectively, being the speed and direction of the horizontal wind motion and  $w$  the vertical motion at the height being sampled. From the amplitude, phase and dc component of the VAD signature it is possible to compute the horizontal speed and direction and vertical velocity of the wind field.

In the present mode of operation it is the absolute value of  $v_r$  ( $|v_r|$ ) that is sensed, a deficiency that allows an ambiguity of  $\pi$  in the wind direction estimate. The modifications that this makes to the VAD profile and the respective equations for the velocity components are indicated in Fig.2-14.

While operating in the VAD mode the system is capable of interrogating  $n$  ( $n = 1$  through 8) altitudes (that can be dialed in by using thumbswitches) in sequence over a total time period of  $5np$  sec where

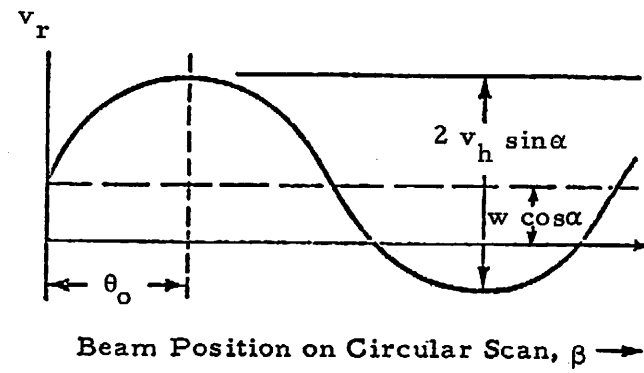
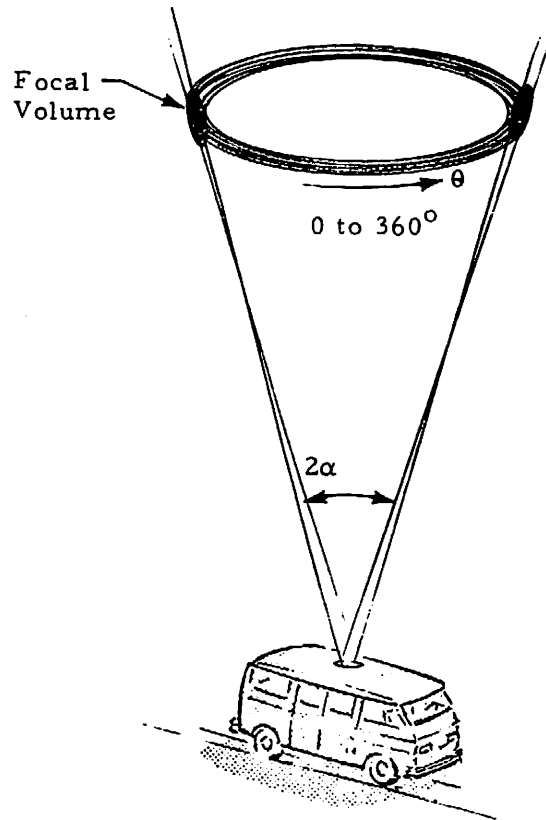
- 5 sec = time for conical sweep at one altitude
- $n$  = number of altitudes to be interrogated
- $p$  = number of VAD scans at each altitude  
(can be chosen to be 1 through 7).

During this investigation  $n = 8$ ,  $p = 1$  were utilized thus allowing the interrogation of eight altitudes every 40 seconds and the sequence was repeated for the required test duration.

### 2.3.2 Coordinated Range and Elevation Scanning and Point Sensing Mode of Operation

The basic LDV has the capability of determining the wind velocity component along the optical system's line of sight and within the system's sensing volume (Section 2.5). The hardware is arranged to range scan along a selectable

2-24



$w$  = vertical wind component  
 $v_h$  = horizontal wind component  
 $\theta_0$  = direction of horizontal wind component

Fig.2-13 - VAD Principle of Operation

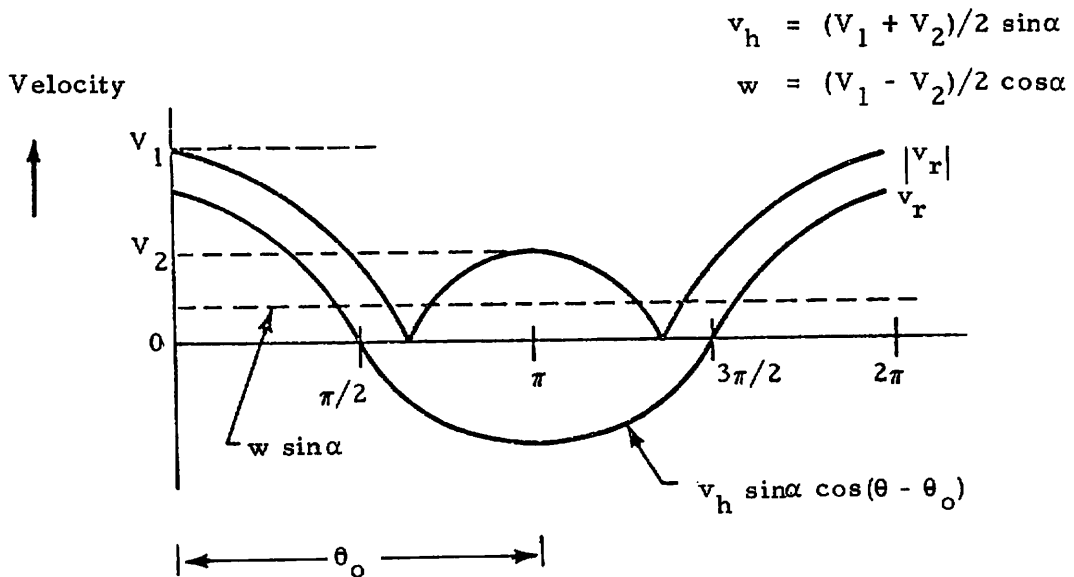


Fig. 2-14 - Azimuth Angle Dependence of Measured Velocity Component

line of sight by varying the position of the telescope secondary mirror, E, relative to the primary, D, (Fig. 2-3) so as to scan the system's sensing volume linearly between fixed range limits. The relationship between the separation, DE, and the range to the sensing volume is given by the lens equation. This procedure will result in the line-of-sight velocity profile along the chosen line of sight and between the range limits. The elevation angle can also be scanned in a controlled manner by scanning the output mirror shown in Fig. 2-3. A coordinated range and elevation scan was the basic mode of operation during vortex tracking. Fast range and slow elevation scans generate a "finger scan" pattern in the plane of interest. Any location of interest could be "dialed in" using the scanner controls and that region interrogated continuously. The scan patterns traced out in the two modes of operation are shown in Fig. 2-15.

#### 2.4 ON-LINE DATA MANIPULATION

The data from the LDV system are transferred to the computer along four digital input channels. It is reformatted and recorded on 7-track magnetic tape for off-line data processing. Software to locate the peak intensity within

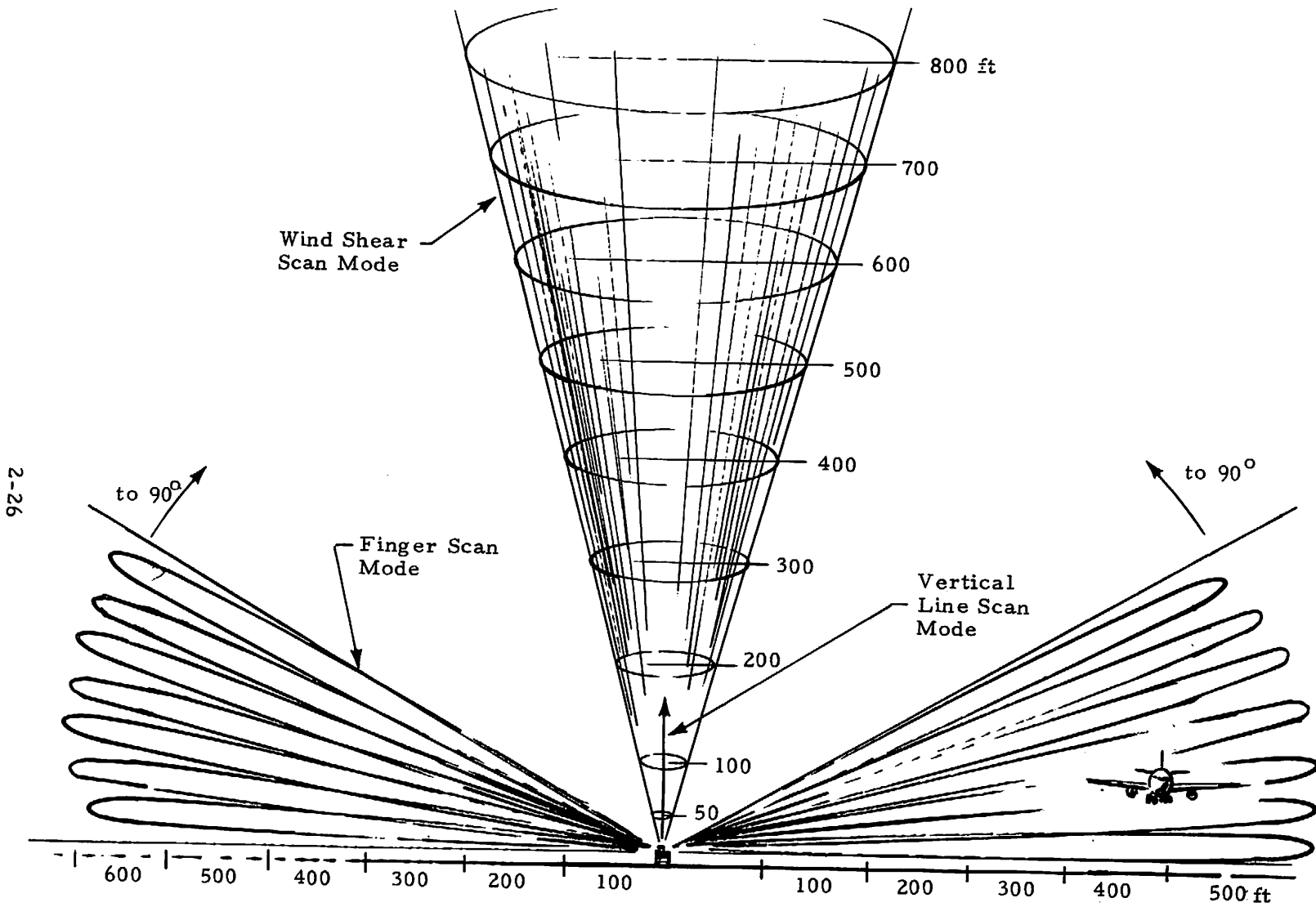


Fig. 2-15 - Scan Configurations

each spectrum, subject to the constraints of frequency and amplitude thresholds and the associated sample count number (velocity), is also incorporated. Additional details of the latter process are included in Appendix B.

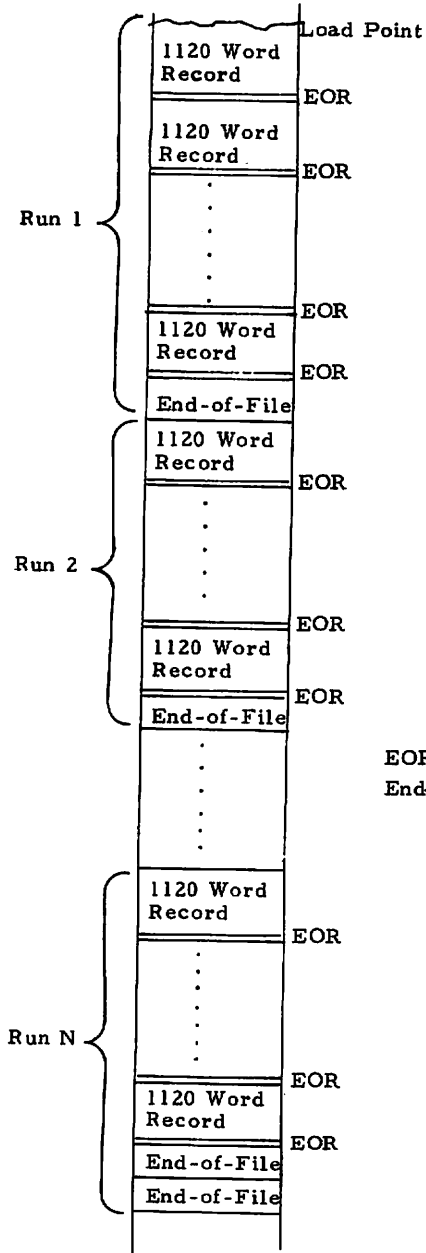
Recorded data consist of four 16-bit words for each spectrum analyzer sweep. These four words correspond to the four SEL logical input channels (60, 61, 62 and 63) read for the spectrum analyzer sample count at which the peak intensity occurred during a given sweep. The logger identifies the peak intensity condition independent of the "data acceptable" condition<sup>\*</sup>; four 16-bit words (identifying sample count location, range or altitude, angle, and appropriate scanning parameters) are saved for each spectrum analyzer sweep with the data acceptable consideration left to the off-line software. After 280 spectrum analyzer sweeps an 1120-word buffer is filled (four words/sweep x 280 sweeps) and a block transfer to magnetic tape are accomplished. The logger ensures that this block transfer is completed before permitting data acquisition to proceed. Thus, a period of one spectrum analyzer sweep and two spectrum analyzer flybacks are occupied with the block transfer of data; thus one spectrum analyzer sweep is lost every 280 sweeps. At the 70-Hz rate, the 1120-word buffer is filled and written to tape approximately every four seconds. The format of the 7-track magnetic tape for the peak intensity logger is given in Fig. 2-16. In general, each run (VAD or aircraft fly-by), will generate a distinct number of 1120-word records (one every four seconds at 70-Hz rate) with one end-of-file at the end of the run. At the end of the day (or data taking period) two (2) end-of-files are marked at the end of the last run on tape.

---

<sup>\*</sup>"Data acceptable" condition is an indication as to whether a Doppler burst above both velocity and amplitude thresholds occurred during a spectrum analyzer sweep.

MAG. TAPE FORMAT

1120 WORD RECORD DESCRIPTION



	Ch. 60	Ch. 61	Ch. 62	Ch. 63
Sweep 1	Word 1	Word 2	Word 3	Word 4
Sweep 2	Word 5	Word 6	Word 7	Word 8
.	.	.	.	.
.	.	.	.	.
.	.	.	.	.
Sweep 280	Word 1117	Word 1118	Word 1119	Word 1120

EOR is standard 3/4 inch  
End-of-Record gap

Fig. 2-16 - SEL 810A Magnetic Tape Format (Peak Intensity Logger)

## 2.5 PERTINENT LDV PERFORMANCE PARAMETERS

### 2.5.1 Theory

The performance characteristics of an LDV system can be quoted in terms of the signal-to-noise ratio of the output and the dimensions of the sensing volume interrogated. Expressions for these parameters are derivable from an electromagnetic wave treatment of the laser radiation propagation and interaction with the aerosol medium. For the Cassegrainian optical system of interest here the field,  $u$ , generated by the telescope assuming a  $TEM_{00n}$  laser beam mode shape is given by (Ref. 2)

$$u(t, x', y', z') = -\frac{ika}{z'} \sqrt{\frac{2N(t-z/c)}{\pi}} \exp[i(kz' - \omega t)] \exp\left(\frac{ik\rho'^2}{2z'}\right) \int_{a_i/a}^{a_o/a} J_0\left(2\frac{\beta\rho'}{a}x\right) \exp\left\{-[1 - i\beta(1 - \xi)]x^2\right\} x dx,$$

where  $\rho'^2 = x'^2 + y'^2 =$  radius at range  $z'$  from the telescope,  $k = 2\pi/\lambda$ ,  $\lambda =$  laser wavelength,  $a = \exp(-2)$  radius of the  $TEM_{00n}$  laser mode at the telescope exit,  $N =$  number of photons transmitted per second,  $a_o =$  telescope outer radius,  $a_i =$  radius of telescope inner hole,  $J_0(\ ) =$  zeroth order Bessel function,  $\beta = \pi a^2/\lambda z$ ,  $\xi = z/f$ ,  $f =$  range to focus in the atmosphere,  $(x', z')$  are dimensions in the plane of telescope,  $c =$  speed of light, and  $t =$  time.

For  $a_o \gg a$  (laser beam width considerably smaller than the telescope diameter, i.e., the telescope does not truncate the laser beam) a simple treatment of the total LDV system is possible. Specifically the following results apply (see Ref. 2 for details):

The signal-to-noise ratio ( $S/N$ ) at the output of the monostatic continuous wave LDV system is given by

$$S/N = \eta(\overline{n\sigma}) \lambda P / 4h\nu B,$$

where

- $\eta$  = the photodetector quantum efficiency
- $n\sigma$  = the scattering cross section of the aerosol at a wavelength,  $\lambda$  (units of inverse length)
- $P$  = laser power transmitted
- $h\nu$  = photon energy at the wavelength,  $\lambda$ , and
- $B$  = bandwidth of the filter being used to monitor the Doppler frequency.

Note that the above is independent of the range to focus and also of the optic diameter. The physical reason is that the sensed volume varies as  $(f/R)^4$  where  $f$  is the range to focus and  $R$  the optic diameter. The number of targets is therefore  $\propto f^4$  which cancels the  $f^{-4}$  dependence of the return from a single target.

Substituting typical parameters in the S/N equation, namely,

- $\eta = 0.3$
- $n\sigma = 5.03 \times 10^{-7} \text{ ft}^{-1}$  (14 mi visibility)
- $\lambda = 10.6\mu$
- $P = 15 \text{ W}$
- $B = 30 \text{ kHz}$  (i.e., a filter with  $\sim 0.5$  fps resolution)
- $h\nu = \text{photon energy at } 10.6\mu = 1.78 \times 10^{-23} \text{ Btu,}$

we have an estimate of 45.5 dB for the signal-to-noise ratio. This estimate should be further adjusted by no more than 5 dB of system optical losses. Such signal-to-noise ratios are routinely observed from wind returns.

The spatial resolution cell parameters of interest are the length along the optic line of sight and its diameter. The latter is always small for the ranges of interest here ( $\sim 0.4$  in) and will not be considered further.

The along-axis resolution is given by  $2\lambda f^2/\pi a^2$  for the untruncated theory (where  $a$  can be considered to be the telescope diameter). In practice, achieving the condition  $a_o \gg a$  is difficult for a given beam diameter,  $a$ , because optic sizes become unwieldy. Studies have shown that the optimum arrangement for a given optic size is to illuminate the telescope such that the  $\exp(-2)$  points of the intensity pattern coincide with the extremity of the mirror. Under such a condition the LDV sensing volume length,  $\Delta L$ , along the optic axis between the 3 dB antenna pattern points is given by

$$\Delta L = 4.4 \frac{\lambda f^2}{\pi a_o^2} \quad (a_o = \text{telescope primary radius}).$$

This equation represents a degradation of a factor of 2.2 over the untruncated case. The truncated effects on the signal-to-noise ratio ( $\sim 3$  dB loss) are of little concern here since in practice under a variety of weather conditions in various parts of the continental United States the signal-to-noise ratios have always been ample ( $> 25$  dB).

For the one-foot diameter optic size of interest the sensing volume length at various ranges are:

Range (ft)	Sensing Volume Length (ft)
100	+0.975
500	+24.4
1000	+97.4
2000	+390.0

## 2.5.2 Summary of Pertinent Performance Data

### Spatial Resolution vs Range Results

The antenna pattern of the laser Doppler system was investigated by interrogating a target of known velocity and position — a rotating disc at various ranges from the LDV. The procedure involved adjusting the line of sight to intersect the disc at some radius to yield a convenient Doppler shift. Range scanning along this line of sight was then initiated. The disc surface consisted of No. 600 grit sandpaper and four ranges between 230 and 800 ft were carefully measured. The heterodyne output of the Pb-Sn-Te detector was monitored by the spectrum analyzer adjusted to operate in the fixed frequency receiver mode and tuned to the Doppler frequency. As the secondary mirror was scanned the receiver response was recorded on a strip chart recorder along with the range command voltage. The range increment at which the Doppler signal deteriorated to the one-half power level was then graphically obtained from the chart data. A typical strip chart record is shown in Fig. 2-17 and the resolution data calculated from such profiles are shown in Fig. 2-18 on which is also plotted the expected theoretical behavior for the nominal system parameters, i.e., a beam diameter of 12 inches at the telescope primary (defined at the exp (-2) intensity points).

It is observed that the measured values are some 40% larger than theoretical (i.e., above diffraction limit) which is indicative of some system inefficiencies. Among the contributing factors are respectively: aberrations, alignment difficulties, and beam size and shape deviations from nominal. Experience has shown that beam shape deformation is probably the chief culprit in that occasionally, when the laser beam output is observed to be non-gaussian (i.e., when it contains multiple intensity peaks), serious degradation of the system spatial resolution capability occurs. Analysis shows aberration effects to be small and also that beam size deviations from nominal are not overly important (a fact not obvious from the theoretical equation for the resolution, i.e.,  $\Delta L = \frac{4.4 \lambda f^2}{\pi a_o^2}$ , since the degree of beam truncation by the telescope primary has been

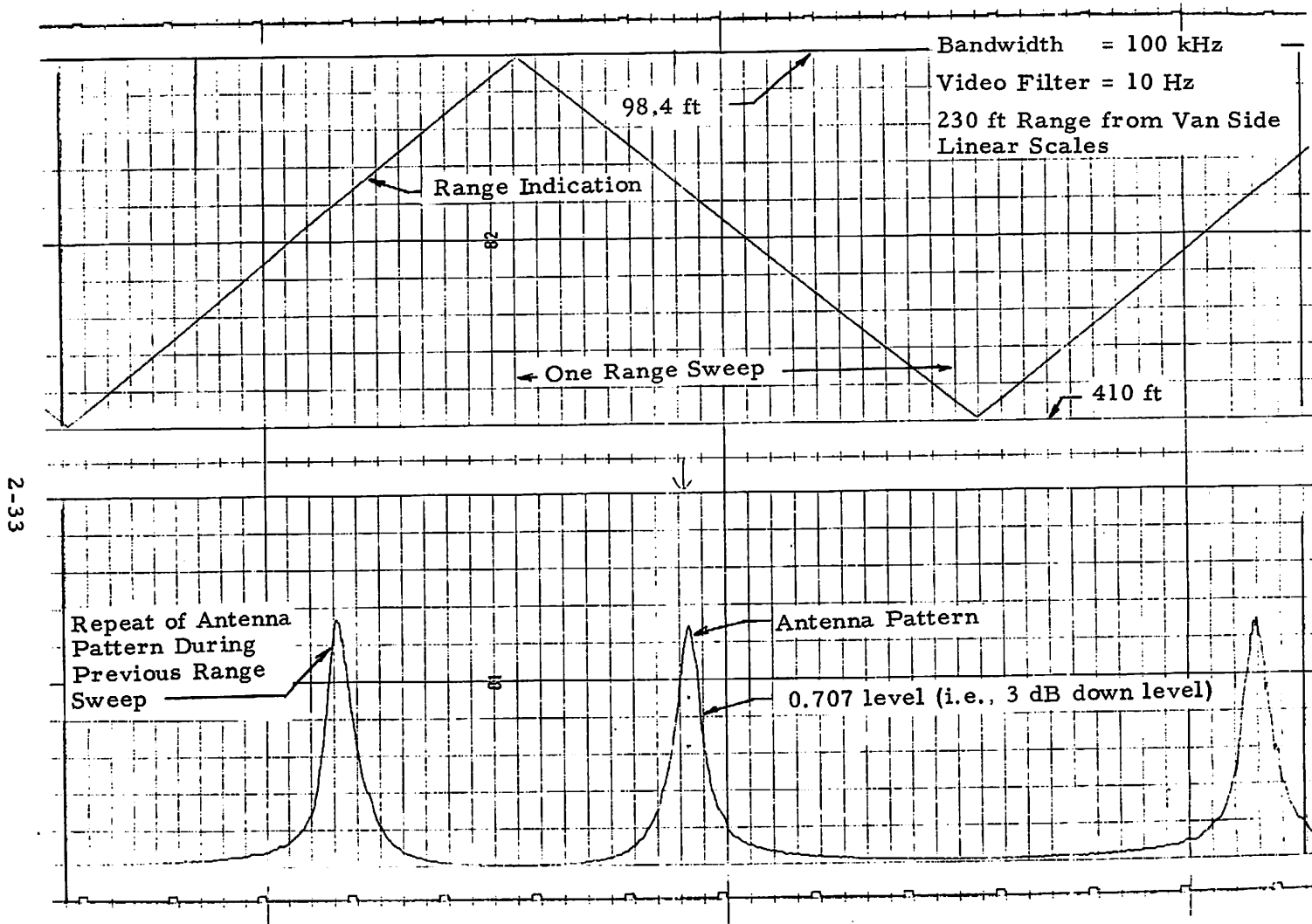


Fig. 2-17 Typical Spatial Resolution Experiment Traces

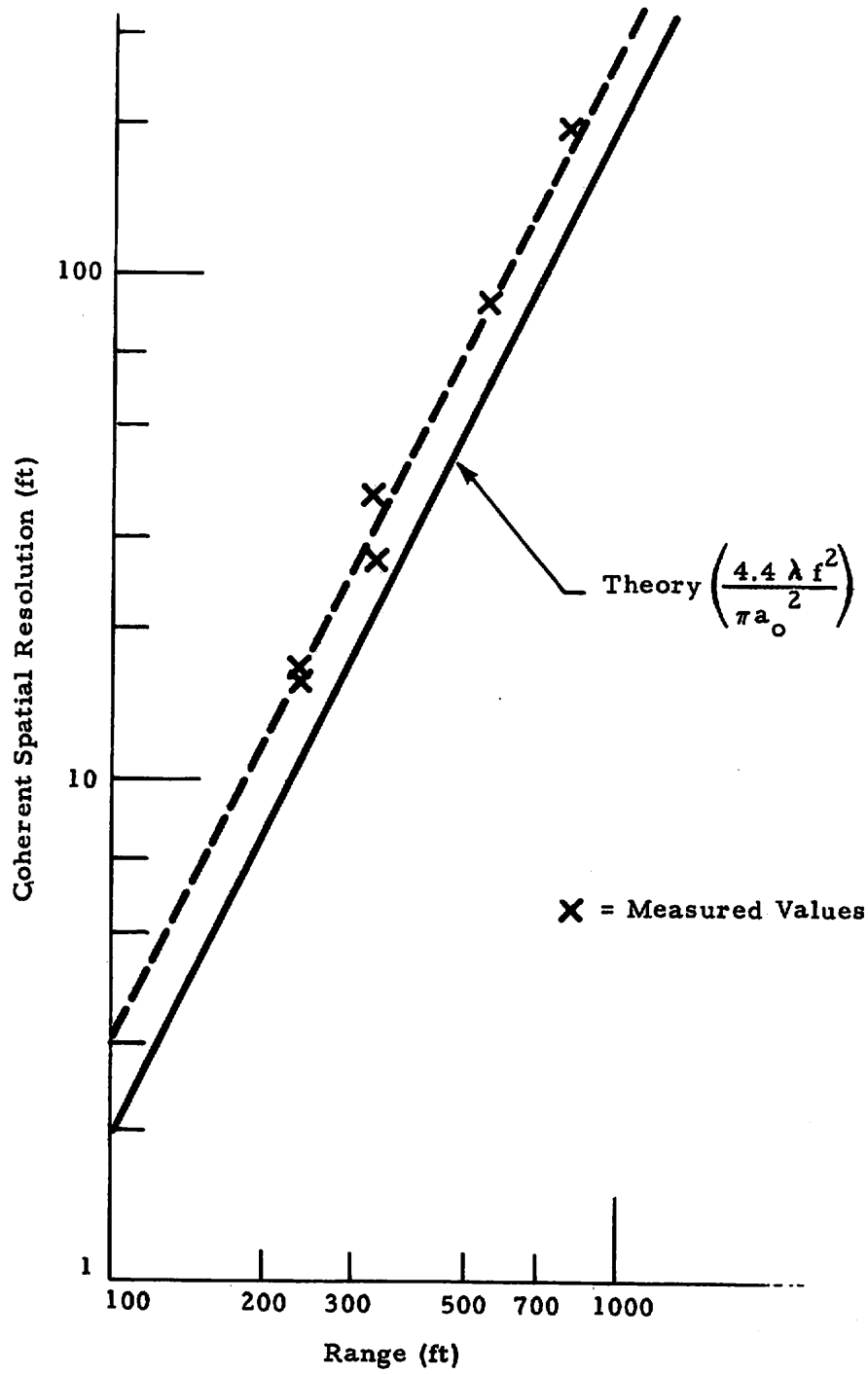


Fig.2-18 - Field Measurements of Coherent Spatial Resolution

factored out). Greater consideration of laser beam quality is merited during the design of future systems.

### Signal-to-Noise Ratio Performance

The signal-to-noise ratio performance of the laser Doppler unit is monitored by interrogating a target of known reflectance, the same rotating disc as used for the spatial resolution measurement. The reflectance of the No. 600 grit sandpaper surface was determined by comparing LDV system efficiency while interrogating such a surface with a similar measurement using a specially prepared 'flowers of sulphur' surface which is well documented to be very nearly Lambertian and of essentially unit reflectance (80%) at the 10-micron wavelength. In this way the sandpaper surface reflectance was determined to be .08. The surface presented a 45° angle of incidence ( $\alpha$ ) to the laser beam.

The signal-to-noise ratio for such a scattering configuration is given by the relation

$$SNR = K_1 K_2 \frac{\eta P a^2 \rho \cos \alpha}{h \nu B L^2},$$

$\eta$  = detector quantum efficiency = 37% ( including 82% detector window transmission loss).

$P$  = transmitted laser power = 15 watt.

$a$  = primary radius (6 inches)

$\rho$  = target reflectivity (0.08)

$\alpha$  = angle of incidence on target = 45°

$h\nu$  = photon energy at 10 $\mu$  = 1.88 x 10<sup>-20</sup> joules

$B$  = spectrum analyzer bandwidth (30 kHz)

$L$  = range to target (560 ft in typical set up)

$K_1$  = beam truncation loss = 0.5

$K_2$  = optical system transmission losses (typically 10%).

Substituting

$$\begin{aligned} SNR &= K_2 \times 2.2 \times 10^8, \\ &= 83.5 \text{ dB less optical transmission losses.} \end{aligned}$$

Two way optical efficiency losses were determined to be 11.2 dB by comparing power measurement at the focus in the atmosphere to a measurement of the laser output power, resulting in a 'target' SNR of 72.3 dB.

Observed, and what was considered satisfactory for operational usage during this investigation, was a SNR of 60 dB at the 560 ft nominal range. The additional 12 dB or so additional loss is due to such factors as optical misalignment and mismatch of beams on the photodetector.

Inasmuch as the quoted optical system transmission (11.2 dB) and alignment (12.3 dB) losses are excessive, these represent areas where the system could be improved. Typical of the improvements required are incorporation of:

- a. Improved alignment methods
- b. Acquisition of improved optical components
- c. Updating the interferometer design, especially in the area of beam interaction with the photodetector.

With the system "peaked up" such that the signal-to-noise ratio obtained while interrogating the rotating disc was 60 dB, a degree of performance was obtained which was satisfactory for wind shear and vortex detection at both Huntsville and JFK. Signal-to-noise ratios of wind returns were generally in the range of 10-20 dB.

## 2.6 DISCUSSION OF LIMITATIONS OF PRESENT SYSTEM

The system as presently configured has several limitations some of which were known before the investigation was initiated and some became more obvious during contract performance. They were not corrected during the effort due to lack of availability of operational components, time and budget constraints, lack of the required technology, etc. The technology areas represented by the limitations should be given prime consideration in the development of any future systems. These areas are now considered.

### Data Rate

The present system is capable of a 70-Hz acquisition rate of velocity samples which is marginal, for example, in the vortex tracking mode. Range scanning at a 5-Hz rate over a 1000 ft range results in range 'smearing' of approximately 150 ft. Typically during the JFK testing the range scan limits were separated by approximately 500 ft with scanning at a rate of 4 Hz resulting in a range smearing of approximately 60 ft. There is room for at least an order of magnitude improvement here which can be partly achieved by increasing the sweep rate in the present processing technique of using a sweeping spectrum analyzer to interrogate the Doppler spectrum. Increasing this, of course, would place an additional burden on the data acquisition system - especially the minicomputer currently in use. The ultimate solution is a parallel filter system or filter bank with the integration time chosen to be sufficiently short to allow for the required data rate, say 1 kHz. This device would also increase the duty cycle of the processing system (Doppler tracker) to essentially unity, an increase of two orders of magnitude over the present system, thus yielding improved signal-to-noise ratio performance. The increased data rate would also accommodate an increased rate of conical scanning. The ultimate improvements suggested here would represent a major addition to the present hardware.

### Doppler Signal Processing

The duty cycle of the present Doppler signal processor (a scanning spectrum analyzer) is given by the ratio of the spectral region spanned to the instantaneous filter bandwidth, typically 2 MHz and 30 kHz, respectively. This approximately 1.5% duty cycle could be improved by the incorporation of an integrating filter bank as alluded to above.

### Rate of VAD Sampling

A VAD scan at a single altitude is accomplished every 5 seconds (0.2 Hz) in the present hardware, which results in a 40-second time interval for interrogating eight altitudes. For operational usage this is too long since it can,

for example, yield false estimates of vertical shear because of the time lag in interrogating the various altitudes. An increase in the rate of scanning is mechanically possible and is consistent with system performance criteria. A limit to the conical scan rate does exist, however, since the antenna pattern should not translate considerably in the round-trip radiation time. The limiting angular rotation rate which ensures that the antenna pattern does not move by more than half its width during the round trip time is given by

$$\omega \leq \frac{1.22 \lambda c}{4 R D \theta} ,$$

where  $\lambda$  = laser wavelength (10.6 microns),  $c$  = velocity of light,  $R$  = range to focus,  $D$  = optic diameter,  $\theta$  = conical scan angle. For  $R = 1154$  ft (corresponding to an altitude of 1000 ft),  $D = 1$  ft, and  $\theta = 0.5$  radian, the limit is  $\omega \leq 18$  rad/sec ( $\leq 3$  Hz). A conical scan capability of up to 3 Hz could therefore be incorporated in the system. The change would be relatively minor and would reduce the time of interrogating eight altitudes to less than 10 seconds.

#### System Range Resolution

The only fundamental limitation of the present system (i.e., monostatic focused) is its spatial resolution capability at the longer ranges. Without a radical change in system concept this can only be improved by increasing the size of the transmitter optics. The spatial resolution at a given range improves as the square of the size of the optics.

Updating the existing system's spatial resolution capability would require incorporation of techniques to increase the time-bandwidth product of the outgoing beam by imposition of modulation on the transmitted waveform such as through pulsed, FM CW, or phase coding methods. This would represent a major modification.

#### Wind Direction Ambiguity

The system as presently configured yields a value for the wind direction that contains an ambiguity of  $\pi$ . This is because the system is homodyne and

not superheterodyne in nature. The solution to the problem is to offset in frequency the local oscillator so that there is never any folding of the Doppler spectrum about zero frequency. A device to accomplish this function, an acousto-optic modulator (Bragg cell), was to be incorporated in the system prior to the system evaluation tests but its suboptimal performance precluded this. Based on current research efforts it appears that the problems are now resolved.

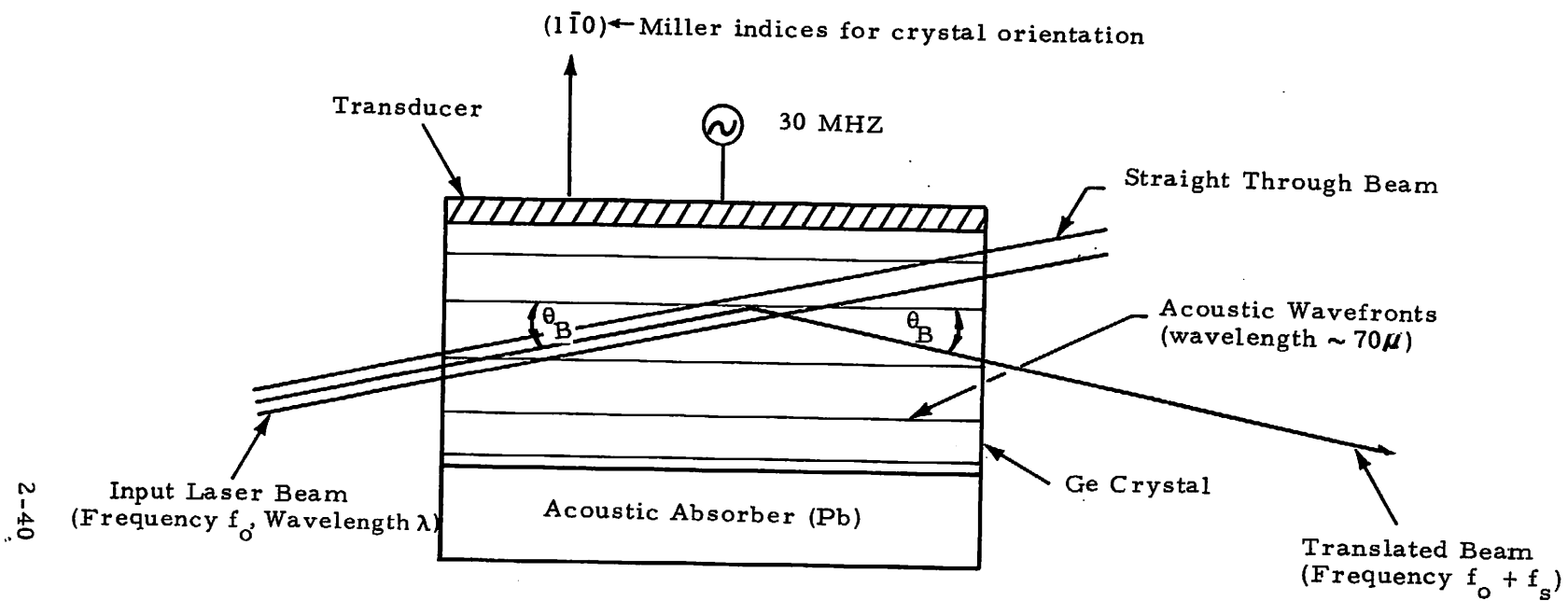
Because of the mandatory nature of having a device in the system to resolve the direction ambiguity, the device is described here in considerable detail along with some performance results obtained from its use. Reference is made to Fig. 2-19.

A lithium-niobate transducer is bonded to a germanium crystal (cut along the axes shown); the acoustic vibrations generated by the transducer are absorbed by a lead backing plate attached to the opposite side. The transducer is excited at the desired offset frequency. A laser beam propagating through the crystal undergoes reflection at the acoustic wavefronts which results in the reflected beam being upshifted\* in frequency relative to the initial laser beam frequency. For the precise geometry shown, i.e., the angle between the acoustic wavefronts and the incident laser beam in the crystal is the Bragg angle, a single definite beam at the upshifted frequency is obtained. It is this beam that is used as the local oscillator beam as shown in the optical arrangement in Fig. 2-20.

For design purposes it is important to consider the origin of the various frequency components in the local oscillator and receiver optical paths, respectively. They are as follows:

---

\*For the geometry shown.



2-40

$$\sin \theta_B = \frac{\lambda}{2\Lambda} , \lambda = \text{Laser Wavelength}, \Lambda = \text{Acoustic Wavelength}$$

= Bragg Angle

Fig. 2-19 - Acoustic-Optic Modulator (Bragg Cell)

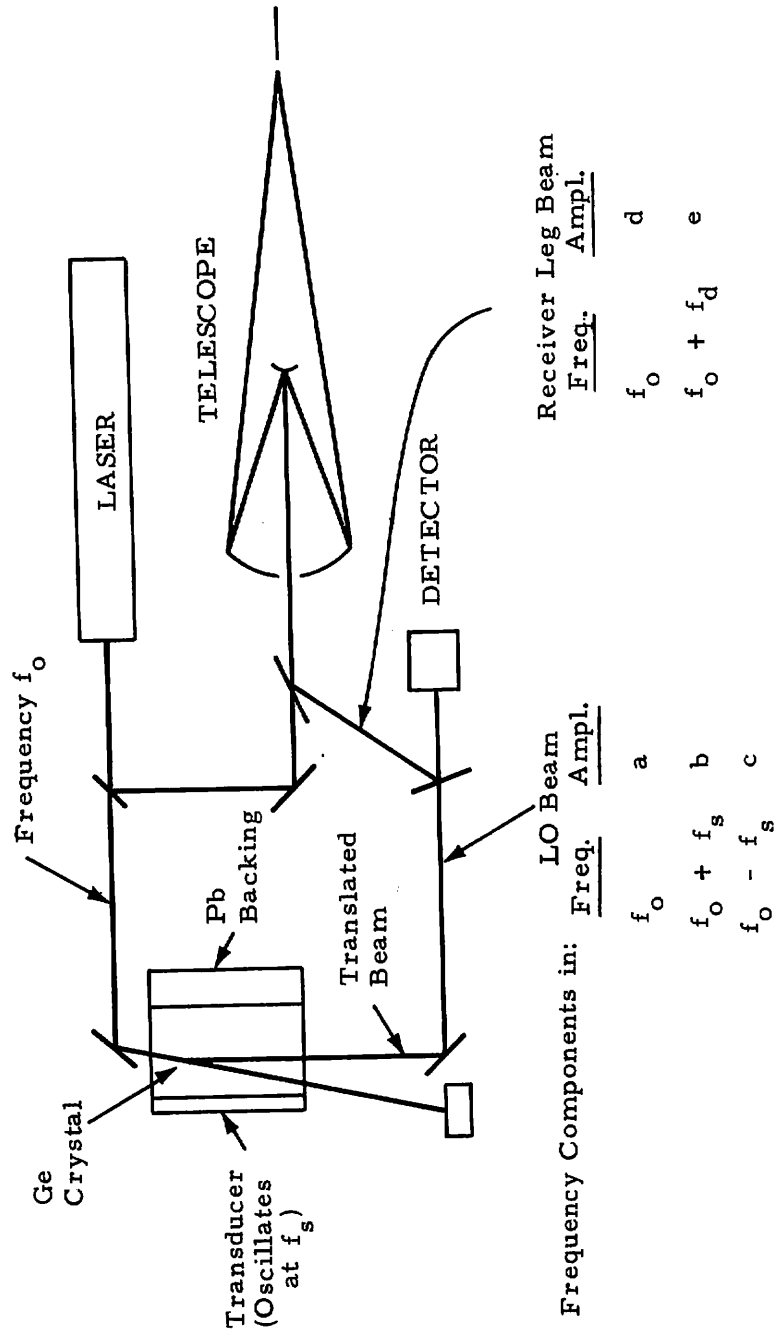


Fig. 2-20 - Optical Arrangement of LDV with Acoustic Modulator Included

### Local oscillator beam

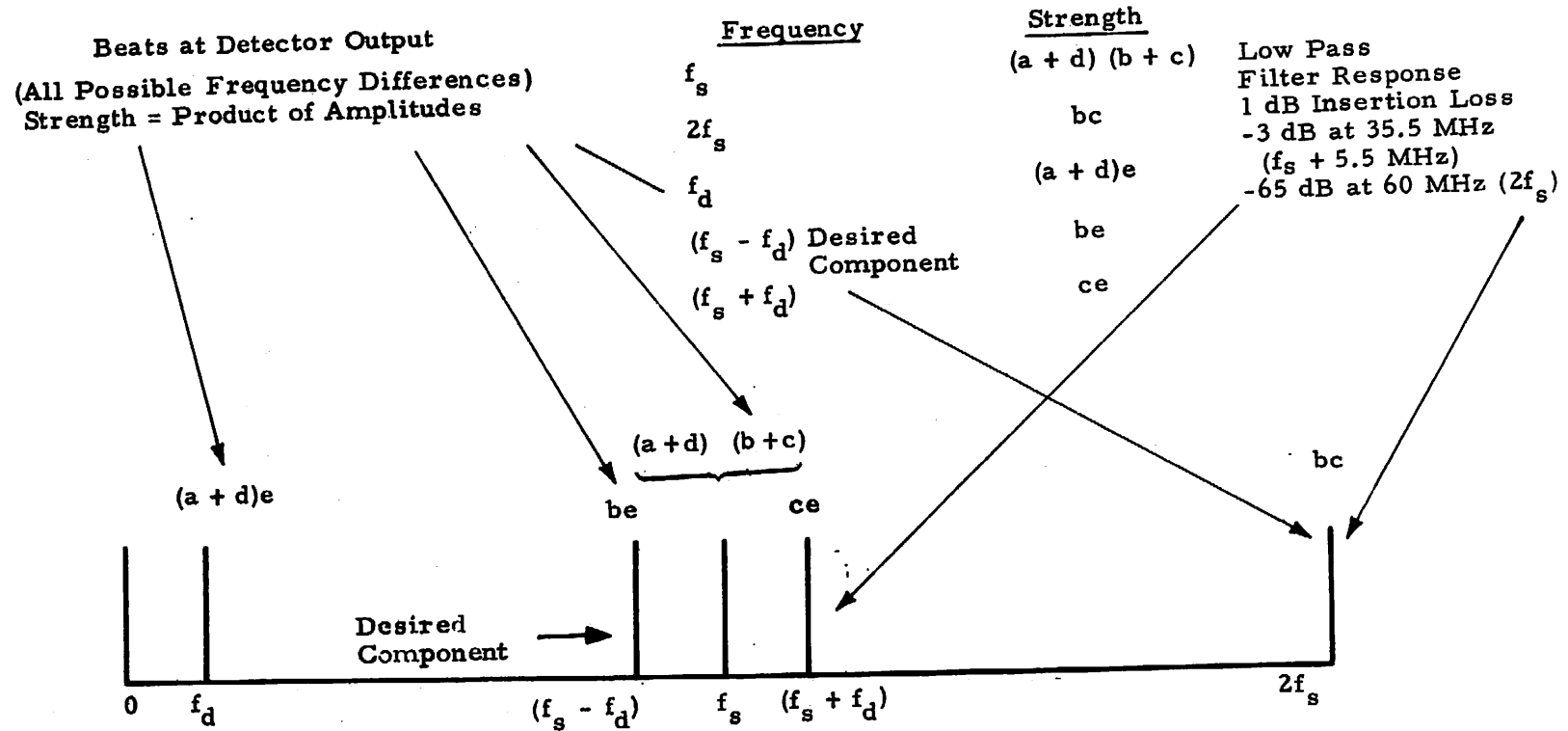
- $f_o$  - feedthrough from the input laser beam of amplitude a
- $f_o + f_s$  - desired upshifted beam of amplitude b
- $f_o - f_s$  - undesired downshifted beam of amplitude c due to the acoustic reflection from germanium-lead interface.

### Receiver beam

- $f_o$  - backreflection from secondary mirror of amplitude d
- $f_o + f_d$  - desired Doppler component of amplitude e,  $f_d$  being the Doppler shift due to moving target.

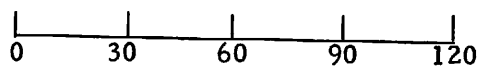
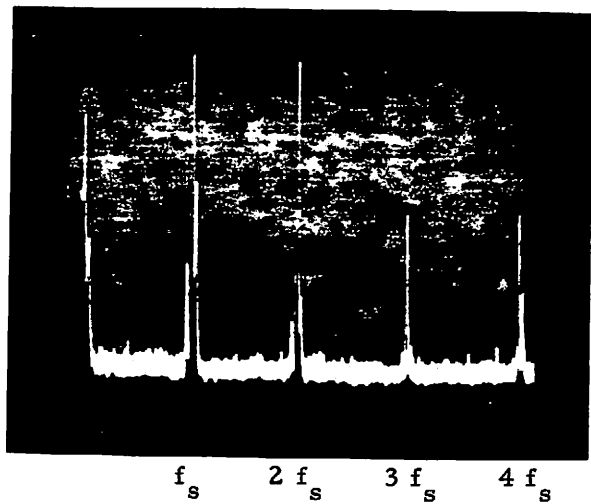
The spectrum that results at the output of the photodetector is summarized in Fig. 2-21 which also summarizes considerations regarding the signal level budget. The relative magnitudes indicated are generally borne out in the observed spectrum analyzer indications (see Fig. 2-22a). Satisfactory separation between the peaks at  $(f_s - f_d)$  (desired) and at  $(f_s + f_d)$  is achievable (see Fig. 2-22b).

The problem encountered with the device involved an insertion loss of 12 dB which precluded the observation of wind signals. This was attributed initially to transducer bonding deficiencies, a problem that seems to be solved. Satisfactory wind returns using the device have been observed. The remaining problem is a saturation of the receiver amplifier due to the strong feedthrough at  $f_s$ . A notch filter is currently being designed to alleviate the problem.

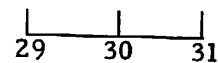
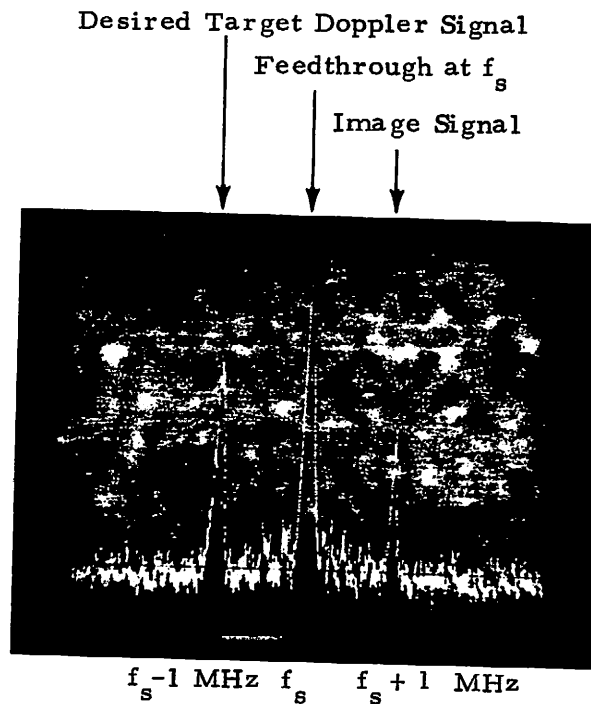


Need  $b \gg c$ ,  $be \gg ce$ ;  $bc \gg be$  expected – use filter to eliminate  $bc$ ; ( $be$  at  $f_s - f_d$  is the desired component).  
 $d \gg a$ ,  $d < b$  (hopefully), then  $(a + d)e < be$ .  
 $d \gg a$ ,  $d > c$ ,  $(a + d)(b + c) \approx db$  – large peak – must live with it (use notch filter to help reduce it).

Fig. 2-21 - Signal Budget for Various Bragg Cell Frequency Components



(a) Doppler Frequency (MHz) →



(b) Doppler Frequency (MHz) →

Fig. 2-22 - Frequency Translator Spectrum Analyzer Signatures (Spinning Disk as Target)

### 3. COMPUTER SOFTWARE SYSTEM DEVELOPMENT

Acquisition and processing of the LDV signature is accomplished by means of a compact data handling system developed specifically for the Lockheed-Huntsville LDV. The general elements of the LDV data acquisition and data processing system are shown in Fig. 3-1. The digitized LDV intensity versus frequency signal along with its coordinates in space are fed into the SEL 810 minicomputer. Reprocessing of the LDV signal is carried out on the minicomputer utilizing on-line computer programs written in SEL machine language. Information from the SEL 810 is stored on magnetic tape and is used as an input to the off-line processing algorithms. Off-line processing of the LDV signal is carried out on a Univac 1108 computer with programs written in FORTRAN language and using card inputs with information from the logs to supplement the data. The flow of data from the LDV is sketched in Fig. 3-2 showing both the on-line and off-line data processing routines. On-line manipulation of the data is carried out by the SEL Data Logger program. The off-line processing is carried out by the VAD and Vortex Track program. The final output consists of printouts, plots, and vortex track tapes. A description of the data logger and the VAD and vortex track program and their operational characteristics is given in the following sections.

#### 3.1 DESCRIPTION OF LDV SOFTWARE SYSTEM

Data acquisition in the LDV is carried out by the SEL Data Logger program. The Data Logger program preprocesses and records the LDV signal. A flow chart of the Data Logger program is given in Fig. 3-3. For each sweep of 10, 20 or 50 millisecond duration, the Data Logger saves the maximum amplitude LDV signal,  $I$ , and its corresponding frequency,  $V_{ms}$ , which is above the amplitude and frequency thresholds. The definition of

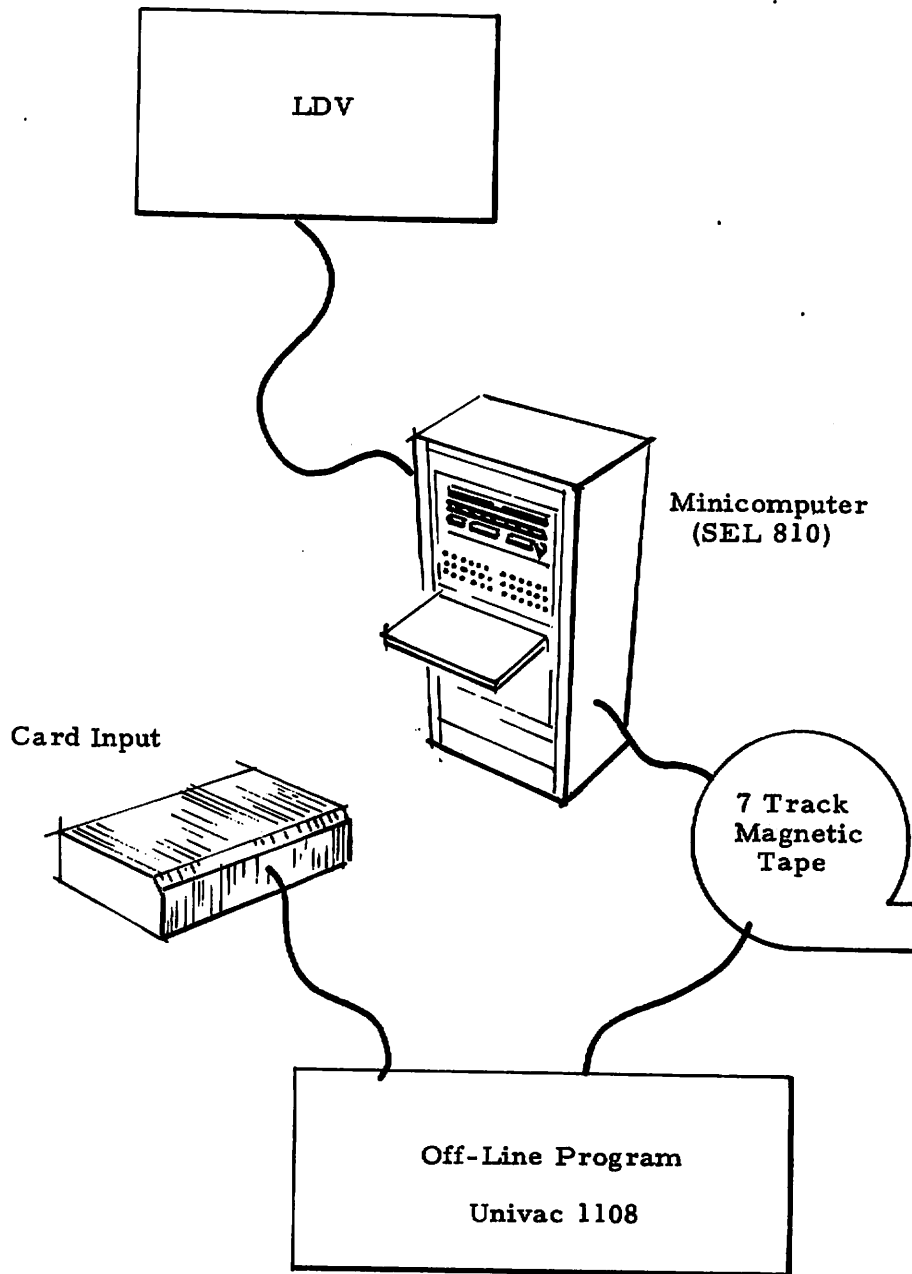


Fig. 3-1 - General Elements of LDV Data Acquisition and Processing System

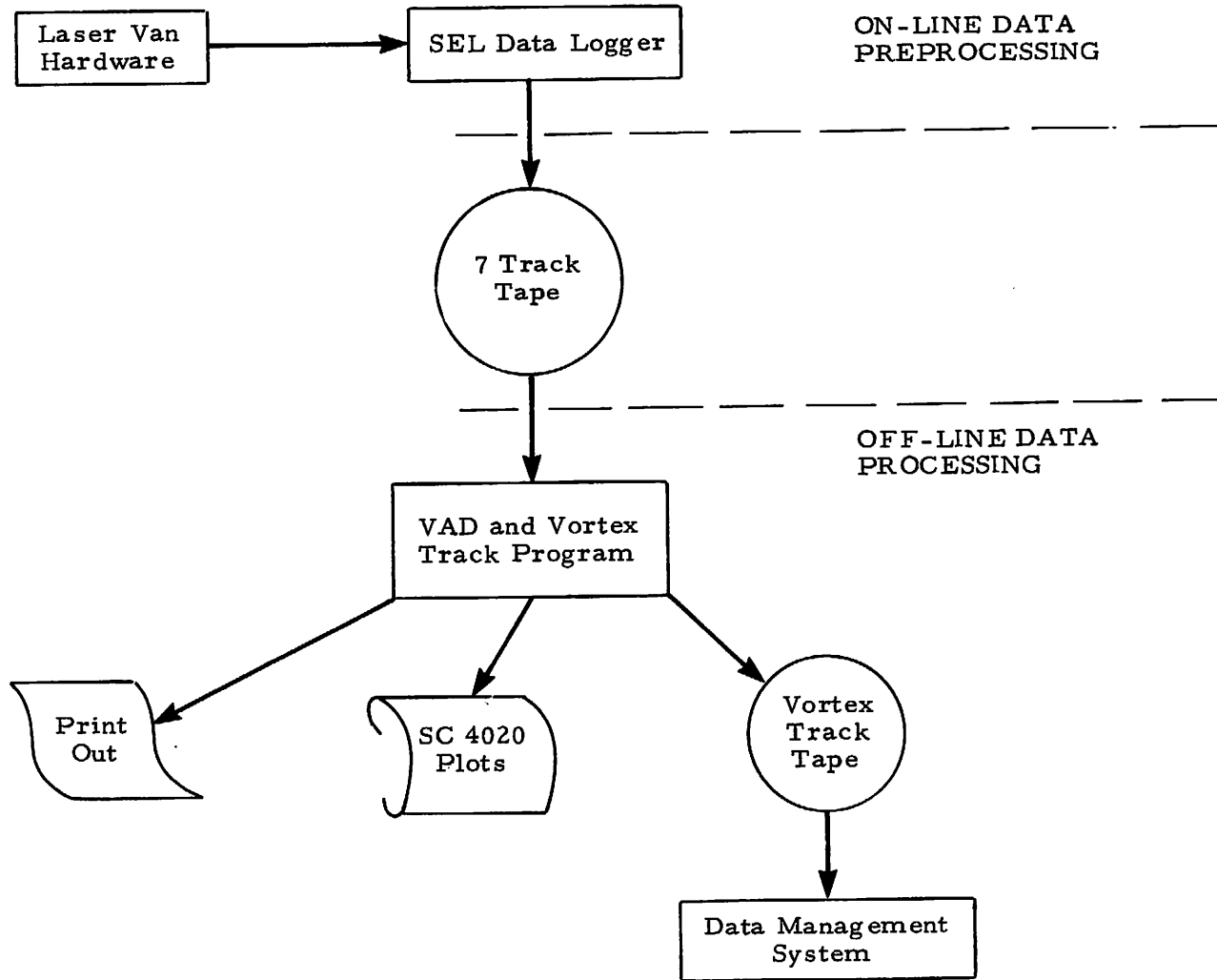


Fig. 3-2 - Data Flow from Lockheed LDV

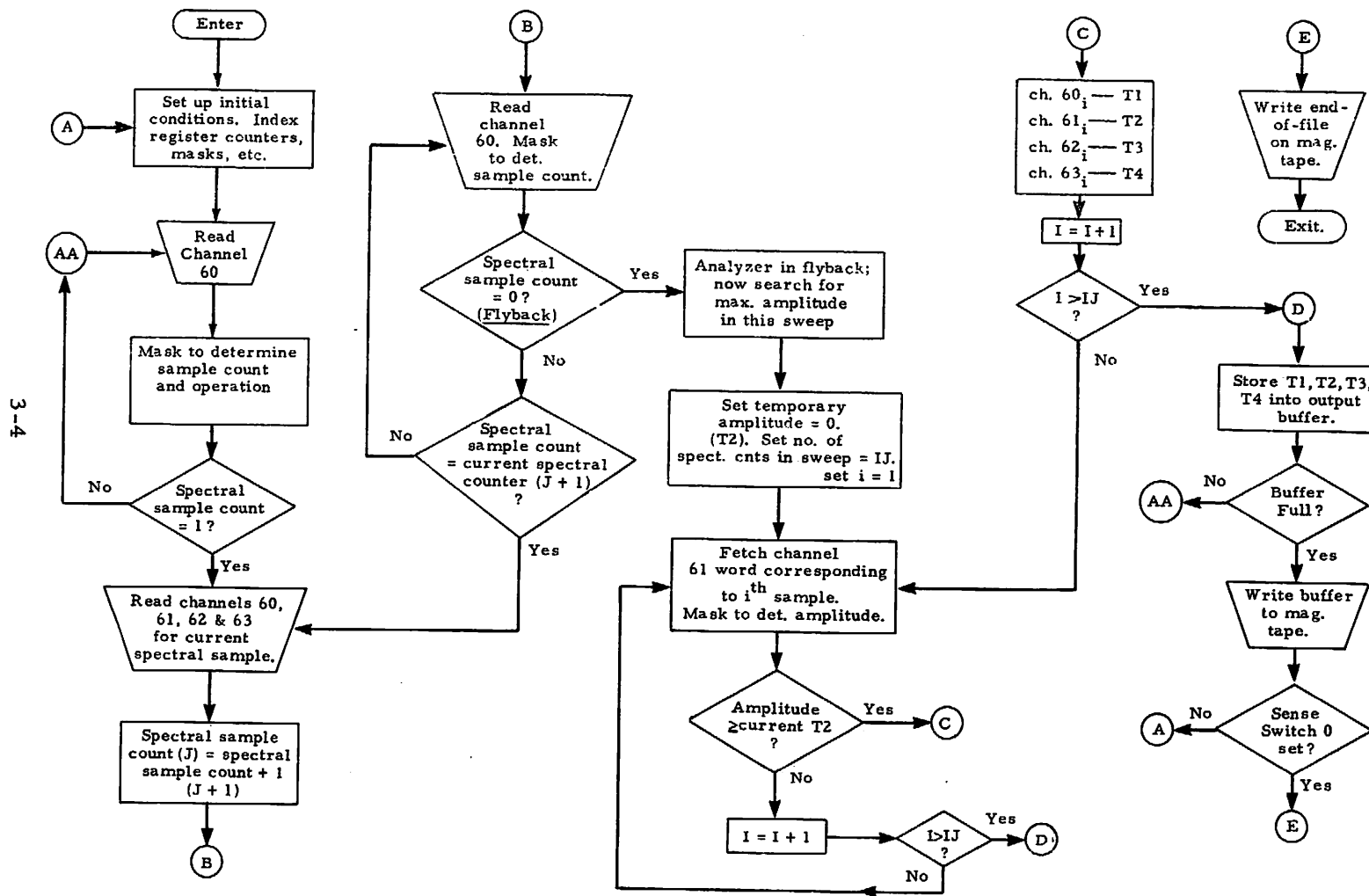


Fig. 3-3 - Data Logger Macro

I and  $V_{ms}$  and the shape of the characteristic LDV spectrum is shown in Fig. 3-4. It can be seen that  $V_{ms}$  is the average velocity associated with the flow phenomena.

The output from the Data Logger program consisting of  $V_{ms}$  as a function of time and space is shown in Table 3-1. Note that the type of information provided in channels 3 and 4 depends on the type of mode, VAD or vortex scan, selected. From the output of the Data Logger, the wake vortex velocity field or wind field can be reconstructed using off-line processing routines.

Final processing of the LDV measurements is carried out by the VAD and Vortex Track program is shown in Fig. 3-5. In this off-line program the array of  $V_{ms}$  values which is a function of time and space is processed to yield the three-dimensional wind field (VAD mode) or the aircraft wake vortex trajectories (vortex mode). The processing of the VAD measurements involves the computation of the  $u, v, w$  wind components from the characteristic sinusoidal VAD LDV signature discussed earlier in Section 2 and described in more detail in Appendix B. The program is geared to handle both the translated and nontranslated LDV signal. However, during the course of this research effort all of the data acquisition and data processing was done in the non-translate mode using an algorithm which processes the peak signals from the VAD spectrum. The final output is a plot (and printout) of the  $u, v,$  and  $w$  velocity components as a function of altitude and time. The peak algorithm was developed under the contract to process the JFK VAD measurements. Subsequently, the capability was added to the processing software to consider spectral processing for the winds using the inverted spectrum and also using a sine curve fit. For the sake of completeness, the details of the full VAD processing are given in Appendix B and are outlined in this report.

$N$  = bandwidth

$V_{pk}$  = velocity of highest channel above amplitude threshold

$V_{ms}$  = velocity of the channel having the peak signal

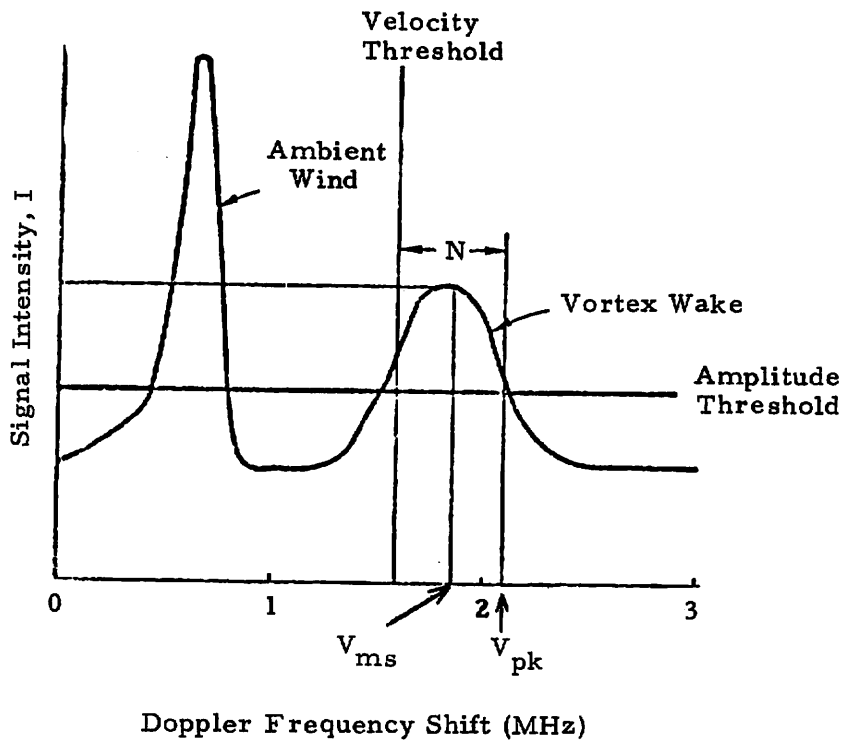


Fig. 3-4 - Typical Vortex Spectrum

Table 3-1

## OUTPUT FROM DATA LOGGER PROGRAM

CHANNEL 1 (OCTAL 60)

WORD FORMAT: NORMAL AND CONICAL SCAN

BIT POSITION	IDENTIFICATION	DESCRIPTION
15(LSB)	$N_s - 1 - 1$	7-BIT UNIPOLAR BINARY WORD (LSB = 1) REPRESENTING SPECTRAL SAMPLE COUNT ACROSS SPECTRUM SWEEP; 1ST SAMPLE, $N_s = 1$ LAST SAMPLE, $N_s = 100$
14	$N_s - 2 - 2$	
13	$N_s - 3 - 4$	
12	$N_s - 4 - 8$	
11	$N_s - 5 - 16$	
10	$N_s - 6 - 32$	
9	$N_s - 7 - 64$	
8	$\tau_s - 1$	SETTING OF SWEEP SPEED PER DIV.; (0, 1) = 1 MILLISEC
7	$\tau_s - 2$	(1, 0) = 2 MILLISEC, (1, 1) = 5 MILLISEC
6	X	NOT USED; ALWAYS OFF OR LOW STATE
5	MODE	MODE INDICATOR; = 1 IF NORMAL, = 0 IF CONICAL SCAN
4		ALL ON OR HI IF SWEEP IS THAT IMMEDIATELY AFTER $\theta = 0$ ; ALL OFF OR LOW, OTHERWISE
3		
2		
1	MAX	= 1 IF PEAK POWER LOCATION, = 0 IF MAX FREQ. LOCATION
0	X	NOT USED; ALWAYS OFF

Table 3-1 - (Continued)

CHANNEL 2 (OCTAL 61)

WORD FORMAT: NORMAL AND CONICAL SCAN

BIT POSITION	IDENTIFICATION	DESCRIPTION
15(LSB)	PS-1-1	12 BIT UNIPOLAR BINARY WORD REPRESENTING MAGNITUDE OF N <sup>TH</sup> POWER SPECTRAL SAMPLE (CHANGES SYNCHRONOUSLY WITH N); SCALE FACTOR FOR THIS PARAMETER MUST BE ENTERED VIA TELETYPE KEYBOARD PRIOR TO BEGINNING OF RUN
14	PS-2-2	
13	PS-3-4	
12	PS-4-8	
11	PS-5-16	
10	PS-6-32	
9	PS-7-64	
8	PS-8-128	
7	PS-9-256	
6	PS-10-512	
5	PS-11-1024	
4	PS-12-2048	
3	TNT	= 1 IF FREQ. TRANSLATOR USED, = 0 IF NOT TRANSLATED
2	PMF	= 1 IF FREQ. REPRESENTS POSITIVE $F_d$ , = 0 IF NEGATIVE $F_d$
1	DA	= 1 IF SPECT. DATA ACCEPTABLE, = 0 OTHERWISE
0	X	= 1 IF SPECT. DATA ACCEPTABLE, = 0 OTHERWISE

Table 3-1 - (Continued)

CHANNEL 3 (OCTAL 62)

WORD FORMAT: NORMAL SCAN

BIT POSITION	IDENTIFICATION	DESCRIPTION
15(LSB)	RTH-1	16 BIT, 4 DIGIT (RHU, RTN, RUN, RTH) BCD (8-4-2-1) REPRESENTATION OF SCANNER RANGE (in meters)  (NOT SYNCHRONOUS WITH SPECTRAL SAMPLING)
14	RTH-2	
13	RTH-4	
12	RTH-8	
11	RUN-1	
10	RUN-2	
9	RUN-4	
8	RUN-8	
7	RTN-1	
6	RTN-2	
5	RTN-4	
4	RTN-8	
3	RHU-1	
2	RHU-2	
1	RHU-4	
0	RHU-8	

Table 3-1 - (Continued)

CHANNEL 4 (OCTAL 63)

WORD FORMAT: NORMAL SCAN

BIT POSITION	IDENTIFICATION	DESCRIPTION
15(LSB) 14 13 12 11 10 9 8 7	$\theta_{el} -1-1$ $\theta_{el} -2-2$ $\theta_{el} -3-4$ $\theta_{el} -4-8$ $\theta_{el} -5-16$ $\theta_{el} -6-32$ $\theta_{el} -7-64$ $\theta_{el} -8-128$ $\theta_{el} -9-256$	9 BIT UNIPOLAR BINARY WORD REPRESENTING SCANNER ELEVATION ANGLE MSB = 51.2°
6 5 4 3 2 1 0	$N_{max} -1-1$ $N_{max} -2-2$ $N_{max} -3-4$ $N_{max} -4-8$ $N_{max} -5-16$ $N_{max} -6-32$ $N_{max} -7-64$	7 BIT UNIPOLAR BINARY WORD REPRESENTING THE SAMPLE COUNT (SPECTRUM) LOCATION OF EITHER (a) THE PEAK SPECTRUM POWER, OR (b) HIGHEST LOCATION AT WHICH THE SIGNAL IS ABOVE NOISE THRESHOLD (BIT 1 OF CHANNEL 1 IDENTIFIES WHICH)

3-10

Table 3-1 - (Continued)

CHANNEL 3 (OCTAL 62)

WORD FORMAT: CONICAL SCAN

BIT POSITION	IDENTIFICATION	DESCRIPTION
15(LSB)	H-1-1	10 BIT BINARY REPRESENTATION OF ALTITUDE IN USE BY CONICAL SCAN LSB = 1 METER
14	H-2-2	
13	H-3-4	
12	H-4-8	
11	H-5-16	
10	H-6-32	
9	H-7-64	
8	H-8-128	
7	H-9-256	
6	H-10-512	
5	$N_a - 1$	4 BIT BINARY WORD REPRESENTING NO. OF AZIMUTH ROTATIONS MADE AT EACH ALTITUDE SETTING IN THE PROGRAM (COMPLIMENT)
4	$N_a - 2$	
3	$N_a - 4$	
2	$N_a - 8$	
1	X	NOT USED; ALWAYS LOW STATE
0	X	

Table 3-1 - (Concluded)

CHANNEL 4 (OCTAL 63)

WORD FORMAT: CONICAL SCAN

BIT POSITION	IDENTIFICATION	DESCRIPTION
15(LSB) 14 13 12 11 10	$\alpha$ -1-1 $\alpha$ -2-2 $\alpha$ -3-4 $\alpha$ -4-8 $\alpha$ -5-16 $\alpha$ -6-32	6 BIT BINARY REPRESENTATION OF CONE ANGLE USED IN CONICAL SCAN LSB = 1°
9 8 7	X X X	NOT USED; ALWAYS OFF OR IN LOW STATE
6 5 4 3 2 1 0	$N_{max}$ -1-1 $N_{max}$ -2-2 $N_{max}$ -3-4 $N_{max}$ -4-8 $N_{max}$ -5-16 $N_{max}$ -6-32 $N_{max}$ -7-64	SAME AS NORMAL MODE. 7 BIT BINARY WORD REPRESENTING EITHER: (a) LOCATION OF PEAK SPECTRUM POWER, OR (b) HIGHEST LOCATION AT WHICH THE SIGNAL IS ABOVE NOISE THRESHOLD  (BIT 1 OF CHANNEL 1 IDENTIFIES WHICH)

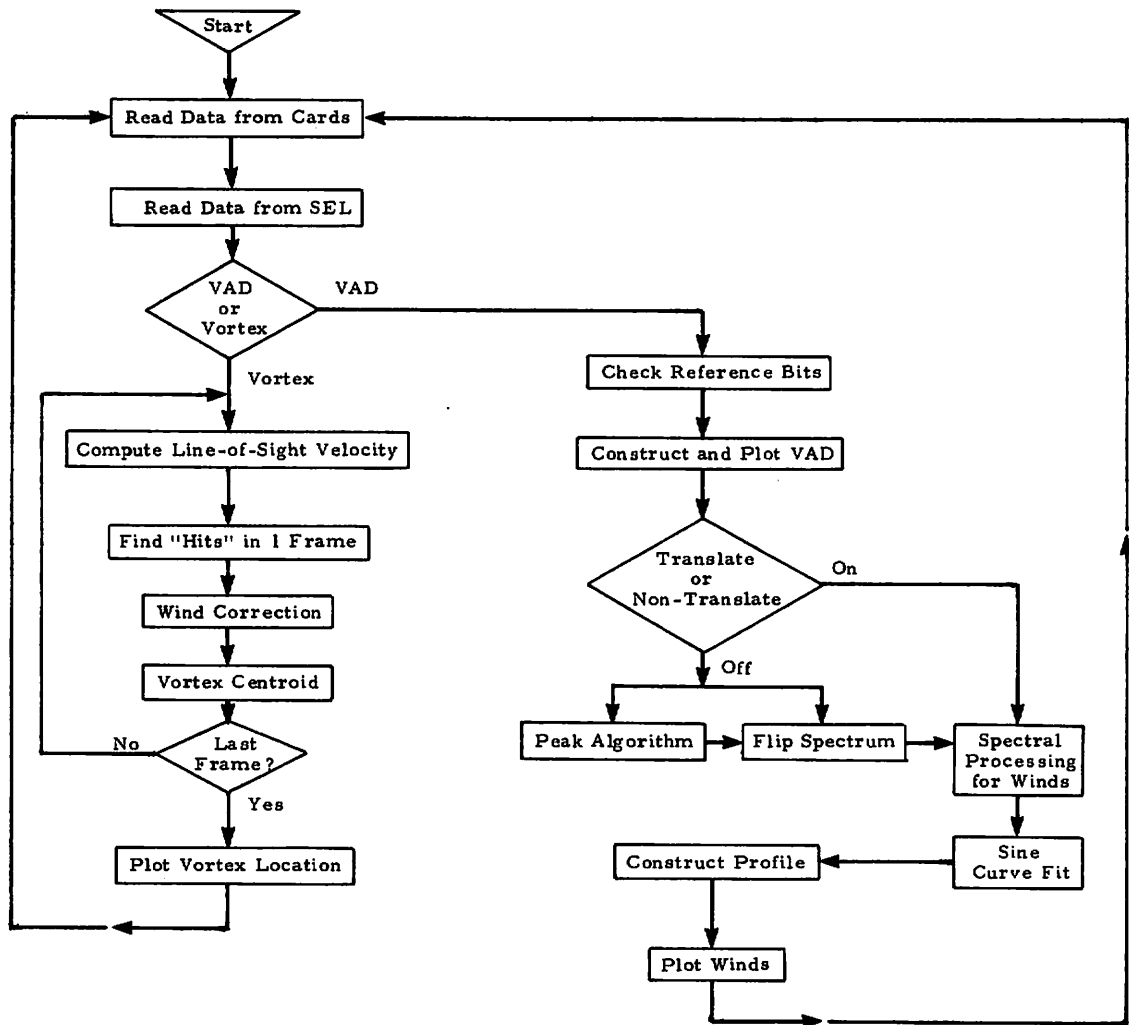


Fig. 3-5 - VAD and Vortex Track Program

When the LDV system is operating in the finger scan vortex track mode, the VAD and Vortex Track program flow-charted in Fig. 3-5 calculates the altitude and lateral location of the port and starboard aircraft vortices as a function of time from the array of  $V_{ms}$  values. The vortex location algorithm calculates and sorts the line-of-sight velocity as a function of elevation angle and time, selects the highest line-of-sight velocities or "hits" observed during each frame, computes the vortex location from the centroid of the high velocity "hits," and plots the track of the vortex centroid. In addition, scatter plots and printouts of the individual hits are generated. A detailed description of the vortex tracker subroutines is given in Appendix B and the basic sorting criteria involving  $V_{ms}$  is described in Ref. 4.

### 3.2 OPERATION OF LDV SOFTWARE SYSTEM

Operation of the Lockheed-Huntsville LDV involves initialization of the SEL Data Logger program and the recording of the LDV signature. After the measurements have been recorded at the proper threshold settings, the VAD and Vortex Track program is used to process the data into VAD or vortex track plots. It is useful to examine the data processing operations involved in determining the wake vortex trajectories and the three-dimensional wind velocity field from the LDV measurements in terms of on-line preprocessing and off-line processing.

#### 3.2.1 On-Line Data Processing

The conical scan VAD and finger scan vortex track measurements are preprocessed and recorded by the SEL computer. The input from the SEL computer consists of the basic  $V_{ms}$  signal as well as additional test parameters which are listed in Table 3-2. The data recorded by the SEL is in a different format depending on which mode (VAD or vortex track) the system is operating in. The SEL records the basic LDV signal with the Data Logger program.

Table 3-2  
INPUT FROM SEL COMPUTER

Note: Each vortex and VAD run are in a separate file. The following data are provided for each spectrum analyzer sweep.

1.	Spectral Sample Count Across Spectrum Analyzer Sweep, Corresponding to $V_{rms}$
2.	Amplitude at the Above Point
3.	Data Acceptable Flag
4.	Flag for Spectrum Analyzer Sweep Speed
5.	Flag for Translator
6.	Flag for Positive or Negative Frequency (used only when translator is used)
7.	Flag for $V_{peak}$ or $V_{rms}$
8.	Flag for Conical Scan or Normal Scan
<u>For Conical Scan</u>	
9.	Height above Van
10.	Flag for Azimuth Switch
11.	Cone Angle
<u>For Finger Scan</u>	
9.	Range
10.	Elevation Angle

A dump of a sample output tape from the Data Logger program operating in the vortex track mode is shown in Fig. 3-6, each row corresponding to information recorded for each spectrum analyzer sweep. The information is separated into 12 columns in the printout with interpretation of the various columns as follows:

<u>Column</u>	<u>Interpretation</u>
1 (PEAK/MAX)	An indication as to whether the peak Doppler frequency, $f_{\text{peak}}$ , or maximum Doppler frequency above amplitude or frequency thresholds ( $f_{\text{ms}}$ ) algorithm is utilized (see Fig. 3-3). (The $f_{\text{ms}}$ algorithm was used at all times during this investigation.)
2 ( $\theta = 0$ )	Inoperative.
3 (NOR/VAD)	An indication as to whether the system is operating in the normal (vortex track) (1) or VAD (0) mode.
4 (SWEEP SPEED)	Sweep speed of the spectrum analyzer trace (1 indicates 10 msec/cm).
5 (DIG TRCK)	The computer calculated estimate of $f_{\text{peak}}$ (percent of full scale).
6 (DATA ACCEPT)	An indication that there was/was not an output above frequency amplitude thresholds during a sweep.
7 (+/-)	An indication as to the sense of the Doppler shift (i.e., target moving toward or away from transceiver). Toward = +, Away = - .
8 (TRANS/NON-TRANS)	An indication as to whether or not a frequency translator was incorporated. (During this investigation it was not incorporated.) No = 0, Yes = 1.
9 (SPECTRUM INTENSITY)	Peak amplitude of the Doppler spectrum in region above a frequency threshold (arbitrary units).
10 (RANGE)	Range to focus of laser Doppler system (ft)
11 (LTRNC TRCK)	On-line frequency tracker estimate of $f_{\text{peak}}$ (should be identical to column 5 with time lag of one sample except when data are not acceptable).
12 (ELEVATION)	Instantaneous scan elevation angle in degrees.

	Word No. 1			Word No. 2			Word No. 3	Word No. 4		
	Peak/ Max. $\theta = 0$	Nor./Sweep VAD	Digital Speed Tracker	Data Accept.	+/-	Trans/ Non	Spectrum Intensity	Range	Electronic Tracker	Elev. Range
	0		1	5	0	1	0	676	176.6	35 17.0
	0		1	38	1	1	0	120	157.6	35 17.2
	0		1	41	1	1	0	118	132.5	36 17.4
	0		1	5	0	1	0	672	115.6	40 17.6
	0		1	5	0	1	0	672	091.3	40 17.8
	0		1	6	0	1	0	662	067.9	40 18.0
	0		1	1	0	1	0	768	064.0	40 18.4
	0		1	5	0	1	0	676	092.1	40 18.6
	0		1	5	0	1	0	670	112.2	40 18.8
	0		1	51	1	1	0	154	141.3	40 19.0
	0		1	42	1	1	0	116	157.6	49 19.2
	0		1	5	0	1	0	678	176.6	41 19.4
	0		1	2	1	1	0	1023	188.9	41 19.6
	0		1	78	1	1	0	128	175.0	41 20.0
	0		1	1	0	1	0	768	167.3	77 20.2
	0		1	49	1	1	0	148	138.2	77 20.4
	0		1	1	0	1	0	896	123.9	48 20.6
	0		1	6	0	1	0	656	099.3	48 20.8
	0		1	6	0	1	0	670	076.3	48 21.0
	0		1	1	1	1	0	1014	058.7	48 21.4
	0		1	2	0	1	0	960	084.0	48 21.6
	0		1	5	0	1	0	672	105.4	48 21.8
	0		1	93	1	1	0	118	141.3	48 22.2
	0		1	39	1	1	0	128	150.2	92 22.2
	0		1	51	1	1	0	128	175.0	38 22.6
	0		1	5	0	1	0	670	183.4	50 22.8
	0		1	5	0	1	0	672	188.9	50 23.0
	0		1	5	0	1	0	678	170.3	50 23.2
	0		1	56	1	1	0	112	145.6	50 23.4
	0		1	73	1	1	0	128	120.7	54 23.8
	0		1	1	0	1	0	1019	10*.*	72 23.8
	0		1	5	0	1	0	662	084.0	72 24.0
	0		1	6	0	1	0	674	060.9	72 24.4

3-17

Fig. 3-6 - Dump of Sample Output Tape from Data Logger with System Operating in Vortex Track Mode

A dump of a sample output tape from the Data Logger operating in the VAD mode is shown in Fig. 3-7, each row of data corresponding to information recorded for each spectrum analyzer sweep. The information, packed into four computer words on tape, is separated into 13 columns in the printout with interpretation of the various columns being as follows:

<u>Column</u>	<u>Interpretation</u>
1 (PEAK/MAX)	An indication as to whether the peak Doppler frequency ( $f_{\text{peak}}$ ) or maximum Doppler frequency above amplitude and frequency thresholds ( $f_{\text{ms}}$ ) algorithm is utilized (see Fig. 3-3). (The $f_{\text{ms}}$ algorithm was used at all times during this investigation.)
2 ( $\theta = 0$ )	A conical scan azimuth reference which is nonzero when the reference switch is activated.
3 (NOR/VAD)	An indication as to whether the system is operating in the normal (vortex track) (1) or VAD (0) modes.
4 (SWEEP SPEED)	Sweep speed of the spectrum analyzer trace in msec/cm.
5 (DIG TRCK)	The computer calculated estimate of $f_{\text{peak}}$ (percent of full scale).
6 (DATA ACCEPT)	An indication that there was/was not an output above frequency and amplitude during a sweep.
7 (+/-)	An indication as to the sense of the Doppler shift (i.e., target moving toward or away from transceiver). Toward = +, Away = - .
8 (TRANS/NON-TRANS)	An indication as to whether or not a frequency translator was incorporated. During this investigation it was not incorporated. No = 0, Yes = 1.
9 (SPECTRUM INTENSITY)	Peak amplitude of the Doppler spectrum in region above a frequency threshold.
10 (NBR ROTN)	Number of successive VAD scans for a particular altitude.
11 (ALT (M))	Altitude of VAD for particular sweep
12 (LTRNC TRCK)	On-line frequency tracker estimate of $f_{\text{peak}}$ (should be identical to column 5 with time lag of one sample except when data is not acceptable).
13 (CONE ANGLE)	Half-angle of VAD cone in degrees.

WORD NO 1					WORD NO 2					WORD NO 3		WORD NO 4	
PEAK/ MAX	6=0	NCR/ VAD	SWEEP SPEED	DIG TRCK	DATA ACCEPT	+/-	TRANS/ NNH	SPECTRUM INTNSITY	NRR R01N	ALT (M)	LTRNC TRCK	COBE ANGLE	
1	C	C	1C	38	1	1	C	232	1	323	37	3C	
1	C	C	1C	38	1	1	C	208	1	323	36	3C	
1	C	C	1C	39	1	1	C	190	1	323	37	3C	
1	C	C	1C	39	1	1	C	254	1	323	39	3C	
1	C	C	1C	38	1	1	C	192	1	323	38	3C	
1	C	C	1C	38	1	1	C	190	1	323	35	3C	
1	C	C	1C	40	1	1	C	144	1	323	36	3C	
1	C	C	1C	40	1	1	C	190	1	323	36	3C	
1	C	C	1C	41	1	1	C	142	1	323	38	3C	
1	C	C	1C	40	1	1	C	144	1	323	40	3C	
1	C	C	1C	42	1	1	C	144	1	323	39	3C	
1	C	C	1C	2	1	1	C	1023	1	323	41	3C	
1	C	C	1C	40	1	1	C	190	1	323	127	3C	
1	C	C	1C	39	1	1	C	140	1	323	38	3C	
1	C	C	1C	41	1	1	C	190	1	323	38	3C	
1	C	C	1C	41	1	1	C	200	1	323	40	3C	
1	C	C	1C	39	1	1	C	280	1	323	40	3C	
1	C	C	1C	40	1	1	C	254	1	323	37	3C	
1	C	C	1C	42	1	1	C	238	1	323	38	3C	
1	C	C	1C	41	1	1	C	126	1	323	41	3C	
1	C	C	1C	39	1	1	C	222	1	323	37	3C	
1	C	C	1C	39	1	1	C	150	1	323	38	3C	
1	C	C	1C	40	1	1	C	254	1	323	38	3C	
1	C	C	1C	41	1	1	C	192	1	323	38	3C	
1	C	C	1C	39	1	1	C	208	1	323	39	3C	
1	C	C	1C	40	1	1	C	190	1	323	37	3C	
1	C	C	1C	41	1	1	C	256	1	323	39	3C	
1	C	C	1C	38	1	1	C	160	1	323	0	3C	
1	C	C	1C	42	1	1	C	128	1	323	37	3C	
1	C	C	1C	38	1	1	C	178	1	323	41	3C	
1	C	C	1C	41	1	1	C	162	1	323	36	3C	
1	C	C	1C	39	1	1	C	144	1	323	39	3C	
1	C	C	1C	41	1	1	C	126	1	323	35	3C	
1	C	C	1C	41	1	1	C	144	1	323	40	3C	
1	C	C	1C	41	1	1	C	256	1	323	40	3C	
1	C	C	1C	42	1	1	C	126	1	323	127	3C	
1	C	C	1C	42	1	1	C	182	1	323	40	3C	
1	C	C	1C	38	1	1	C	176	1	323	40	3C	
1	C	C	1C	43	1	1	C	200	1	323	37	3C	
1	C	C	1C	40	1	1	C	146	1	323	42	3C	
1	C	C	1C	37	1	1	C	128	1	323	39	3C	
1	C	C	1C	43	1	1	C	128	1	323	36	3C	
1	C	C	1C	35	1	1	C	160	1	323	39	3C	
1	C	C	1C	41	1	1	C	128	1	323	33	3C	
1	C	C	1C	41	1	1	C	126	1	323	127	3C	
1	C	C	1C	37	1	1	C	128	1	323	40	3C	
1	C	C	1C	39	1	1	C	150	1	323	34	3C	
1	C	C	1C	40	1	1	C	126	1	323	38	3C	
1	C	C	1C	38	1	1	C	126	1	323	36	3C	
1	C	C	1C	35	1	1	C	128	1	323	36	3C	

Fig. 3-7 - Dump of Sample Output Tape from Data Logger with System Operating in VAD Mode

### 3.2.2 Off-Line Data Processing

Based on the array of line-of-sight velocities recorded by the SEL, the VAD and Vortex Track program computes the wind field and/or wake vortex trajectories. A summary of the basic off-line data processing technique is given in Table 3-3. The data processing steps described in Table 3-2 form the fundamental framework for the VAD and Vortex Track program. The VAD and Vortex Track program is a flexible and comprehensive software package which is the off-line data processing element of the LDV software system.

Table 3-3  
SUMMARY OF OFF-LINE DATA PROCESSING TECHNIQUE

DESCRIPTION OF VAD PROCESSING TECHNIQUE	
1.	Save line-of-sight velocities for one rotation of scanner.
2.	If two or more rotations at same altitude, average with first rotation.
3.	Assign azimuth angle to each point (assuming constant rotation rate). Plot velocity versus angle.
4.	Edit points.
5.	Apply moving average if wanted.
6.	Plot velocity versus angle.
PEAK ALGORITHM TECHNIQUE	
7.	Pick two peak velocity points, $V_{P_1}$ and $V_{P_2}$ , that occur a minimum of 90 deg apart.
8.	Compute horizontal velocity, $V_h$
	$V_h = \frac{V_{P_1} + V_{P_2}}{2 \sin \frac{(\text{cone angle})}{2}}$
9.	Compute horizontal angle with help of estimated wind direction.
10.	Compute vertical wind velocity, $V_v$
	$V_v = \frac{V_{P_1} - V_{P_2}}{2 \cos \frac{(\text{cone angle})}{2}}$
11.	Derectify VAD signal if no translator is present.

Table 3-3 (Continued)

FOURIER COEFFICIENT TECHNIQUE	
12.	<p>Compute Fourier coefficients (program computes first four coefficients).</p> $f(x) = \frac{a_0}{2} + \sum_{n=1}^{\infty} \left( a_n \cos \frac{n\pi x}{L} + b_n \sin \frac{n\pi x}{L} \right)$ $a_n = \frac{2}{L} \sum_{m=1}^L V_m \cos \left( \frac{n\pi 2m}{L} \right); \quad b_n = \frac{2}{L} \sum_{m=1}^L V_m \sin \left( \frac{n\pi 2m}{L} \right)$ <p style="text-align: right;">where L = number of points in VAD sweep.</p>
13.	<p>Compute correction to fundamental harmonic due to frequency cutoff (Ref. 6).</p> $\text{Correction} = \frac{1}{1 - Z + \frac{\sin \pi Z}{\pi}} \quad \text{where } Z = \text{No. Zeros/No. Points}$ <p>Correction Value = (Correction) * (Calculated Fundamental)</p>
14.	<p>Compute vertical wind correction. (Ref. 6)</p> $\text{Correction} = \frac{1}{1 - Z}$
15.	<p>Compute horizontal velocity.</p> $V_h = \frac{\sqrt{a_1^2 + b_1^2}}{\sin \left( \frac{\text{cone angle}}{2} \right)}$

Table 3-3 (Continued)

16.	<p>Compute horizontal angle.</p> $\text{Angle}_h = \text{Atan}(b_1/a_1)$
17.	<p>Compute vertical wind velocity</p> $V_v = \frac{-a_o}{2 \cos(\frac{\text{cone angle}}{2})}$
<b>SINE CURVE FIT TECHNIQUE</b>	
19.	<p>Find least squares curve fit for a sine wave to the data</p> $\text{Minimum} = \sum_{i=1}^L (Y_i - C - A \cos\theta_1 - B \sin\theta_1)^2$ <p>where</p> <p><math>Y_i</math> is line-of-sight velocity at point</p> <p><math>\theta_i</math> is azimuth at point</p> <p>C, A and B are coefficients to be solved for.</p>
20.	<p>Compute horizontal velocity.</p> $V_h = \frac{\sqrt{A^2 + B^2}}{\sin(\frac{\text{cone angle}}{2})}$
21.	<p>Compute horizontal angle.</p> $\text{Angle}_h = \text{Atan}(B/A)$
22.	<p>Compute vertical wind velocity</p> $V_v = \frac{-C}{\cos(\frac{\text{cone angle}}{2})}$

Table 3-3 (Continued)

AFTER THE VELOCITIES HAVE BEEN COMPUTED FOR ALL ALTITUDES:	
1.	<p>Compute a least squares fit for the horizontal speed to a power law curve</p> $V = V_r (H/H_r)^P$
2.	Compute a least squares fit for the horizontal directions to a polynomial.
3.	Plot horizontal speed versus height.
4.	Plot horizontal direction versus height.
5.	Plot crosswind velocity versus height.
DESCRIPTION OF VORTEX TRACKING ALGORITHM	
1.	Frequency, intensity, range, elevation angle, and time are saved for each point in a frame.
2.	The x, y position is computed with adjustment for the wind.
3.	The line-of-sight airspeed is computed. If the translator is used, the crosswind speed is removed.
4.	The points are sorted with respect to velocity and also sorted with respect to intensity.
5.	Depending on algorithm chosen, the highest velocity point or the highest intensity point is picked.
6.	A correlation circle is drawn around the above point. Only points within this circle will be considered for determining the vortex.
7.	The number of points within the correlation circle are counted and compared with NPSUF. If insufficient, throw out the chosen point and return to item 5.
8.	The fraction of points, with a velocity or intensity greater than APERCT of the maximum point, is computed. If this fraction is less than BPERCT, throw out the chosen point and return to item 5.
9.	The velocity at each point is multiplied by its intensity, to be used as a weighting factor in determining the centroid of the points. This centroid is declared to be the vortex location. The relative weighting of intensity versus velocity for computing the centroid may be modified by the use of NOISEF (the noise floor) and ADJI (intensity adjustment or fraction of noise floor added to total intensity).

Table 3-3 (Concluded)

10. An excluding circle, with a radius of EPERCT multiplied by the correlation radius, is drawn around the above vortex.
11. The highest velocity point or the highest intensity point outside the excluding circle is chosen. (In the case of the velocity algorithm, no point with less than half the velocity of the highest velocity of vortex 1 will be considered.)
12. A correlation circle is drawn around the above point and only points within this circle and outside of a correlation circle around vortex 1 will be considered for determining vortex 2.
13. The number of points within the area described above is counted and compared with NPSUF and CPERCT multiplied by (number of points used in determining vortex 1). If insufficient, throw out the chosen point and return to item 11.
14. The fraction of points with a velocity or intensity greater than APERCT of the maximum point is computed. If this fraction is less than BPERCT throw out the chosen point and return to item 11.
15. The velocity at each point is multiplied by its intensity to be used as a weighting factor in determining the centroid of the points. This is declared to be the vortex 2 location.
16. The vortex with a greater Y position is declared to be the starboard vortex with the other vortex being port. If only one vortex is found it is declared unknown.
17. A scatter plot showing the magnitude and location of each velocity point is made for each frame on the printer.
18. SC 4020 plots and printer plots are made of the following
  - a. Vortex height versus horizontal position
  - b. Vortex height versus time
  - c. Vortex horizontal position versus time.

From the type of information shown earlier in Figs. 3-6 and 3-7, the VAD and Vortex Track program is used to reconstruct the ambient wind field or the aircraft wake vortex trajectories. To describe the operation of the software, it is useful to present sample runs and to analyze the results. The list of input parameters to the off-line analysis program and their definitions are provided in Fig. 3-8. A sample VAD run from the VAD and Vortex Track program showing the resulting printout and plots is given in Figs. 3-9 and 3-10, respectively.

TITLE CARD 30 COLUMNS OF COMMENT

OFFLINE DATA REDUCTION PROGRAM FOR LMSC LASER VAN  
HANDLES VAD WIND SCAN AND NORMAL VORTEX ARC SCAN

PROGRAM INPUT

NAMelist (DATA)

IGROUP	NUMBER OF GROUPS OF DATA TO BE SKIPPED
ISFILE(2,10)	SKIP FILES ISFILE(1,K) THROUGH ISFILE(2,K)
NRUN	NUMBER OF FLYBYS AND VAD RUNS TO PROCESS (INCLUDES SKIPPED FILES BUT NOT SKIPPED GROUPS) (IF NRUN=0 PROGRAM IS TERMINATED)
ZLASER	HEIGHT ABOVE GROUND OF LASER M MIRROR FOR VORTEX SCA
ZLASCN	HEIGHT ABOVE GROUND OF CONICAL SCAN MIRROR
INTVEL	FLAG INTVEL = 1 VELOCITY ORIENTED VORTEX DETERMINATION INTVEL = 2 INTENSITY ORIENTED VORTEX DETERMINATION
NPSUF	SUFFICIENT NUMBER OF POINTS TO DETERMINE VORTEX POSITION
APERCT	FRACTION OF THE MAXIMUM PEAK Q
BPERCT	FRACTION OF POINTS OF WHICH THE Q IS AT LEAST APERCT FRACTION OF THE MAXIMUM Q (Q IS VELOCITY OR INTENSITY AS DETERMINED BY INTVEL)
CPERCT	FRACTION OF POINTS USED IN VORTEX ONE REQUIRED FOR VORTEX TWO
RPERCT	FRACTION OF AIRCRAFT WING SPAN USED FOR CORRELATION RADIUS REPRESENTED AIRCRAFT ARE B707, B727, B737, B747, DC8, DC9, DC10, L1011, CSA, CV880
EPERCT	FRACTION OF CORRELATION RADIUS FROM VORTEX ONE FOR EXCLUDING INITIAL POINT OF VORTEX TWO
NOISEF	NOISE FLOOR
ADJI	INTENSITY ADJUSTMENT (FRACTION OF NOISE FLOOR ADDED TO TOTAL INTENSITY)
ANGSW	AZMUTH OF MIRROR WHEN SWITCH IS ACTIVATED
WANGLE	ESTIMATE OF WIND ANGLE (DIRECTION WIND IS FROM) (USED WHEN NO TRANSLATOR IS USED)
WINDHP	WIND HEIGHT TO BE PLOTTED (IF ZERO WIND WILL BE PLOTTED TO HEIGHT OF CONICAL SCAN)
LFLIP	FLAG (APPLYS ONLY FOR NONTRANSLATE MODE) LFLIP = 0 USES PEAKS, DOES NOT FLIP DATA

Fig. 3-8 - Input Parameters to VAD and Vortex Track Program

LFLIP = 1 FLIP SIGN OF HALF VAD DATA  
 (FLIP POINTS MUST BE INPUTED FOR EACH VAD ALT)  
 LFLIP = 2 SAME AS LFLIP = 1 EXCEPT  
 FLIP POINTS ARE COMPUTED  
 WITH THE USE OF THE PEAK ALGORISM  
 LFLIP = 3 SAME AS LFLIP = 2 EXCEPT  
 ONLY ONE PEAK IS FOUND

ISINE FLAG (APPLYS ONLY FOR TRANSLAT OR WHEN LFLIP .GT. 0)  
 ISINE = 0 FOURIER COEFFICIENTS  
 ISINE = 1 SINE WAVE FIT  
 ISINE = 2 BOTH FOURIER AND SINE

EIDT EDIT CRITERIA IN FRACTION OF VELOCITY FOR POINT  
 MOVAVE NUMBER OF POINTS USED IN MOVING AVERAGE OF VELOCITY  
 ALONG AZIMUTH FOR VAD (MOVAVE MUST BE ODD)

YLIM(2) MINIMUM BOUNDARIES IN Y DIRECTION OF SCATTER PLOTS  
 ZLIM(2) MINIMUM BOUNDARIES IN Z DIRECTION OF SCATTER PLOTS  
 ISCALE FLAG  
 ISCALE = 0 ALL VORTEX PLOTS COMPUTE OWN SCALE  
 FACTORS  
 ISCALE = 1 INPUTED SCALE FACTORS FOR VORTEX PLOTS

YR RIGHT EXTREME OF Y POSITION  
 YL LEFT EXTREME OF Y POSITION  
 ZT TOP EXTREME OF HEIGHT  
 TMAX MAXIMUM TIME FOR PLOT  
 VMAX MAXIMUM VELOCITY FOR EACH FRAME  
 NSPLT NUMBER OF VAD SWEEPS FOR EACH VAD PLOT  
 JPROF FLAG  
 JPROF = 0 NO WIND PROFILE COMPUTED  
 JPROF = 1 WIND PROFILE COMPUTED

IMULT FLAG FOR VORTEX TRACK PLOTS  
 IMULT = 0 SINGLE FRAME FOR EACH FLYBY  
 IMULT = 1 MULTIPLE FRAMES FOR EACH FLYBY

IOP1 PRINTING OPTION  
 IOP1 = 0 NO PRINT  
 IOP1 = 1 MINIMUM PRINT  
 IOP1 = 2 MAXIMUM PRINT

IOP2 PRINTER PLOT OPTION  
 IOP2 = 0 NO PRINTER PLOT  
 IOP2 = 1 MINIMUM PRINTER PLOT  
 IOP2 = 2 MAXIMUM PRINTER PLOT

IOP3 SC4020 PLOT OPTION  
 IOP3 = 0 NO SC4020 PLOT  
 IOP3 = 1 MINIMUM SC4020 PLOT  
 IOP3 = 2 MAXIMUM SC4020 PLOT

IOP4 TRACK ON UNIT 21 OPTION  
 IOP4 = 0 NO TRACK WRITTEN  
 IOP4 = 1 TRACK WRITTEN

Fig. 3-8 (Continued)

PRESET VALUES FOR NAMELIST (DATA)

IGROUP	0
ISFILE(2,10)	20*1000
NRUN	1000
ZLASER	7.
ZLASCN	0.
INTVEL	1
NPSUF	3
APERCT	.75
BPERCT	.5
CPERCT	.5
RPERCT	.3141592654
EPERCT	1.5
NOISEF	0
AUJI	0.
ANGSN	0.
WANGLE	0.
WINDHP	800.
LFLIP	2
ISINE	2
EIDT	.2
MOVAVE	5
YLIM(2)	0.,0.
ZLIM(2)	0.,0.
ISCALE	1
YK	400.
YL	-400.
ZT	200.
TMAX	120.
VMAX	80.
NSPLT	12
JPROF	1
IMULT	0
IOP1	2
IOP2	2
IOP3	2
IOP4	1

Fig. 3-8 (Concluded)

```

                                BOULDER BOD42 RUN01
SDATA
IGROUP =                      +0
ISFILE =                      +1000,      +1000,      +1000,      +1000,
                                +1000,      +1000,      +1000,      +1000,
                                +1000,      +1000,      +1000,      +1000,
                                +1000,      +1000,      +1000,      +1000,
                                +1000,      +1000,      +1000,      +1000
NRUN =                          +1
ZLASER =      .70000000E+01
ZLASCN =      .00000000E+00
INTVEL =                          +1
NPSUF =                          +3
APERCT =      .75000000E+00
BPERCT =      .50000000E+00
CPERCT =      .50000000E+00
RPERCT =      .31415927E+00
EPERCT =      .15000000E+01
NOISEF =                          +0
ADJI =      .00000000E+00
ANGSW =      .74000000E+02
WANGLE =      .27000000E+03
WINDHP =      .00000000E+00
LFLIP =                          +3
ISINE =                          +2
EDIT =      .20000000E+00
MOVAVE =                          +5
YLIM =      .00000000E+00,      .00000000E+00
ZLIM =      .00000000E+00,      .00000000E+00
ISCALE =                          +1
YR =      .40000000E+03
YL =      -.40000000E+03
ZT =      .20000000E+03
TMAX =      .12000000E+03
VMAX =      .80000000E+02
NSPLT =                          +9
JPROF =                          +0
IMULT =                          +0
IOP1 =                          +1
IOP2 =                          +2
IOP3 =                          +2
IOP4 =                          +0

SEND
                                BOULDER BOD42 RUN01      000000 2/ 7/76      TABLE MT.      HD270.
DATE      2/ 7/76
LOCATION TABLE MT.
AIRCRAFT HEADING      .27000000+03 DEGREES
X POSITION OF LASER      .00000000 FEET
Y POSITION OF LASER      .00000000 FEET

```

Fig. 3-9 - Sample of VAD and Vortex Track Program Operating in VAD Mode

AIRCRAFT TYPE .4000000+06 HZ  
 STARTING FREQUENCY .2900000+07 HZ  
 CORRELATION RADIUS VAD .46181412+02 FEET  
 VELOCITY STEP PER DIVISION .34776906+00 FT/SEC PER DIVISION  
 INCREMENT CORRESPONDING TO ZERO VELOCITY -20  
 TIME IS 15:40: 0  
 CONICAL SCAN  
 TRANSLATOR NOT ON  
 TIME BETWEEN SPECTRUM ANALYZER SWEEPS IS .199400-01 SEC.  
 CONE ANGLE IS 30. DEGREES  
 RUN NO. 1 TIME IS 15:40: 5  
 ALTITUDE 92. FT WIND SPEED 59.4 FT/SEC WIND DIRECTION 310.3 DEGREES  
 WIND SPEED ONE 59.6 FT/SEC WIND DIRECTION ONE 336.1 DEGREES  
 WIND SPEED TWO 59.1 FT/SEC WIND DIRECTION TWO 104.5 DEGREES  
 AVERAGE WIND DIRECTION 310.3 DEGREES  
 AVERAGE WIND DIRECTION REVERSED 130.3 DEGREES  
 VERTICAL WIND VELOCITY IS 2.677-01  
 LOWER ANGLE = 123.72 UPPER ANGLE = 303.72  
 RUN NO. 1 TIME IS 15:40: 5  
 ALTITUDE 92. FT WIND SPEED 49.3 FT/SEC WIND DIRECTION 284.9 DEGREES  
 VERTICAL WIND SPEED -1.0 FT/SEC.  
 PHASE ANGLE OF 20 HARMONIC 8.3  
 PHASE ANGLE OF 30 HARMONIC 74.6 DEGREES  
 ZERO FACTOR = 1.5148  
 331 POINTS WITH 209 ZEROS  
 RAW VERTICAL DATA -1.0 FT/SEC.  
 ALTITUDE 92. FT WIND SPEED 52.6 FT/SEC WIND DIRECTION 284.7 DEGREES  
 VERTICAL WIND SPEED 1.1 FT/SEC.  
 STANDARD DEVIATION ABOUT THE SINE WAVE IS .316725+01  
 NUMBER OF POINTS = 331  
 NUMBER OF ZEROS = 209

Fig. 3-9 - (Concluded)

ALTITUDE IS 91.8 FEET  
TIME IS 15:40:46

RUN NO. 1  
VAD 2/17/76

ND270.

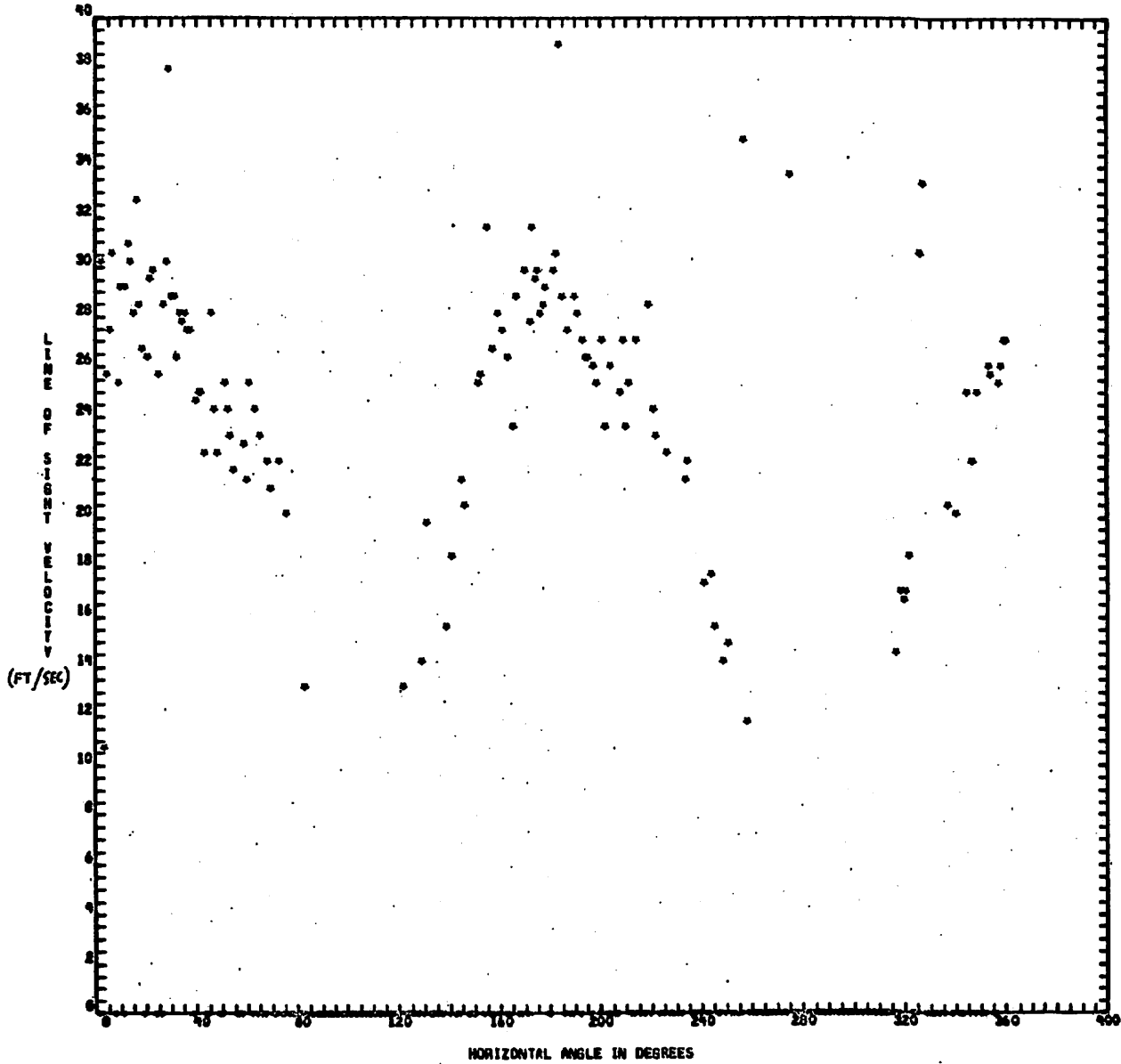


Fig. 3-10 - Sample of VAD and Vortex Track Program Operating in VAD Mode

a. Basic Signal

ALTITUDE IS 91.8 FEET  
TIME IS 15°40'46

RUN NO. 1  
VAD 2/17/76  
21 POINT AVERAGE

HD270.

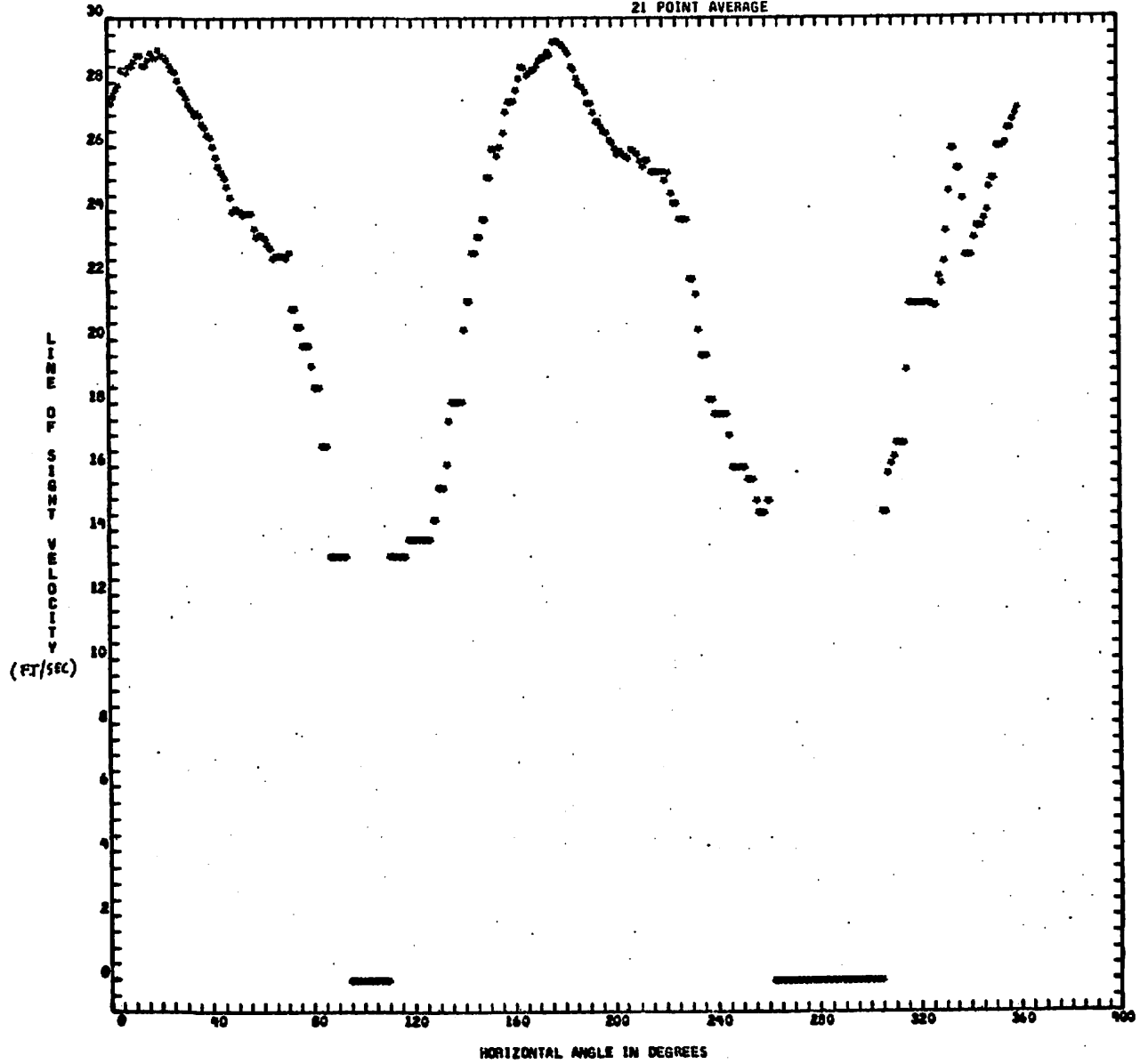


Fig. 3-10 (Continued)

b. Twenty-One Point Average of Basic Signal

ALTITUDE IS 91.8 FEET  
TIME IS 15°40'46

RUN NO. 1  
VAD 2/17/76  
COMPUTED FLIP

ND270.

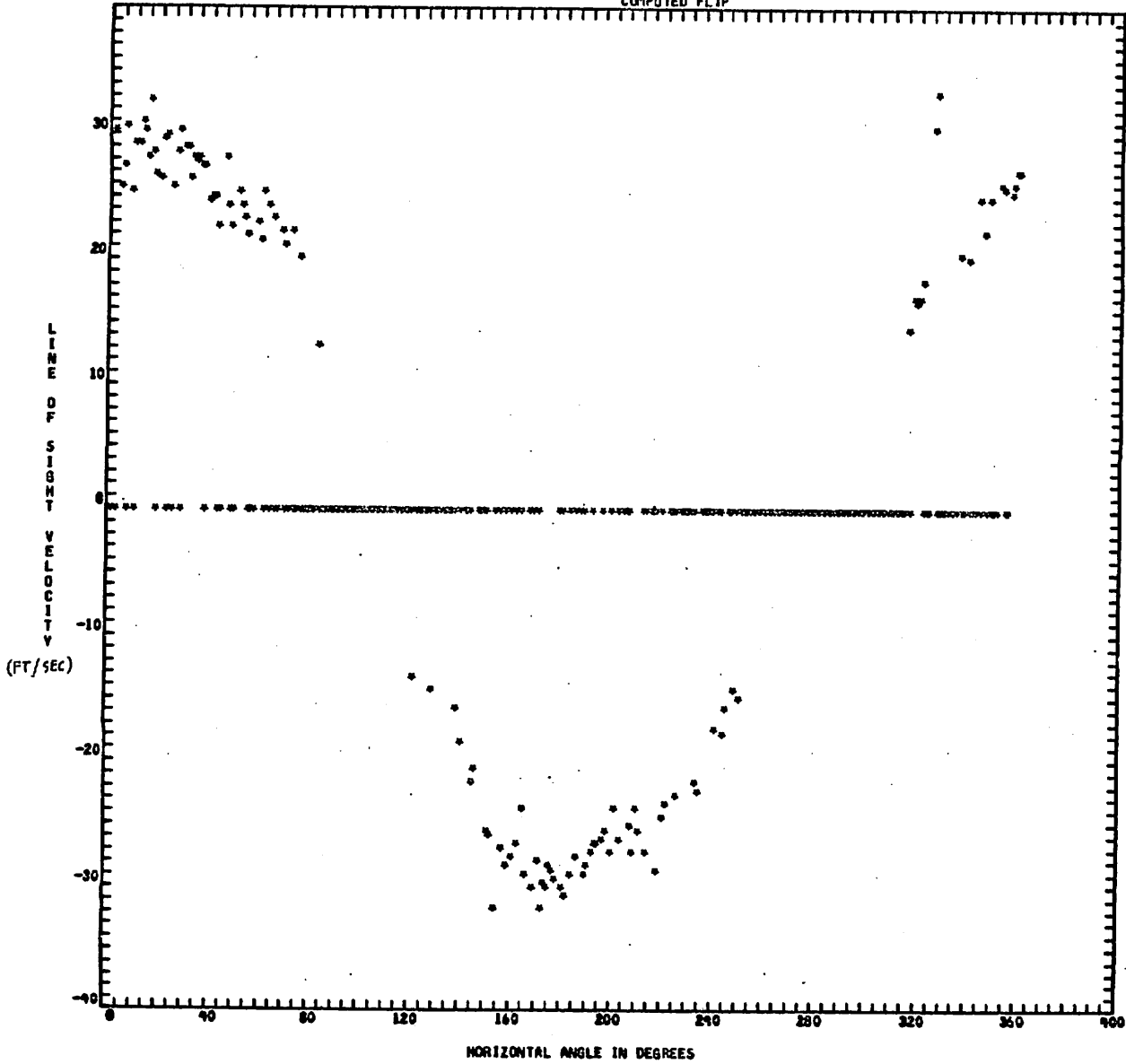


Fig. 3-10 (Concluded)

c. Computed Flip of Basic Signal

The plots corresponding to the sample printout shown in Fig. 3-9 are presented in Fig. 3-10. The plots include the observed line-of-sight velocity as a function of azimuth angle, the signature filtered by a 21-point moving average, and the signal derectified. For the latter two cases, the signal is edited. The edit criterion is applied to all of the points whose magnitude is above the specified velocity threshold. The edit program compares successive points in the velocity versus horizontal scan angle distribution and deletes those points where the magnitude of the velocity differs by more than a specified fraction (20% for the JFK tests) from the adjacent values. The purposes of this edit criteria is to filter out high frequency turbulence and to isolate the fundamental mean flow components.

The printout from the off-line program, illustrated in Fig. 3-9, consists of the list of input parameters, test parameters, and VAD measurements. The VAD measurements show the wind speed and wind direction as a function of altitude and time. In the sample output the wind speed and direction at each altitude (and time interval) is computed three different ways according to: (1) the peak algorithm, (2) the spectral analysis, and (3) the sine curve fit.

The winds are computed with the peak algorithm for the two highest line-of-sight velocities observed in the VAD (resulting in wind speed and direction 1 and 2, respectively, in Fig. 3-9). The average of wind speed and direction 1 and 2 is also given by the peak algorithm and is assumed to be more representative of the actual phenomenon. In the printout the reversed wind direction is also given since a 180 degree ambiguity is present in the non-translated LDV mode which is resolved by specifying the wind quadrant as an input. The lower and upper angle refer to the angle over which the VAD signal is flipped or derectified (see Fig. 3-10).

The spectral analysis program computes the wind speed and direction based on the first harmonic of the VAD signal as shown in the results in Fig. 2-10. In addition, the second and third harmonic contributions are computed and printed out. The number of points observed in the VAD scan (the number

of hits) and the number of zeros are tabulated and printed out. The zero factor is a scale correction factor to adjust the wind speed of the fundamental biased by the frequency threshold. As shown in Fig. 3-10, when the VAD signal is derectified gaps occur at the crossover regions due to the frequency (velocity) threshold. The zero factor is computed to adjust the wind speed based on the number of zeros in the VAD scan (i.e., in Fig. 3-9 the wind speed computed from the first harmonic was multiplied by 1.5148 to derive the actual wind speed). The RAW VERTICAL DATA refers to the measured vertical velocity without the frequency cutoff correction, and the VERTICAL WIND SPEED in refers to the corrected value as shown in Fig. 3-9.

The sine curve fit algorithm computes the wind speed and direction making a least square fit to the VAD signature with a sine wave and the results are shown in Fig. 3-9. The standard deviation of the line-of-sight velocity about the sine wave is also computed and given.

Data processing of the finger scan LDV measurements is carried out by the vortex track routines in the VAD and Vortex Track program. The operation of the vortex tracking software was summarized earlier in Table 3-1, and is illustrated by the sample output shown in Fig. 3-11. Typical printout from the program includes the number of saved hits (IP) and the observed signal frequency ( $IFREQ = V_{ms}$ ) which is tabulated as a function of time, range, and elevation angle for each scan. The line-of-sight velocity (SPEED in ft/sec) and lateral and vertical coordinates (YP and ZP in feet) are computed from the above parameters. The points are sorted according to their intensity, selected by the tracking algorithm for the determination of the centroid of the port, starboard, or undefined vortex (YC, ZC). For each elevation sweep a scatter plot of the intensity of all of the hits is given labeled A through O and a list of points used in determining the centroids is given. In the scatter plots the Z's represent the points about which the correlation circle are drawn and the P's and S's are the centroids of the correlation circles and denote the location of the port and starboard vortices, respectively. The line-of-sight velocity is processed and displayed in this manner for each

TIME OF SWEEP START = 4.510 SEC.  
 TIME OF SWEEP END = 5.513 SEC.  
 MID TIME OF SWEEP = 4.911 SEC.

IP	TIME	RANGE	ANGLE	YP	ZP	DELTA TIME	C WIND	SPEED	IFREQ	INTENSITY
1	2.510	391.1	33.6	74.3	223.4	1.501	.00	33.04	95	126
2	3.122	325.8	30.4	119.0	171.9	.889	.00	10.78	31	174
3	3.152	414.4	30.2	41.9	215.4	.859	.00	11.82	34	176
4	3.167	400.3	30.2	2.2	236.5	.844	.00	11.48	33	152
5	3.182	504.6	30.0	-37.0	259.3	.829	.00	12.17	35	152
6	3.217	625.7	29.8	-142.9	317.9	.784	.00	12.87	37	126
7	3.232	530.2	29.2	-62.2	265.7	.680	.00	12.87	37	126
8	3.247	481.3	29.2	-28.1	241.8	.665	.00	13.91	40	128
9	3.261	431.7	29.2	18.0	220.5	.650	.00	11.82	34	238
10	3.276	388.8	29.0	60.0	195.5	.635	.00	11.82	34	160
11	3.293	324.1	28.8	115.9	163.2	.575	.00	12.52	36	160
12	3.451	375.4	28.6	74.8	184.3	.560	.00	12.87	37	128
13	3.490	535.6	28.4	-43.9	247.0	.515	.00	14.26	41	178
14	3.501	458.8	27.8	-182.8	314.3	.411	.00	15.30	44	116
15	3.575	434.7	27.4	14.1	207.1	.336	.00	15.65	45	126
16	3.705	341.9	27.2	95.9	163.3	.300	.00	10.78	31	188
17	3.750	320.9	27.0	114.1	152.7	.261	.00	12.52	36	128
18	3.765	365.8	27.0	74.1	173.1	.247	.00	11.13	32	126
19	3.780	409.1	26.8	34.8	191.5	.232	.00	11.82	34	124
20	3.805	625.7	26.4	-160.4	285.2	.157	.00	14.26	41	112
21	3.864	711.3	26.2	-238.2	321.0	.127	.00	22.95	66	112
22	3.899	687.7	26.2	-217.0	310.0	.112	.00	23.65	68	118
23	3.929	625.7	26.0	-162.3	281.3	.082	.00	24.00	69	112
24	3.959	521.7	25.8	-69.7	234.0	.052	.00	31.65	91	128
25	3.974	477.7	25.8	-30.1	214.9	.037	.00	25.73	74	192
26	3.989	440.6	25.8	3.3	198.8	.022	.00	13.56	39	128
27	4.004	374.7	25.6	62.1	168.9	.007	.00	29.21	84	126
28	4.019	325.8	25.6	106.2	147.8	-.007	.00	27.47	79	128
29	4.034	289.7	25.6	138.7	132.2	-.022	.00	15.30	44	144
30	4.064	333.0	25.4	99.2	149.8	-.052	.00	28.86	83	188
31	4.079	365.8	25.2	69.0	162.8	-.067	.00	15.65	45	114
32	4.094	425.9	25.2	14.7	188.3	-.082	.00	29.91	86	128

3-35

AIRCRAFT TYPE DC9  
 STARTING FREQUENCY .00000000 HZ  
 END FREQUENCY .20000000+07 HZ  
 CORRELATION RADIUS .28085838+02 FEET  
 VELOCITY STEP PER DIVISION .34776900+00 FT/SEC PER DIVISION  
 INCREMENT CORRESPONDING TO ZERO VELOCITY 0  
 TIME IS 11:34: 0  
 JFK13 DC9 11/17/75 JFK RUNWAY 31R HD310  
 VORTEX SCAN  
 TRANSLATOR NOT ON  
 TIME BETWEEN SPECTRUM ANALYZER SWEEPS IS .149400-01 SEC.

Fig. 3-11 - Sample of VAD and Vortex Track Program Operating in Vortex Track Mode

33	4.109	466.9	25.3	-23.1	204.3	-0.097	.00	29.21	84	176
34	4.196	386.2	24.0	47.2	164.1	-0.187	.00	20.17	58	154
35	4.213	327.8	23.8	100.1	139.3	-0.202	.00	28.86	83	136
36	4.228	255.8	23.8	138.5	122.3	-0.217	.00	21.56	62	128
37	4.243	279.5	23.8	144.2	119.8	-0.232	.00	28.52	92	128
38	4.258	331.0	23.6	96.7	139.5	-0.247	.00	28.52	82	144
39	4.273	374.7	23.6	56.7	157.0	-0.261	.00	28.52	82	120
40	4.288	409.1	23.4	24.5	169.5	-0.276	.00	16.69	48	126
41	4.303	463.6	23.4	-25.5	191.1	-0.291	.00	29.21	84	124
42	4.318	508.9	23.4	-67.0	209.1	-0.306	.00	25.73	74	116
43	4.333	544.3	23.2	-100.3	221.4	-0.321	.00	24.34	70	126
44	4.347	437.7	22.4	-4.6	173.8	-0.486	.00	21.91	63	128
45	4.362	388.8	22.2	40.0	153.9	-0.500	.00	20.87	60	142
46	4.377	340.2	22.2	85.0	135.6	-0.515	.00	20.52	59	190
47	4.392	289.7	22.2	131.8	116.5	-0.530	.00	19.82	57	128
48	4.407	264.1	22.0	155.1	105.9	-0.545	.00	10.78	31	128
49	4.422	311.4	22.0	111.3	123.6	-0.560	.00	11.82	34	152
50	4.437	363.8	21.8	62.2	142.1	-0.575	.00	18.43	53	128
51	4.452	401.2	21.8	27.4	156.0	-0.590	.00	14.61	42	112
52	4.466	453.4	21.8	-21.0	175.4	-0.605	.00	18.78	54	152
53	4.781	530.2	20.8	-95.6	195.3	-0.769	.00	28.17	81	112
54	4.811	446.9	20.6	-18.3	164.2	-0.799	.00	15.65	45	128
55	4.826	396.0	20.6	29.3	146.3	-0.814	.00	13.91	40	128
56	4.841	347.8	20.6	74.5	129.4	-0.829	.00	15.65	45	142
57	4.855	352.2	20.4	116.8	112.3	-0.844	.00	11.13	32	124
58	4.870	264.1	20.4	152.5	99.1	-0.859	.00	11.48	33	126
59	4.885	311.4	20.2	107.8	114.5	-0.874	.00	13.91	40	192
60	4.900	357.6	20.2	64.4	130.5	-0.889	.00	14.26	41	224
61	4.915	396.0	20.2	28.4	143.7	-0.904	.00	10.78	31	256
62	5.109	504.6	19.0	-77.1	171.3	-1.098	.00	12.17	35	126
63	5.124	456.7	19.0	-31.8	155.7	-1.113	.00	12.52	36	128
64	5.139	403.9	19.0	18.1	138.5	-1.128	.00	12.17	35	174
65	5.154	353.7	18.8	65.2	121.0	-1.143	.00	12.17	35	214
66	5.169	303.8	19.8	112.8	104.9	-1.158	.00	11.13	32	190
67	5.184	264.1	19.6	149.7	91.2	-1.173	.00	11.13	32	316
68	5.199	305.1	18.6	110.8	104.3	-1.188	.00	10.78	31	256
69	5.214	353.7	18.6	64.8	119.8	-1.203	.00	11.82	34	174
70	5.229	393.7	18.4	26.4	131.3	-1.218	.00	10.78	31	222
71	5.244	443.9	18.4	-21.2	147.1	-1.233	.00	11.82	34	128
72	5.483	306.3	17.0	106.6	96.7	-1.472	.00	10.78	31	128
73	5.498	262.8	17.8	145.7	83.8	-1.487	.00	10.78	31	120
74	5.513	302.2	16.8	110.7	94.3	-1.501	.00	10.78	31	192

Fig. 3-11 (Continued)

ORDER	VELOCITY	INTENSITY
1	1	67
2	24	61
3	32	9
4	27	60
5	33	70
6	41	65
7	30	68
8	35	25
9	37	57
10	38	74
11	39	46
12	53	66
13	28	16
14	25	30
15	42	3
16	43	33
17	23	2
18	22	64
19	21	69
20	44	10
21	36	11
22	45	34
23	46	4
24	34	5
25	47	49
26	52	52
27	50	29
28	50	36
29	15	45
30	31	56
31	54	35
32	56	8
33	14	12
34	29	13
35	51	17
36	13	24
37	20	26
38	60	28
39	8	32
40	55	36
41	59	37
42	26	44

Fig. 3-11 (Continued)

43	6	47
44	7	48
45	12	54
46	11	54
47	17	55
48	63	63
49	5	71
50	62	72
51	64	1
52	65	6
53	3	7
54	9	15
55	14	18
56	19	27
57	49	45
58	69	43
59	71	58
60	4	62
61	58	19
62	18	41
63	57	57
64	66	39
65	67	73
66	2	22
67	16	14
68	48	42
69	61	31
70	68	23
71	70	21
72	72	23
73	73	51
74	74	53

11	113	N1	N2	R2
67	48	2	2	245.55
67	58	3	3	68.84
67	73	4	4	55.84
KV = 1		JJJ = 67	YC = 150.4	ZC = 92.8
CIRCULATION ESTIMATE A		3984.	FT**2/SEC.	
CIRCULATION ESTIMATE B		3568.	FT**2/SEC.	
AVERAGE VELOCITY IS		14.54	FT/SEC	
AVERAGE INTENSITY IS		163.6		
AVERAGE VELOCITY*INTENSITY IS		2257.		

Fig. 3-11 (Continued)

II	III	N1	N2	R2	
61	70	2	2	159.13	
61	64	3	3	132.15	
61	34	4	3	769.26	
61	45	5	3	239.67	
61	55	6	3	7.64	
61	40	7	3	677.45	
61	51	8	3	151.46	
KV = 2		JJK = 61		YC = 30.8	ZC = 149.2
CIRCULATION ESTIMATE A		3136		FT**2/SEC.	
CIRCULATION ESTIMATE B		3246		FT**2/SEC.	
AVERAGE VELOCITY IS		16.53		FT/SEC.	
AVERAGE INTENSITY IS		159.3			
AVERAGE VELOCITY*INTENSITY IS		2476			

3-39

Fig. 3-11 (Continued)



TIME OF SWEEP START = 72.564 SEC.  
 TIME OF SWEEP END = 76.941 SEC.  
 MID TIME OF SWEEP = 74.752 SEC.

IP	TIME	RANGE	ANGLE	YP	ZP	DELTA TIME	C WIND	SPEED	IFREQ	INTENSITY
1	72.564	619.8	5.8	-216.6	69.6	2.189	.00	11.13	32	148
2	72.593	525.9	6.0	-123.0	62.0	2.159	.00	11.48	33	126
3	72.623	428.5	6.2	-26.0	53.3	2.129	.00	10.78	31	126
4	72.698	329.4	6.6	72.8	44.9	2.054	.00	10.78	31	144
5	72.713	371.7	6.6	27.8	50.1	2.039	.00	11.13	32	112
6	72.742	463.6	6.8	-60.3	61.9	2.009	.00	11.82	34	136
7	72.758	508.9	6.8	-105.3	67.3	1.994	.00	11.48	33	224
8	72.773	548.9	7.0	-144.8	73.9	1.980	.00	11.13	32	188
9	72.789	595.1	7.0	-191.7	79.6	1.965	.00	10.78	31	192
10	72.803	632.2	7.0	-227.5	84.0	1.950	.00	11.13	32	128
11	72.818	666.1	7.2	-274.8	92.2	1.935	.00	11.13	32	160
12	72.842	579.4	7.6	-174.3	83.6	1.860	.00	11.13	32	112
13	72.907	534.8	7.6	-130.1	77.7	1.845	.00	10.78	31	112
14	72.922	481.3	7.8	-76.8	72.3	1.830	.00	11.13	32	128
15	72.937	431.4	7.8	-27.4	65.6	1.815	.00	11.48	33	128
16	72.952	381.6	7.8	22.0	58.8	1.800	.00	10.78	31	112
17	73.012	325.8	8.2	77.5	53.5	1.741	.00	10.78	31	112
18	73.027	372.4	8.2	31.4	60.1	1.726	.00	11.48	33	192
19	73.042	417.3	8.4	-12.8	68.0	1.711	.00	11.48	33	126
20	73.072	504.6	8.6	-98.9	82.5	1.681	.00	10.78	31	128
21	73.116	632.2	8.8	-224.8	103.7	1.636	.00	10.78	31	162
22	73.131	600.1	8.8	-272.1	111.0	1.621	.00	11.13	32	150
23	73.146	711.3	9.0	-302.5	118.3	1.606	.00	11.13	32	124
24	73.176	658.8	9.2	-250.3	112.3	1.576	.00	11.48	33	126
25	73.191	625.7	9.2	-217.6	107.0	1.561	.00	10.78	31	164
26	73.206	579.4	9.2	-171.9	99.6	1.546	.00	10.78	31	126
27	73.266	303.9	9.6	21.5	71.0	1.487	.00	12.52	36	126
28	73.281	335.3	9.6	68.4	63.1	1.472	.00	10.78	31	170
29	73.326	325.8	10.0	79.2	63.6	1.427	.00	11.48	33	128
30	73.340	370.4	10.0	35.2	71.3	1.412	.00	13.22	38	126
31	73.355	411.7	10.0	-5.5	78.5	1.397	.00	10.78	31	144
32	73.365	505.6	10.2	-96.6	96.4	1.367	.00	11.82	34	160
33	73.415	598.2	10.4	-160.5	113.5	1.337	.00	11.13	32	190
34	73.430	625.7	10.4	-215.4	119.9	1.322	.00	11.13	32	128
35	73.475	695.2	10.8	-282.9	137.3	1.277	.00	10.78	31	288
36	73.505	625.7	10.8	-214.6	124.2	1.247	.00	11.13	32	152
37	73.520	575.4	11.0	-168.8	117.6	1.233	.00	10.78	31	158
38	73.550	484.8	11.2	-79.5	102.0	1.203	.00	11.13	32	122
39	75.835	672.9	24.2	-213.8	282.8	-1.083	.00	31.99	92	112
40	76.941	305.1	30.0	135.8	159.6	-2.189	.00	25.73	74	126

3-41

Fig. 3-11 (Continued)

ORDER	VFLOCITY	INTENSITY
1	39	35
2	40	7
3	30	9
4	27	18
5	6	33
6	32	0
7	2	25
8	7	21
9	15	11
10	18	32
11	19	22
12	24	37
13	29	36
14	1	1
15	5	4
16	8	31
17	10	6
18	11	2
19	12	10
20	14	14
21	22	15
22	23	20
23	33	27
24	34	34
25	36	3
26	38	19
27	3	24
28	4	26
29	9	27
30	13	30
31	16	40
32	17	23
33	20	38
34	21	28
35	25	5
36	26	12
37	28	13
38	31	16
39	35	17
40	37	39

Fig. 3-11 (Continued)

Fig. 3-11 (Continued)

11 113 NI N2 R2  
 35 2 746.45  
 11 113 NI N2 R2  
 7 2 343.23  
 7 3 271.59  
 7 4 724.83  
 7 7 JJJ = YC = -109.4 ZC = 69.5  
 CIRCULATION ESTIMATE A 973.1 FT\*\*2/SEC.  
 CIRCULATION ESTIMATE B 1308. FT\*\*2/SEC.  
 AVERAGE VELOCITY IS 11.13 FT/SEC  
 AVERAGE INTENSITY IS 148.0  
 AVERAGE VELOCITY\*INTENSITY IS 1657.

11 113 NI N2 R2  
 9 1 720.05  
 9 12 317.85

11 113 NI N2 R2  
 18 27 217.20  
 18 30 140.00  
 18 5 114.07  
 18 16 91.31  
 18 JJJ = YC = 29.3 ZC = 61.9  
 CIRCULATION ESTIMATE A 853.8 FT\*\*2/SEC.  
 CIRCULATION ESTIMATE B 914.9 FT\*\*2/SEC.  
 AVERAGE VELOCITY IS 11.82 FT/SEC  
 AVERAGE INTENSITY IS 133.6  
 AVERAGE VELOCITY\*INTENSITY IS 1580.

Fig. 3-11 (Continued)



	TIME OF SWEEP START #	78.540 SEC.																		
	TIME OF SWEEP END #	79.331 SEC.																		
	MID TIME OF SWEEP #	78.935 SEC.																		
IP	TIME	RANGE	ANGLE	YR	ZP	DELTA TIME	C WIND	SPEED	IFREQ	INTENSITY										
1	78.540	255.1	31.2	173.2	144.3	.396	.00	31.30	90	112										
2	78.331	711.3	27.0	-233.8	329.9	-.374	.00	25.33	73	125										

Fig. 3-11 (Continued)

JFK13 DC9 11/17/75 JFK RUNWAY 31R HD310. RUN NO. 9  
 TIME IS 11:34: 0

11	12 1975	321	11	34	0	JFK13	DC9	11/17/75	JFK RUNWAY 31R	HD310.
	00.000		150.405			92.7861		6.22251	158.243	113.117
	11.6607		148.584			85.3546		17.4649	150.953	107.046
	22.4175		129.460			48.2157		28.2291	156.919	110.292
	38.6274		148.087			145.892		44.6407	111.161	99.6225
	49.5933		149.406			94.3061		59.7525	150.913	93.3778
	70.7409		29.3316			61.9182		.000000	30.8184	149.193
	6.22251		117.536			121.869		11.6607	106.205	91.8576
	17.5049		67.6995			130.856		28.2291	73.2864	163.482
	34.6394		108.370			100.183		38.6274	77.3429	167.869
	44.8407		63.4752			114.380		49.5933	101.923	103.596
	55.2033		113.197			58.1507		59.7525	66.7935	119.959
	70.7409		-109.407			69.5113				

STARBOARD VORTEX

TIME	Z	Y
4.01139	92.7861	150.405
10.2339	113.117	158.243
15.6721	85.3546	148.584
21.4762	107.046	150.953
32.2405	110.292	156.919
42.6388	145.892	148.087
48.6521	99.6225	111.161
53.6047	94.3061	149.406
63.7639	93.3778	150.913
74.7523	61.9182	29.3316

3-46

Fig.3-11 (Continued)









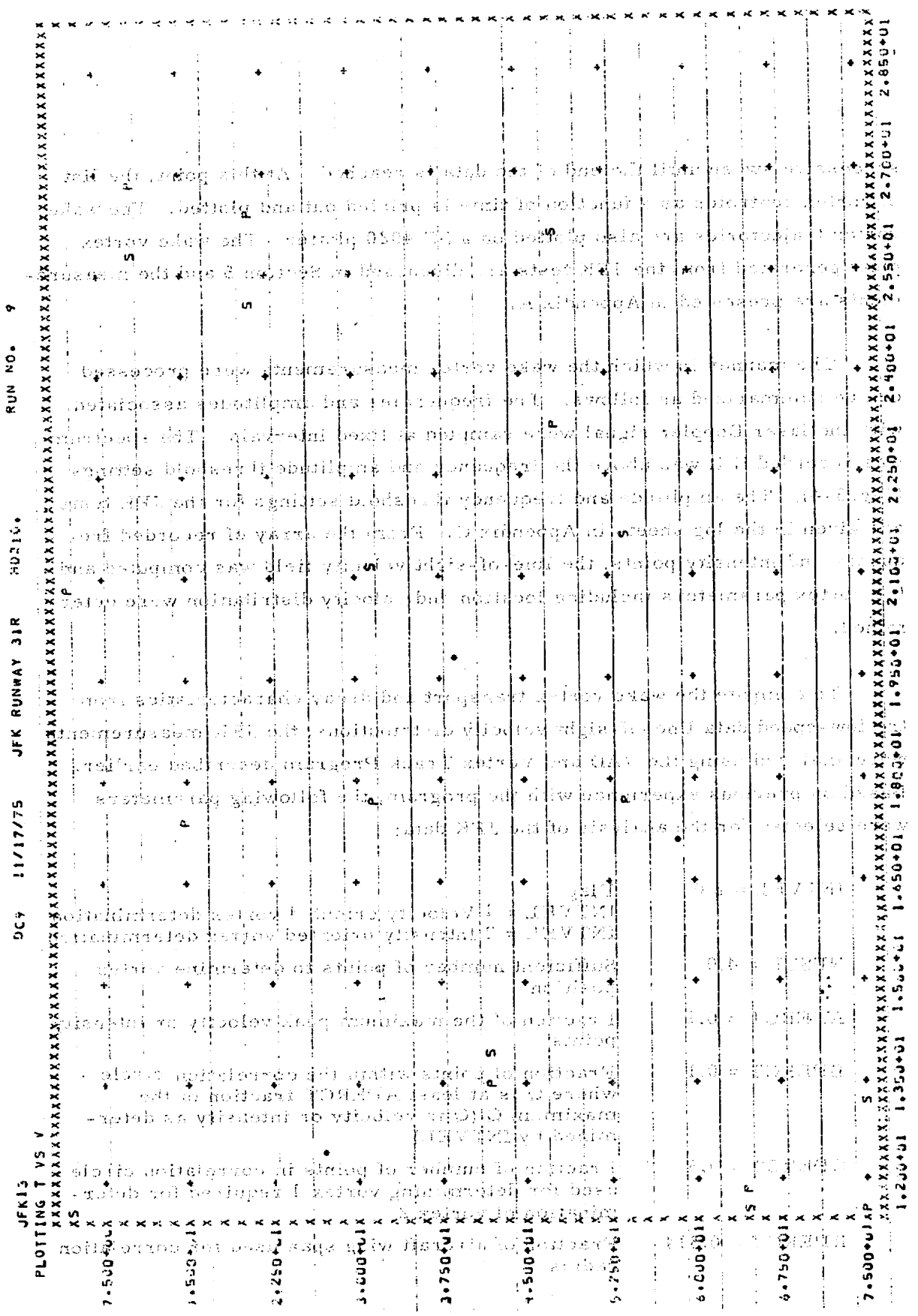


Fig. 3-11 (Concluded)

successive sweep until the end of the data is reached. At this point, the list of vortex centroids as a function of time is printed out and plotted. The wake vortex trajectories are also plotted on a SC 4020 plotter. The wake vortex plots generated from the JFK tests are discussed in Section 5 and the measurements are presented in Appendix A.

The manner in which the wake vortex measurements were processed can be summarized as follows. The frequencies and amplitudes associated with the laser Doppler signal were sampled at fixed intervals. The spectrum was recorded if it was above the frequency and amplitude threshold settings (Fig. 3-4). The amplitude and frequency threshold settings for the JFK tests are given in the log sheets in Appendix C. From the array of recorded frequency and intensity points, the line-of-sight velocity field was computed and the vortex parameters including location and velocity distribution were determined.

To compute the wake vortex transport and decay characteristics from the low-speed data line-of-sight velocity distributions, the JFK measurements were analyzed using the VAD and Vortex Track Program described earlier. Based on previous experience with the program, the following parameters were selected for the analysis of the JFK data:

INTVEL = 2.0	Flag INTVEL = 1 Velocity oriented vortex determination INTVEL = 2 Intensity oriented vortex determination
NPSUF = 4.0	Sufficient number of points to determine vortex position
APERCT = 0.1	Fraction of the maximum peak velocity or intensity points
BPERCT = 0.1	Fraction of points within the correlation circle where Q is at least APERCT fraction of the maximum Q (Q is velocity or intensity as determined by INTVEL)
CPERCT = 0.5	Fraction of number of points in correlation circle used for determining vortex 1 required for determination of vortex 2
RPERCT = 0.314	Fraction of aircraft wing span used for correlation radius

EPERCT = 1.5

Fraction of correlation radius from vortex 1 for  
excluding initial point of vortex 2

NOISEF = 0.0

Noise floor

ADJI = 0.0

Intensity adjustment (Fraction of noise floor  
added to total intensity)

Fraction of correlation radius from vortex 1 for  
excluding initial point of vortex 2  
Noise floor  
Intensity adjustment (Fraction of noise floor  
added to total intensity)

EPRECT = 1.5

NOISEF = 0.0

ADJ1 = 0.0

#### 4. FIELD TESTS OF LDV SYSTEM

To evaluate the capability of the Lockheed-Huntsville LDV to measure the wind, wind shear, and wake vortex phenomena in terminal areas; the system was deployed at the Huntsville Jetplex, Huntsville, Alabama, and at Kennedy International Airport, Jamaica, New York.

The LDV was deployed and tested at the Huntsville Jetplex in October 1975 to check out the basic operation of the system. The location of the LDV at the Jetplex was as shown in Fig. 4-1. On 15 October 1975 wake vortex measurements were made behind an L-1011 aircraft and the following day, measurements were made behind a FAA CV-880 aircraft conducting touch and go landings and approaches. The wake measurements at the Huntsville Jetplex were intended primarily to test the operation of the system. The ability of the LDV system to identify and track wake vortices was demonstrated at the Jetplex tests. A sample wake vortex trajectory measured by the LDV at the Jetplex is shown in Fig. 4-2. The vortex track in Fig. 4-2 shows the lateral motion of the L-1011 wake vortices. Similar wake measurements were obtained at Huntsville for the CV-880 aircraft. The ability of the LDV system to monitor wake vortices at an airport for extended periods of time under various weather conditions was demonstrated during the JFK tests.

Wake vortex and wind profile measurements were taken with the Lockheed-Huntsville LDV at Kennedy International Airport (JFK) in two test sequences from 30 October 1975 to 19 November 1975 and from 13 January to 31 January 1976. (Between these tests, the LDV was transported to Rosamond, California, to participate in the DOT/NASA B-747 wake vortex decay studies.) In the 14 days of operation at JFK in November 1975, 13 tapes of vortex, VAD, and range scan data were generated. During the second test series in January 1975 another 13 tapes of VAD and wake vortex

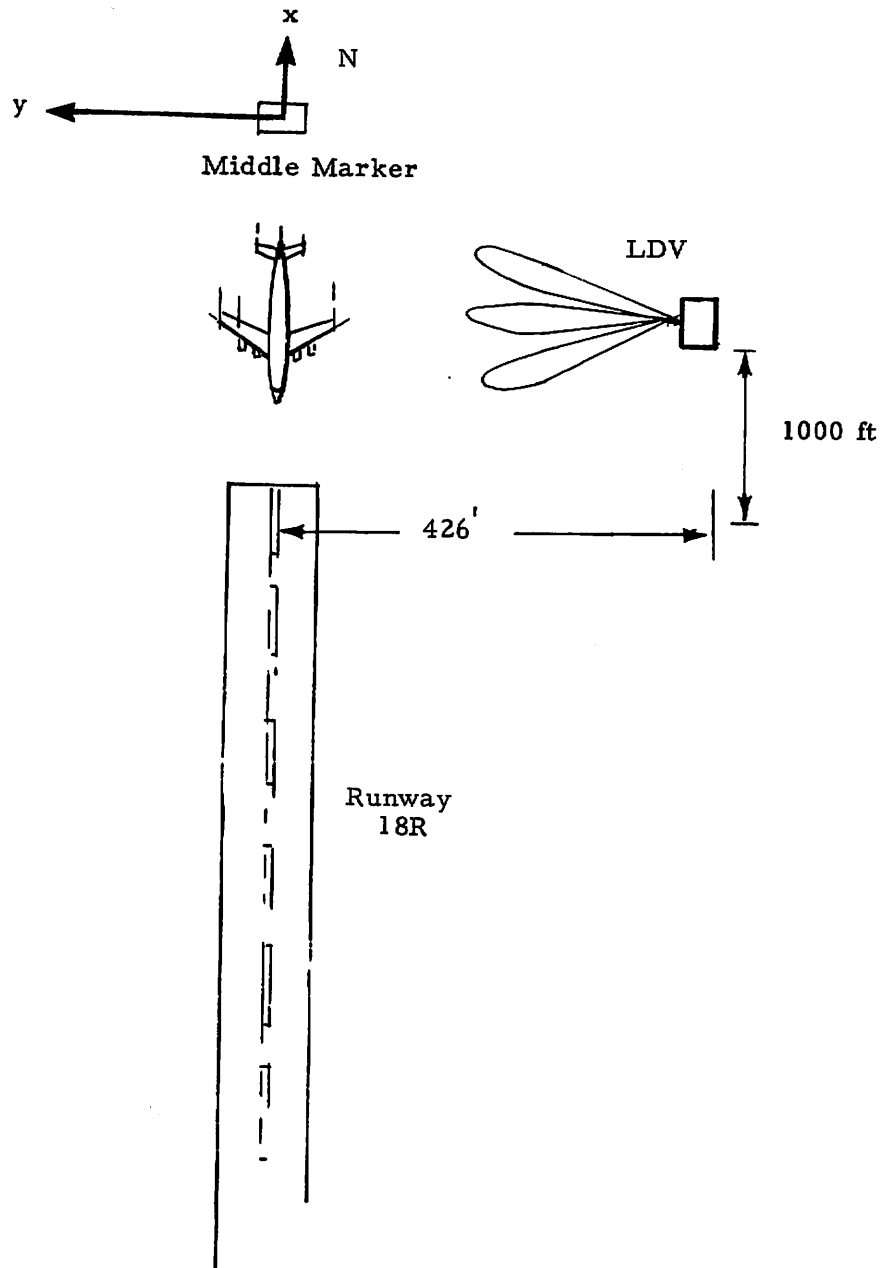


Fig. 4-1 - Field Site Location for Huntsville Jetplex LDV Tests

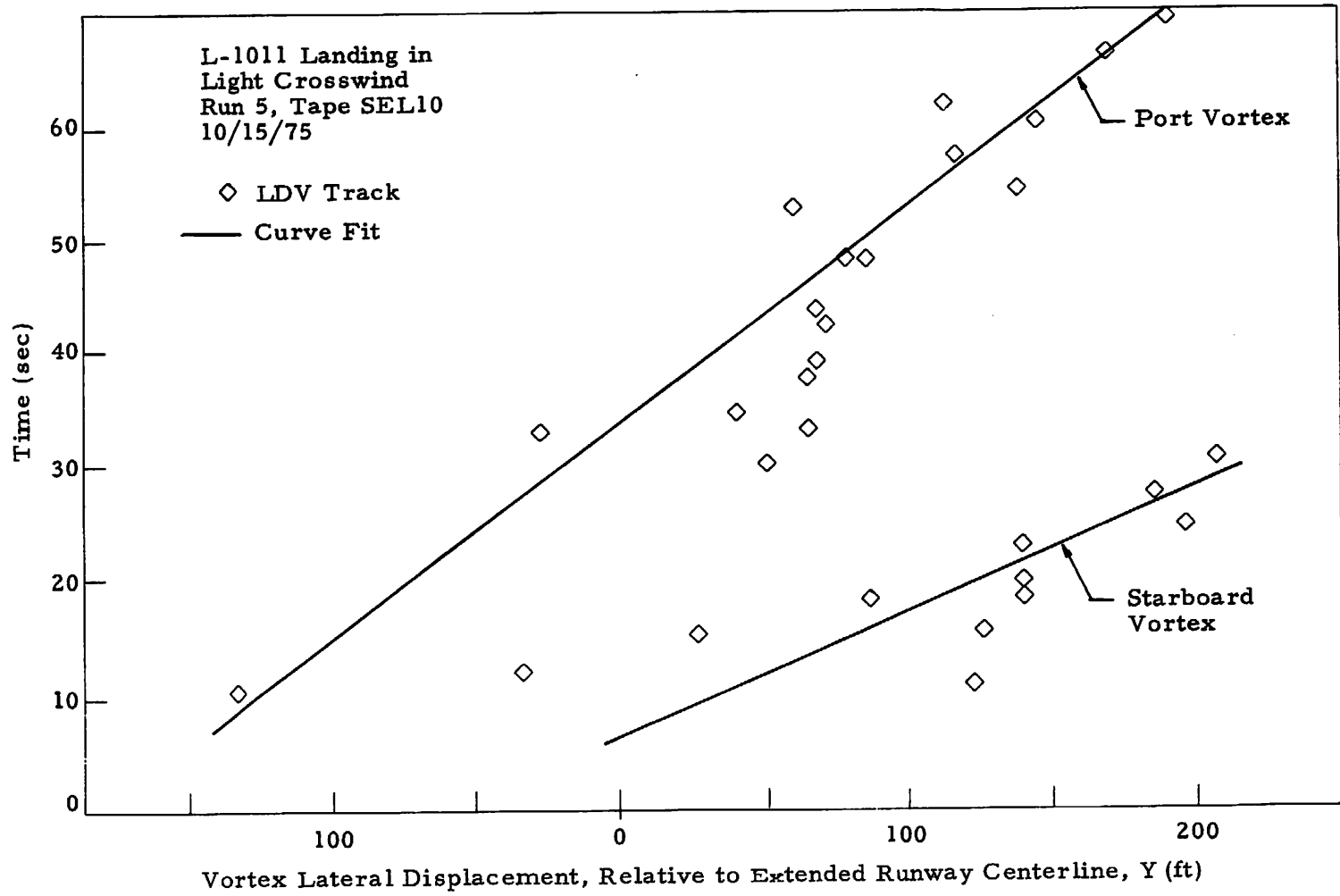
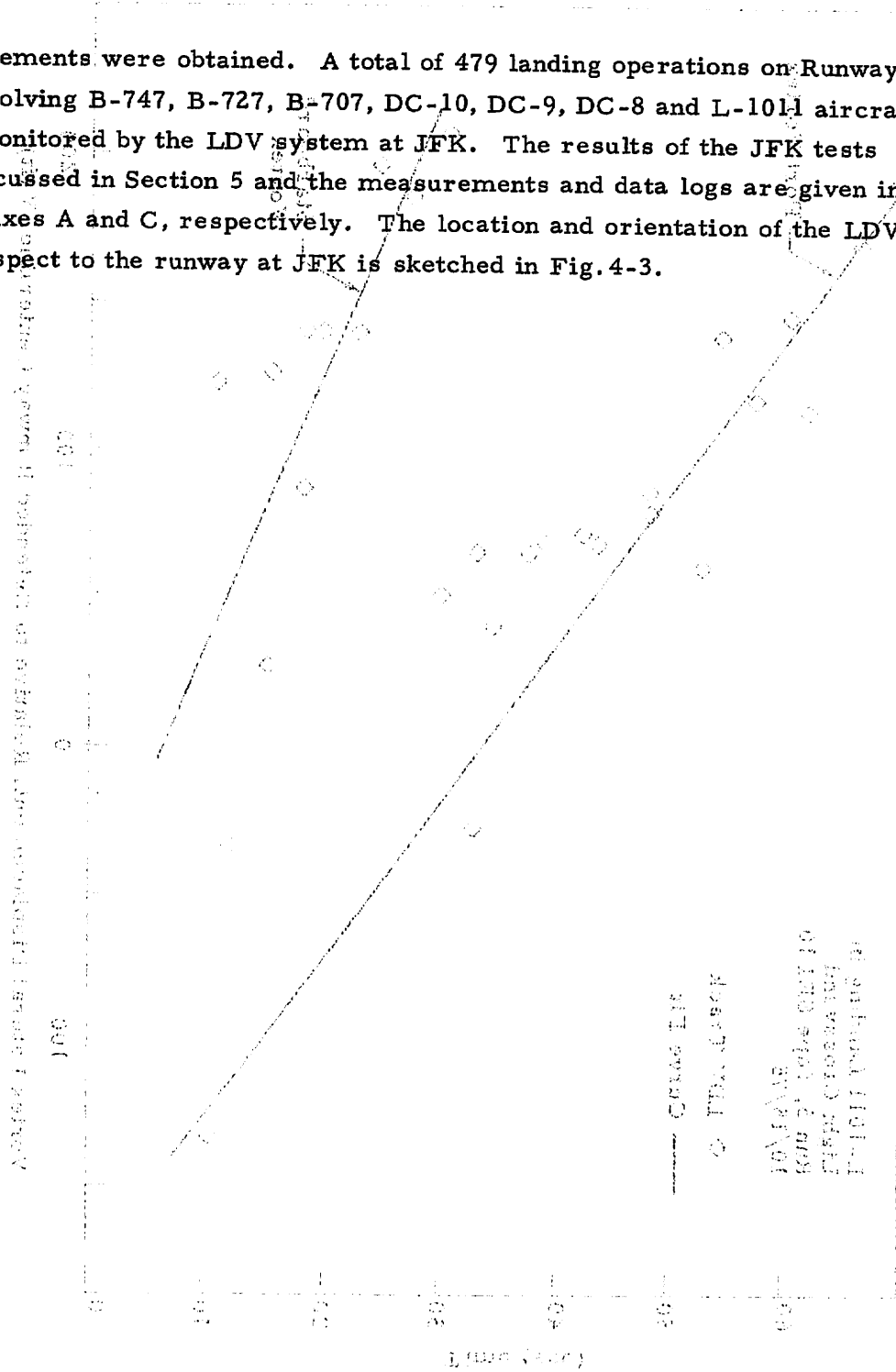


Fig. 4-2 - Sample Wake Vortex Trajectory Measured by LDV at Huntsville Jetplex

measurements were obtained. A total of 479 landing operations on Runway 31R involving B-747, B-727, B-707, DC-10, DC-9, DC-8 and L-1011 aircraft were monitored by the LDV system at JFK. The results of the JFK tests are discussed in Section 5 and the measurements and data logs are given in Appendixes A and C, respectively. The location and orientation of the LDV with respect to the runway at JFK is sketched in Fig.4-3.



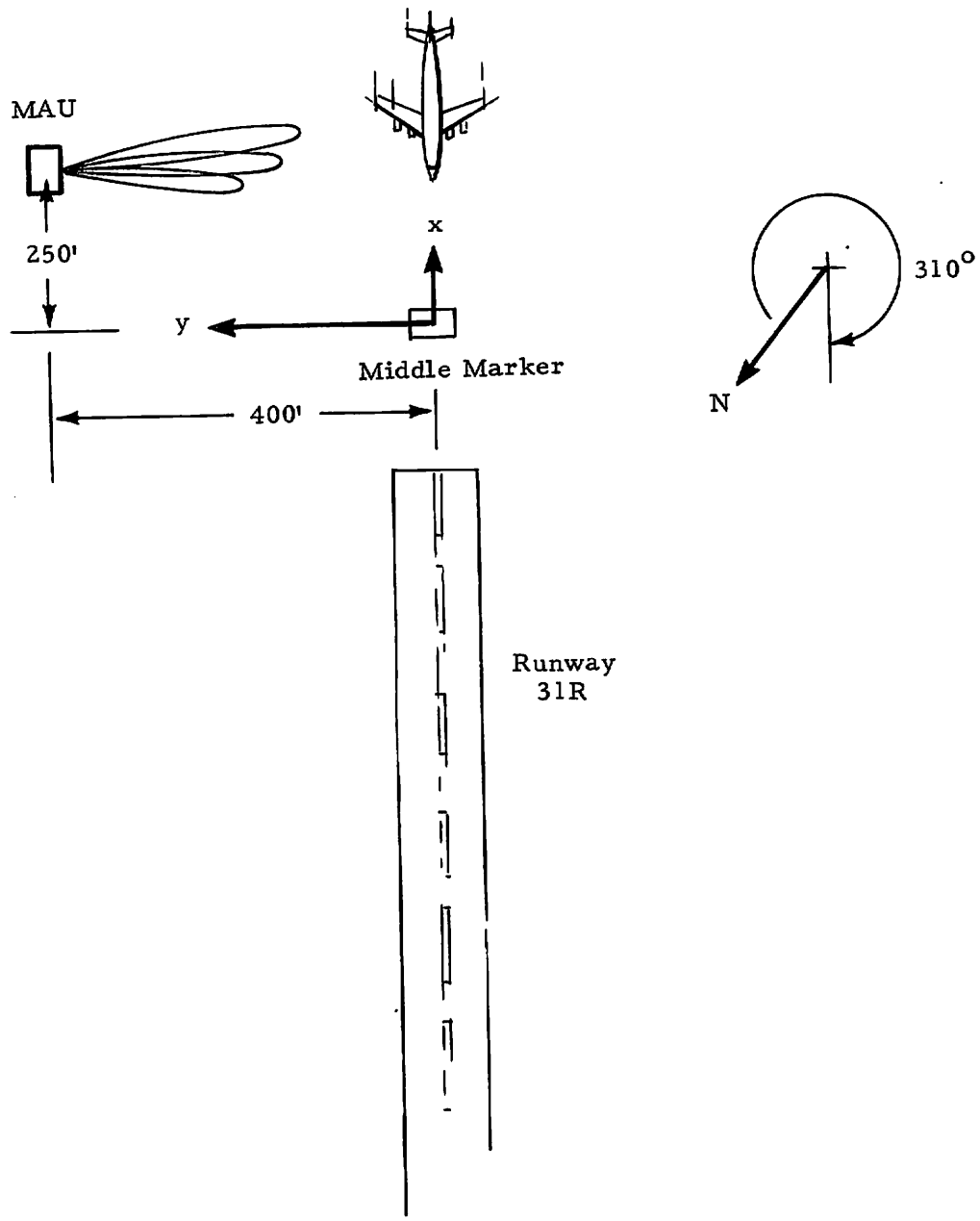


Fig. 4-3 - Field Site Location for the JFK LDV Tests

## 5. RESULTS OF WAKE VORTEX MEASUREMENTS

To demonstrate the operational capability of the LDV for monitoring wake vortices at airports, wake vortex measurements were carried out with the LDV system for 479 landing operations on runway 31R at Kennedy International Airport (JFK). From the logged data, 460 flybys have been processed and the presence of the wake vortex was clearly detected with the system for 379 flybys (i.e., one or more vortex centroids were computed) which includes 82% of the processed data. For the remaining 18% of the data (81 cases) no clear identification of the wake vortex pair was made. The lack of vortex identification is attributed to: (1) light aircraft types (such as DC-9 and others) where the vortex strength is too small for the LDV to detect them; (2) operator error in initializing the start of the scan or in setting the frequency and amplitude thresholds; and (3) windy and/or gusty conditions where the wake vortex is rapidly dispersed or transported out of the field of view. A summary of the wake vortex measurements is listed in Table 5-1 including the date, the number of flybys logged, the number of flybys processed, the number of observed wake trajectories, and pertinent comments. The individual wake vortex trajectories are given in Appendix A for those flybys out of the total of 379 where the vortex tracks were within the field of view of the LDV system (i.e., six or more vortex centroids were located). The general trends are described below.

Sample wake vortex trajectories recorded with the LDV at JFK are presented in Figs. 5-1 through 5-10. These flybys have been selected since they illustrate the wake vortex measuring capability of the systems in terms of:

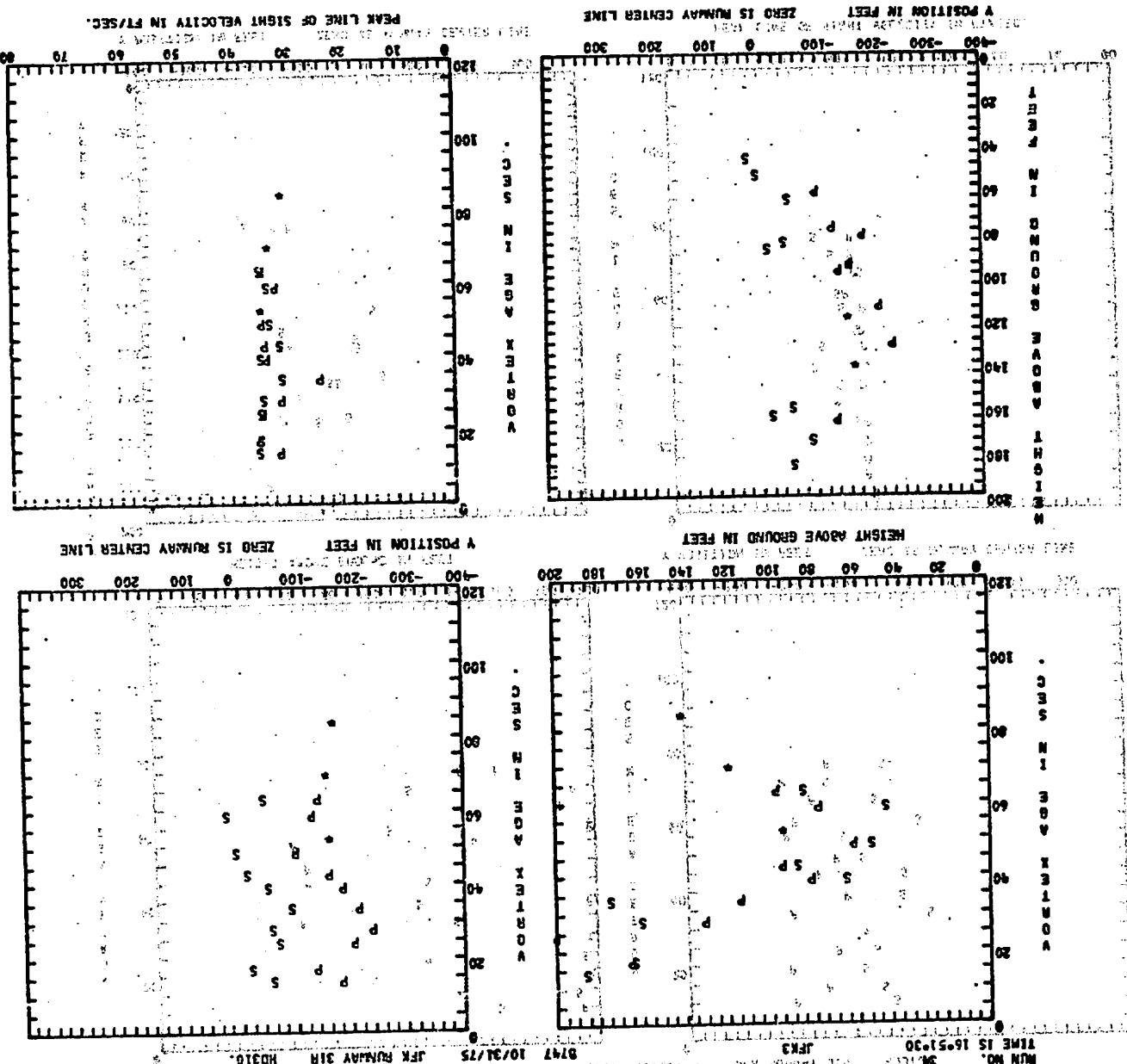
- a. Discriminating the port and starboard vortices from the overall flowfield,
- b. Tracking the lateral and vertical location of the vortex wake,

Table 5-1

SUMMARY OF WAKE VORTEX MEASUREMENTS CONDUCTED  
AT KENNEDY INTERNATIONAL AIRPORT WITH  
LOCKHEED-HUNTSVILLE LDV

JFK Tape	Date	No. of Flybys Logged	No. of Flybys Processed	No. of Wake Trajectories	Comments
2	10/30/75	18	18	7	
3	10/31/75	45	45	38	
6	11/4/75	21	16	15	
9	11/7/75	7	7	6	
13	11/18/75	9	9	7	Run stopped
14	11/18/75	51	51	38	Good runs
21	1/14/76	60	58	55	Short vortex life
22	1/15/76	99	99	70	Good runs
27	1/27/76	34	34	26	Few hits
28	1/28/76	70	68	63	
30	1/30/76	56	55	54	Good runs
31A	1/31/76	9	0	0	Not processed
	Totals	479	460	379	

Fig. 5-1 - Wake Vortex Trajectory of B-747 Aircraft - Date, 10/31/75; Time, 16:51:30



RUN NO. 36107  
 TIME IS 16:51:30  
 JFK  
 8797 10/31/75  
 JFK RUNWAY 31R HD310

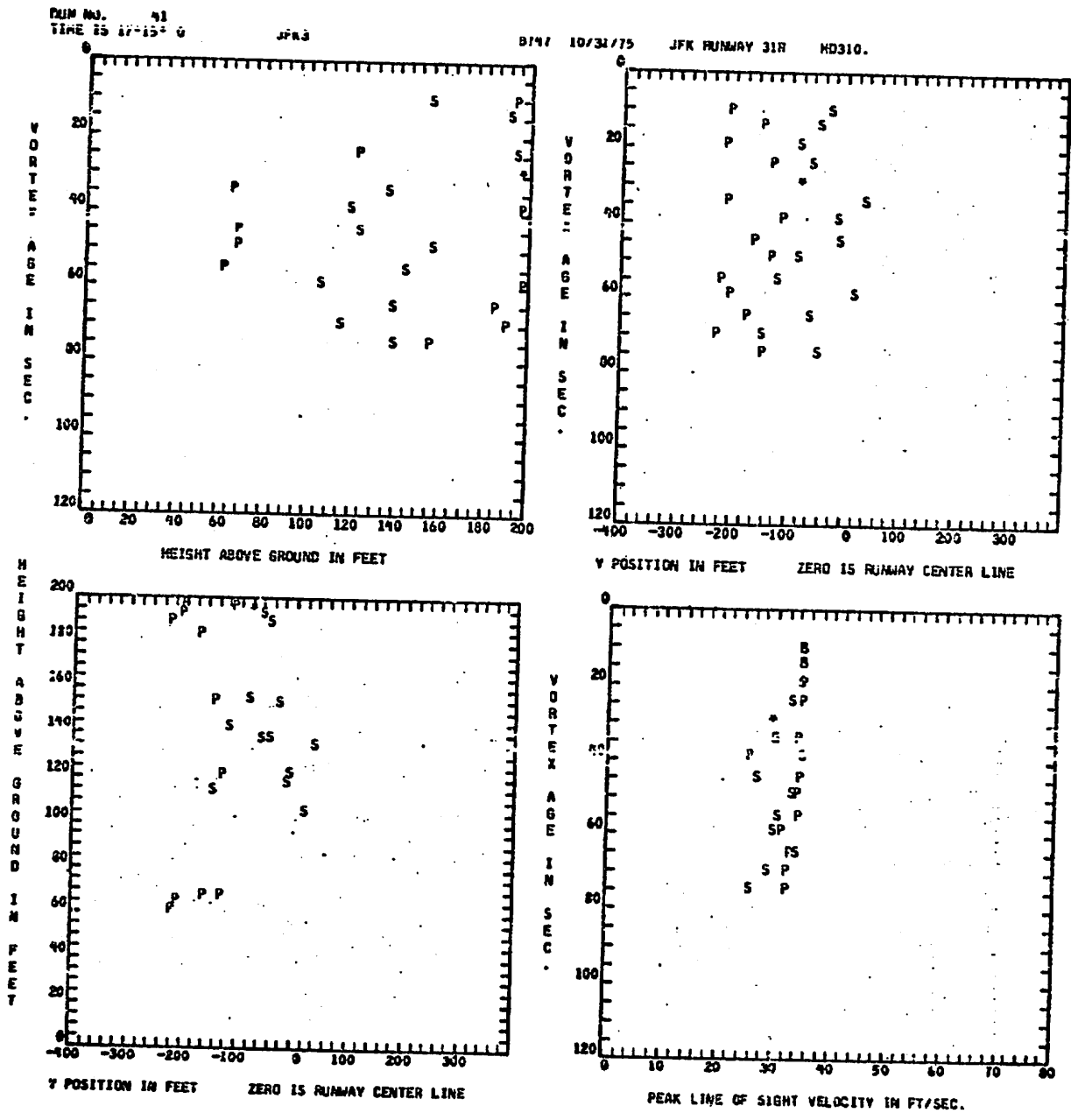


Fig. 5-2 - Wake Vortex Trajectory of B-747 Aircraft - Date, 10/31/75; Time, 17:15:00

RUN NO. 99  
TIME IS 17:27:00

JFK3

B747 10/31/75 JFK PRIMARY DIR 10310.

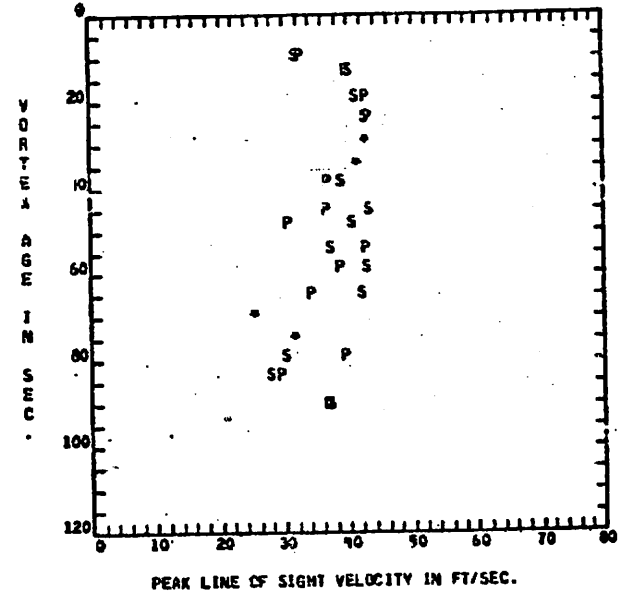
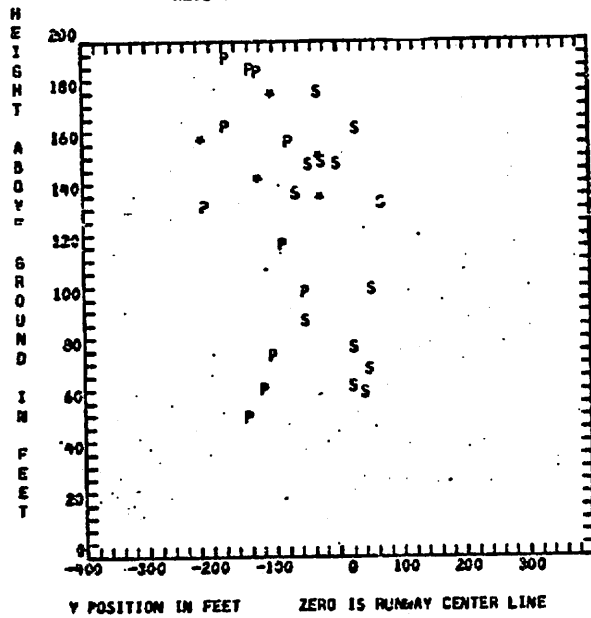
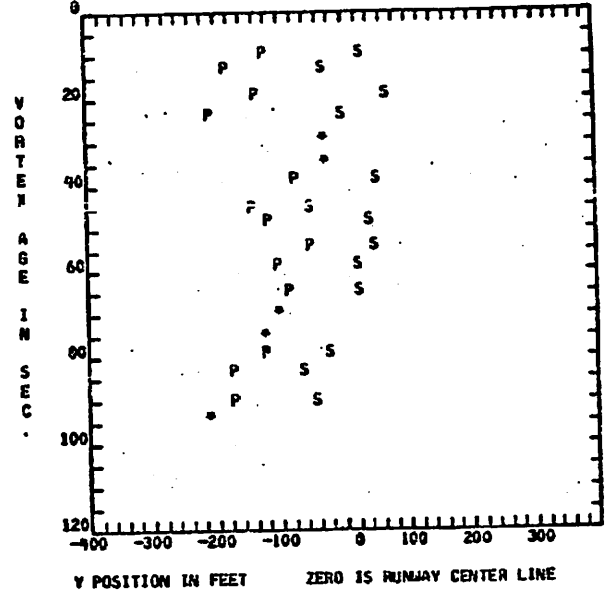
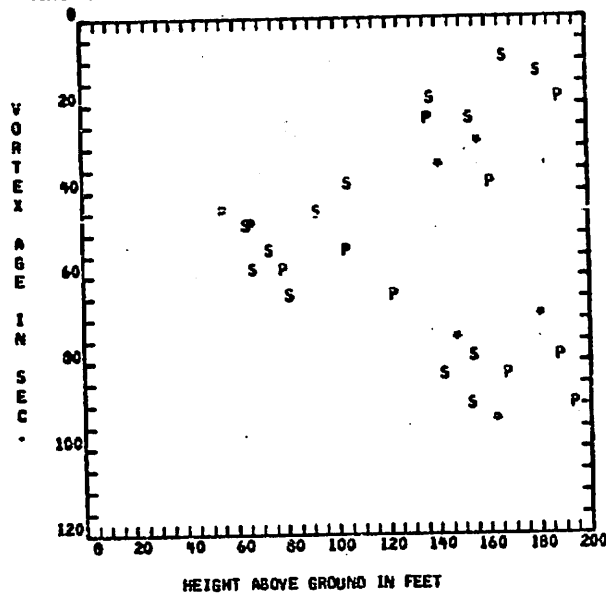


Fig.5-3 - Wake Vortex Trajectory of B-747 Aircraft - Date 10/31/75;  
Time 17:27:00

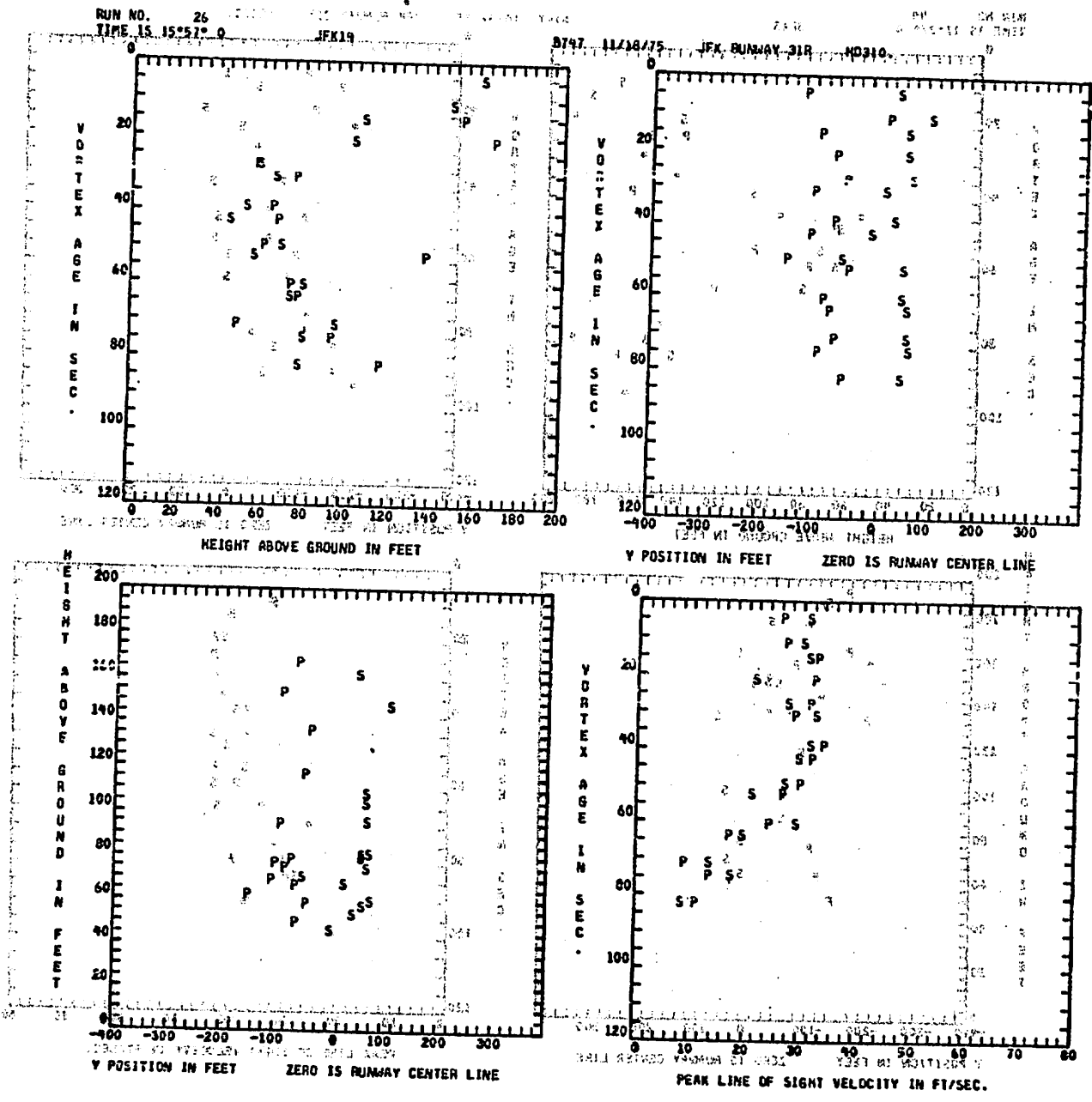


Fig. 5-4 Wake Vortex Trajectory of B-747 Aircraft - Date 11/18/75;  
 Time, 15:57:00

RUN NO. 99  
TIME IS 17:20

JFK19

B747 11/18/75

JFK RUNWAY 31R

MD310.

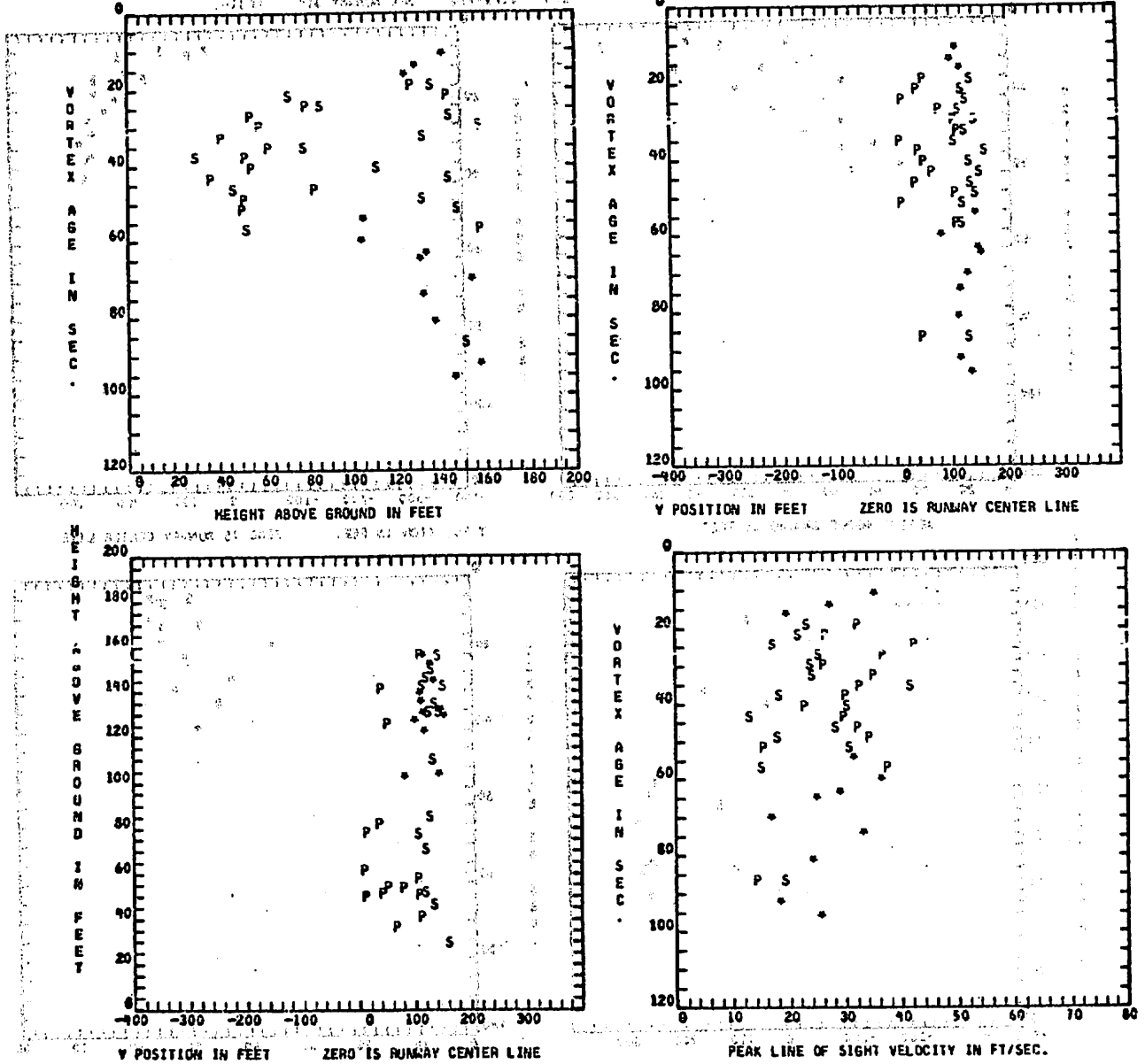


Fig. 5-5 - Wake Vortex Trajectory of B-747 Aircraft - Date 11/18/75;  
Time, 17:20

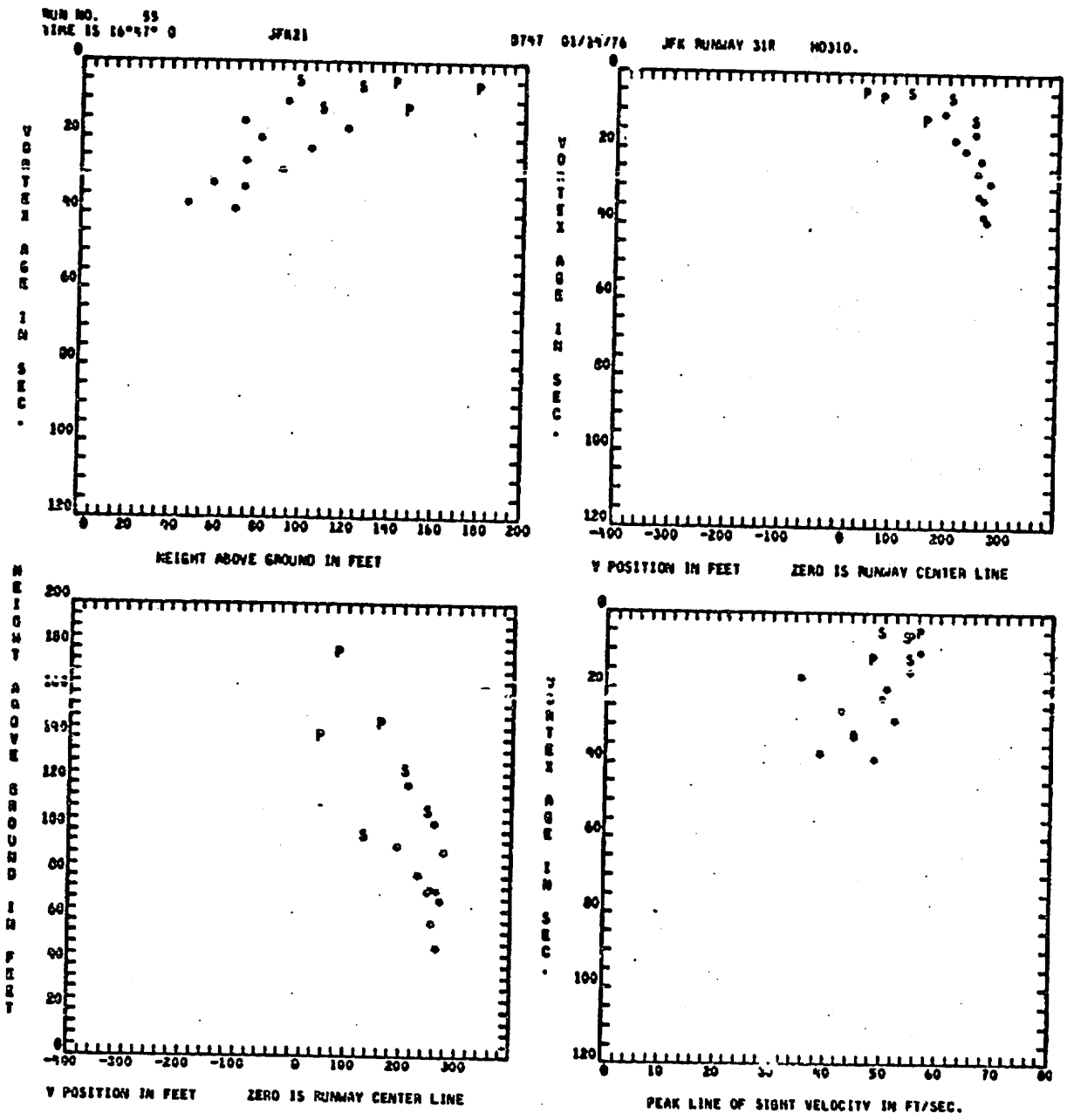


Fig.5-6 - Wake Vortex Trajectory of B-747 Aircraft - Date, 1/14/76;  
Time, 16:47:00

UN NO. 43  
TIME IS 14:41:00

JFK22

B747 01/15/76

JFK RUNWAY 31R N0310.

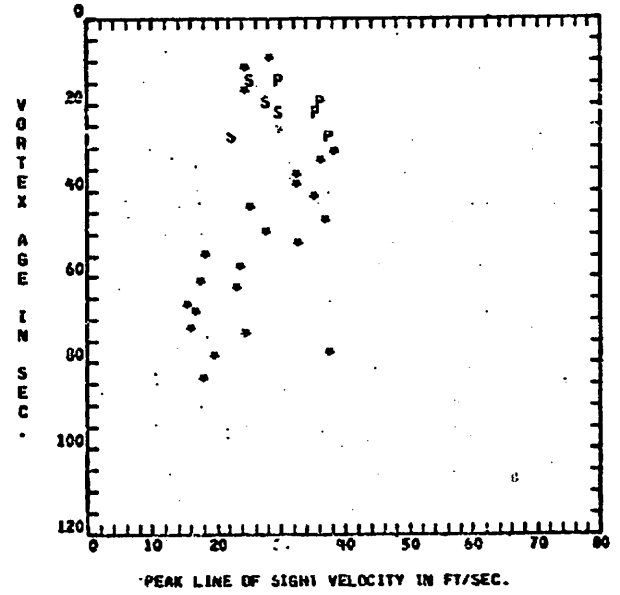
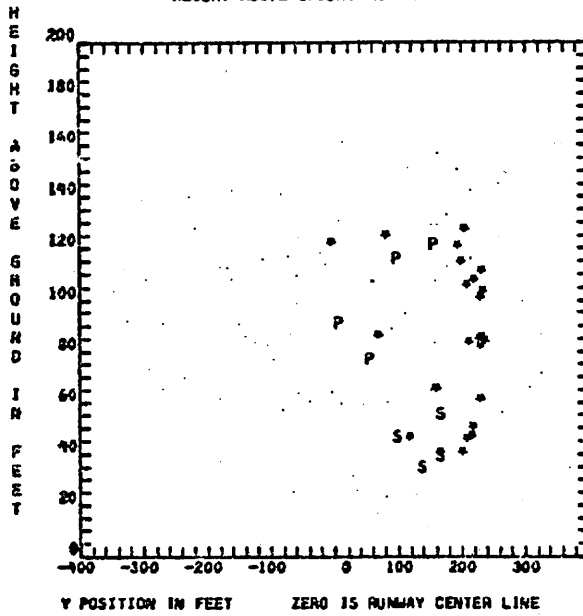
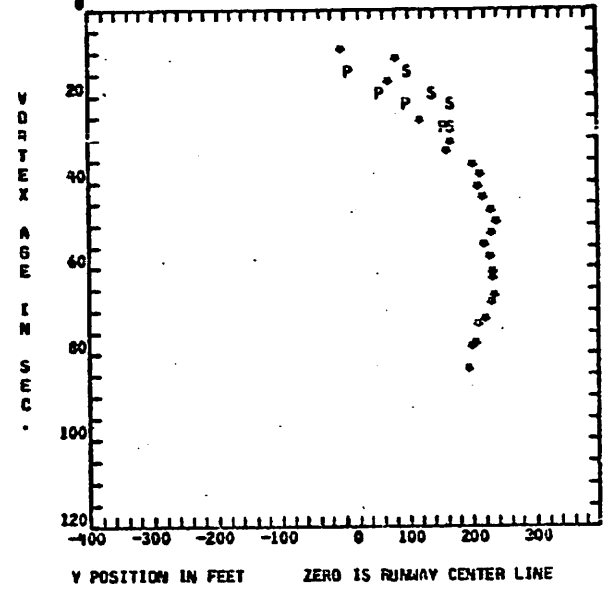
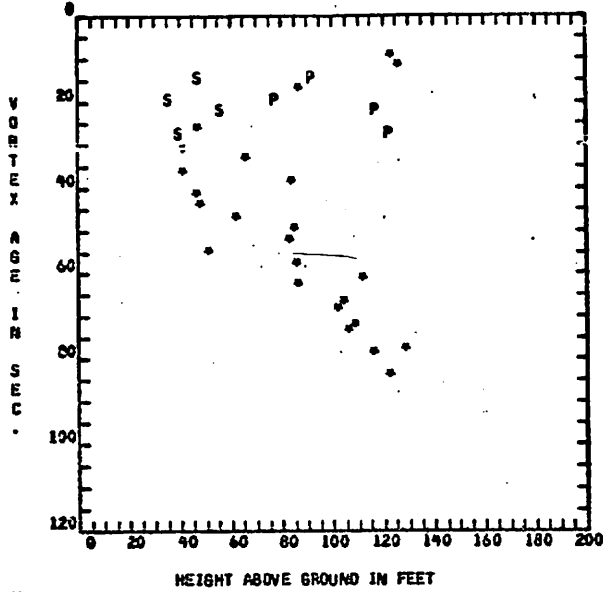


Fig.5-7 - Wake Vortex Trajectory of B-747 Aircraft - Date 1/15/76;  
Time, 14:41:00

MIN NO. 8  
TIME 15:15:00

JFK30

B707 1/30/76

JFK RUNWAY 31R

HD310.

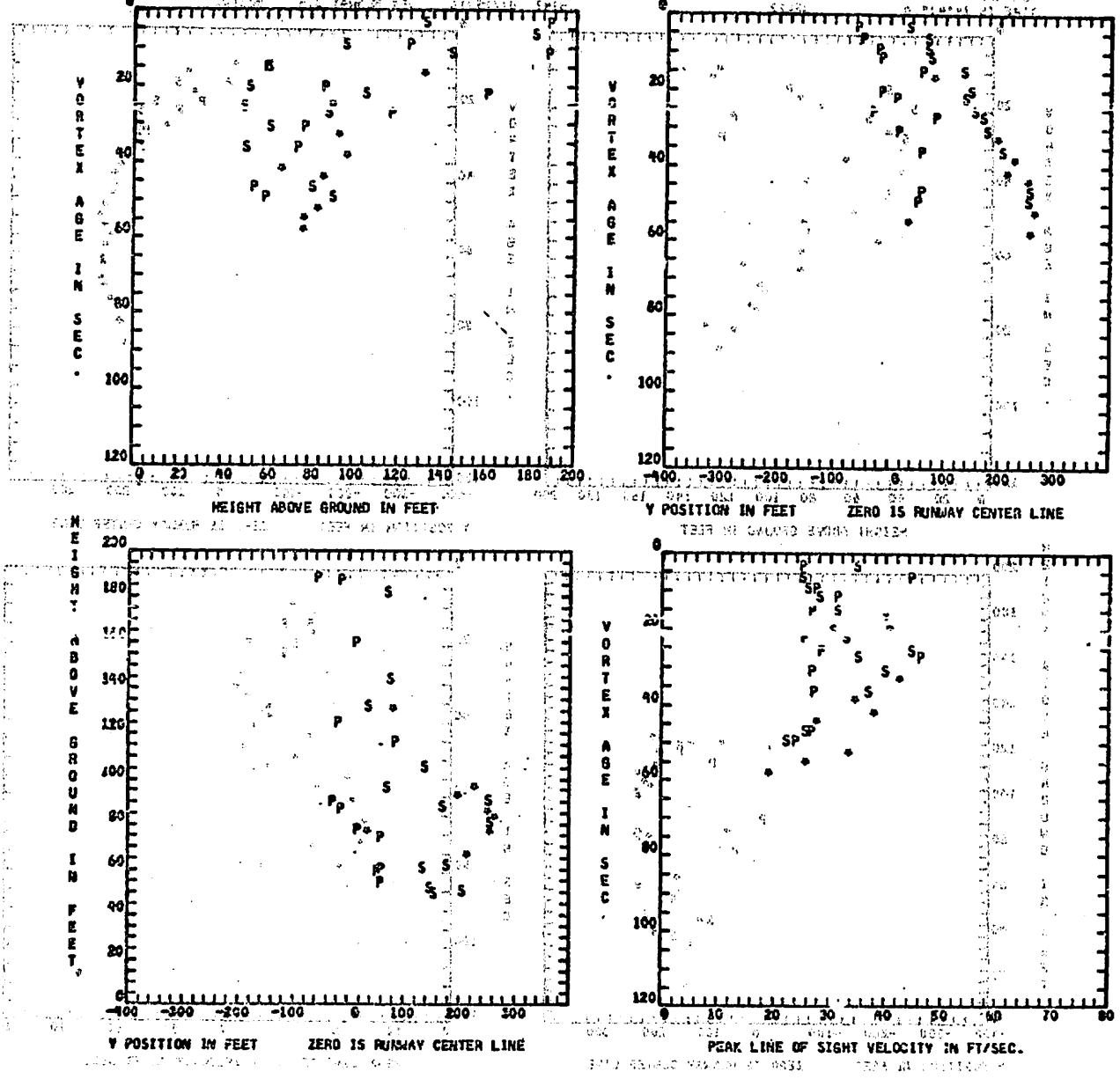


Fig. 5-8 - Wake Vortex Trajectory of B-747 Aircraft - Date, 1/30/76;  
Time, 15:15:00

RUN NO. 25  
 TIME IS 16:10:00  
 JFK30  
 B707 1/30/76  
 JFK RUNWAY 31R HD310.

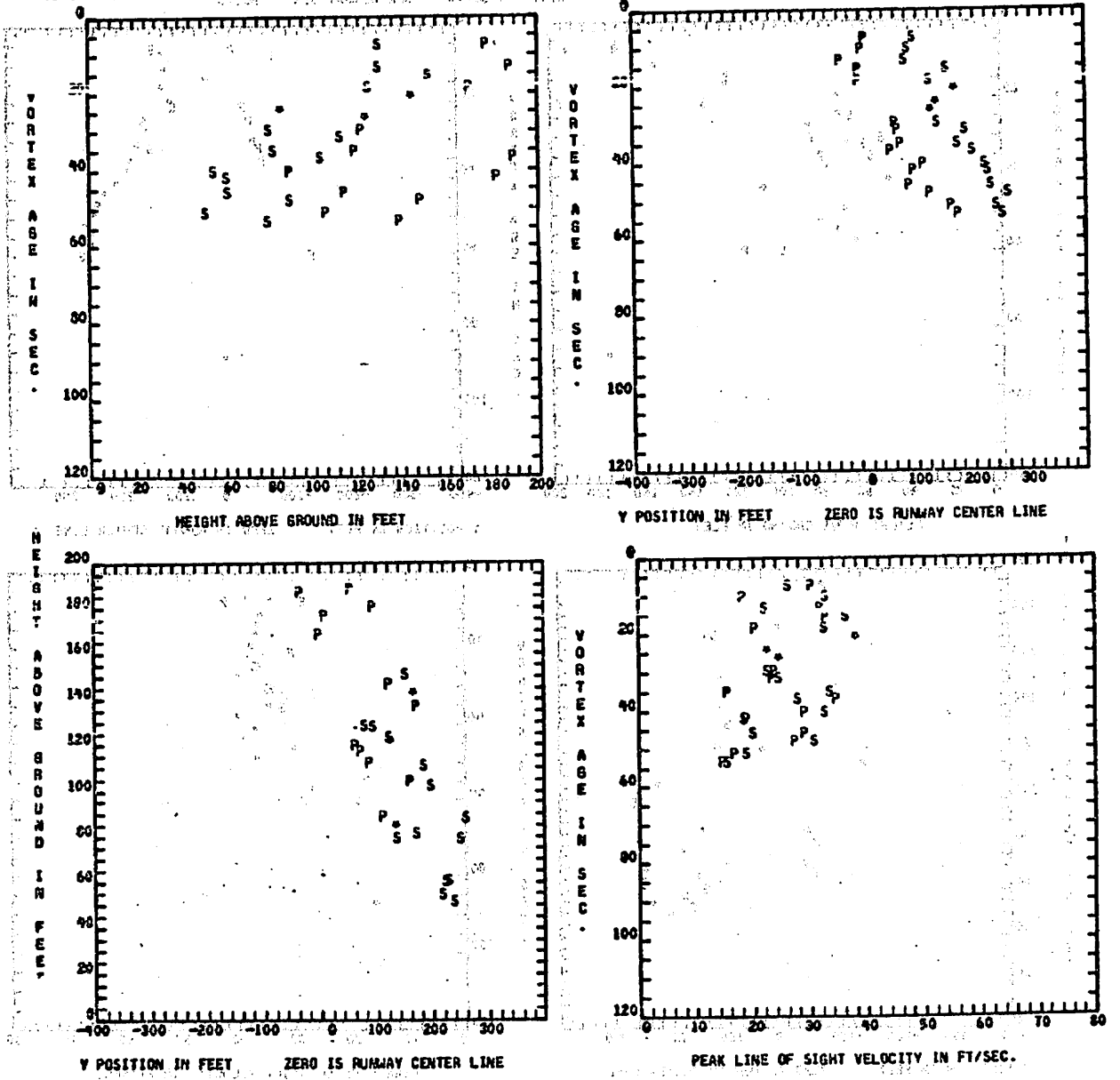


Fig. 5-9 - Wake Vortex Trajectory of B-747 Aircraft - Date, 1/30/76;  
 Time, 16:10:00

RUN NO. 44  
TIME IS 17:00:0

JFK30

B747 1/30/76 JFK RUNWAY 31R HD310.

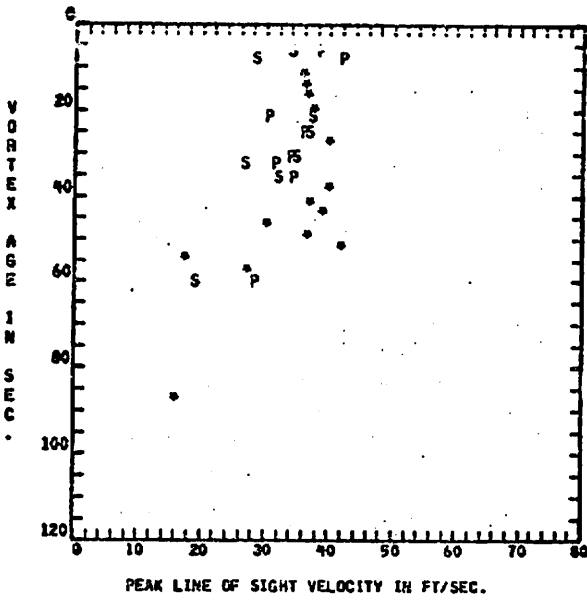
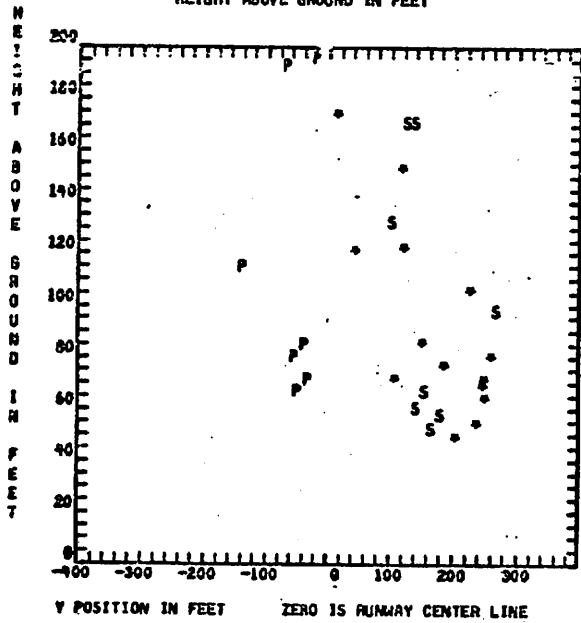
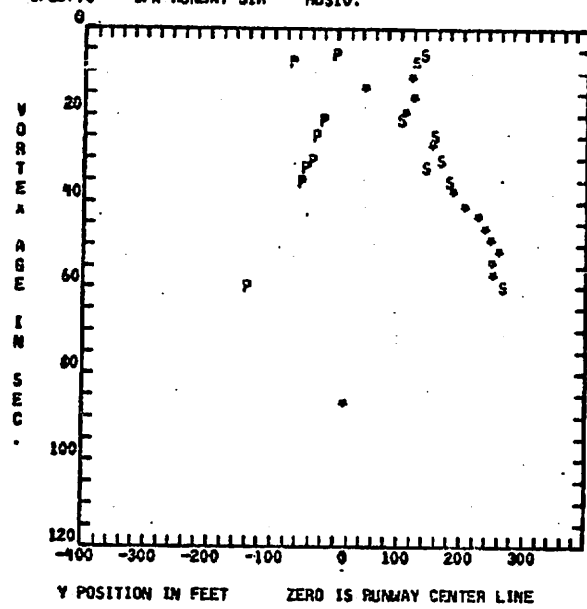
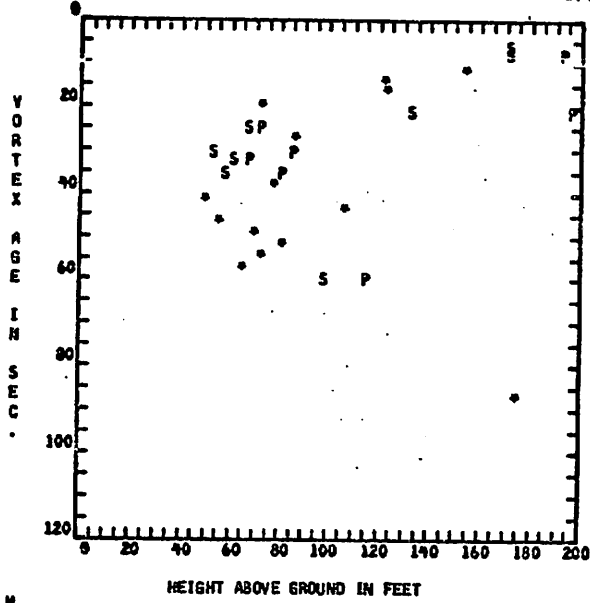


Fig. 5-10 - Wake Vortex Trajectory of B-747 Aircraft - Date 1/30/76;  
Time, 17:00:00

- c. Indicating transport of the vortex pair, and
- d. Indicating decay of the vortex peak velocity.

The port and starboard vortices are labeled by the letters P and S respectively while the symbol (\*) refers to a single vortex whose origin is undefined. In Figs. 5-1 through 5-10 the LDV system consistently locates the port and starboard vortices. At late times, when lateral drift of one vortex out of the LDV field of view can occur, discrimination of the port and starboard vortices is limited.

The lateral trajectory of the wake vortices is indicated by the height versus y position and vortex age versus y position plots. For the sample runs shown in Figs. 5-1 through 5-10 the wake vortex remains in the region  $\pm 150$  ft about the runway centerline for 20 to 60 sec. Some scatter can be seen in the lateral trajectories attributed to: (1) the actual vortex wandering; (2) the range resolution of the LDV system; and (3) the resolution of the vortex track algorithm. Filtering the data or a least squares fit to the vortex trajectory could eliminate some of the scatter. However, the existence of the wake vortices in the vicinity of the runway can be clearly determined from the measurements.

In addition to the scatter in the vortex track measurements attributed to ambient conditions and to computer processing techniques, some of the scatter resulted from constraints in the LDV system hardware. Two possible sources of error in the LDV system included: (1) error in vortex track location due to actual versus commanded focus position, and (2) failure to record vortex signal during periods when the onboard computer was dumping the filled up buffer. Since the location of the LDV focal volume was determined from the commanded rather than the observed mirror orientation and since a small lag occurred between the commanded and observed mirror position, the measured vortex location could be in error by  $\pm 20$  ft for the typical finger scan rates selected at JFK. Hardware problems with the computer interrupt dictated a single buffer data collection mode on the onboard computer which resulted in

data being rejected whenever the computer was in the process of dumping the filled up buffer. As a result, intermittent skips in the recorded vortex tracks lasting a fraction of a second could be observed during the measurements. However, it is noted that the above hardware problems did not seriously hamper the capability of the LDV to identify and to monitor wake vortices in the vicinity of the runway. Appropriate modifications can be made to the LDV system to circumvent the cited hardware limitations.

The vertical trajectory of the wake vortices is indicated by the vortex age versus height and height versus y-position plots. For the sample runs shown in Figs. 5-1 through 5-10 the vortex pair descends at approximately constant velocity until it is within 50 to 100 ft of the ground. The scatter in the vortex altitude measurements appears to be larger than in the vortex lateral position measurements. This is attributed to: (1) the wake vortices can become asymmetric during the descent process, and (2) the uncertainty in the altitude is related to the product of the uncertainty in the elevation angle and range.

Decay of the wake vortex peak velocity is illustrated by the vortex age versus peak line-of-sight velocity plots in Figs. 5-1 through 5-10. The peak line-of-sight velocity is a measure of the maximum rotational velocity of each vortex. In general, no significant decrease of the vortex rotational velocity occurs initially in the vortex wake, i.e., 0 to 40 sec after aircraft passage, while at later times the peak velocity decreases markedly. Some scatter can be noted in the peak velocity time histories which is attributed to: (1) the different velocity decay rates for the port and starboard vortices, (2) unsteadiness in the vortex flow and the lack of axial symmetry, and (3) the uncertainty in determining the exact vortex centroids due to spatial resolution and lack of sample points. However, the velocity decay trends shown in Figs. 5-1 through 5-10 are in agreement with the plateau and the  $1/t$  or  $1/\sqrt{t}$  type of vortex decay characteristics observed in wind tunnel and water tank studies by others (Ref. 7).

The wake vortex trajectories measured with the LDV system at JFK are given in Appendix A and show the same trends as the sample plots discussed above.

## 6. RESULTS OF WIND MEASUREMENTS

The three-dimensional wind field was monitored as a function of altitude near the middle marker position of runway 31R at Kennedy International Airport several times daily during the LDV field tests. The objective of the wind data collection was to: (1) demonstrate the capability of the Lockheed-Huntsville LDV for measuring ambient atmospheric wind fields; (2) compare the LDV measurements with wind measurements obtained by conventional anemometers at the test site; and (3) from the above data, establish the operational capabilities, resolution, and integrity of the LDV for wind monitoring at terminal areas.

During the JFK field tests, a considerable amount of wind data was collected with the LDV as shown in the data logs in Appendix A. However, a detailed comparison of the LDV wind measurements with on-site wind measurements from the DOT-TSC meteorological towers was hampered by lack of data from the meteorological towers. In subsequent tests, summarized in a separate report, LDV u, v, w measurements were carefully correlated with instrumented tower measurements; the results showed that the LDV is a highly sensitive wind monitoring device (Ref. 6).

Wind profile measurements were carried out at JFK with the LDV system operating in the VAD mode. The processed wind speed, direction, and crosswind and downwind profile are shown in Figs. 6-1 and 6-2 for sample cases. For comparison, the hourly 20-foot level NOAA groundwind measurements at JFK are also plotted for each of the wind profiles as obtained from the surface weather charts. Good correlation is noted between the Lockheed-Huntsville LDV measurements fitted by a least squares curve fit and the ground wind observations in Figs. 6-1 and 6-2. A power law wind speed profile and a linear wind direction profile were fitted to the LDV VAD

measurements at different altitudes so as to minimize the sum of the squares of the derivations of the given points from the curve. The LDV measurements have also been compared with observations from the DOT-TSC instrumented meteorological tower at JFK. The LDV system was located 3,700 and 850 ft, from the DOT 135 and 40 ft towers, respectively. The NOAA tower was located approximately 2 miles from the LDV system. The results in Figs. 6-3 and 6-4 show the wind speed measurements obtained from the LDV VAD scans and the meteorological towers. The measurements in Fig. 6-5 show the line-of-sight velocity obtained with the LDV system focused at the location of the anemometer on the 40' tower. The wind measurements from the 40' DOT tower and the 20' NOAA tower, resolved about the LDV line-of-sight, are shown in Fig. 6-5 for comparison. Again, good agreement is noted between the LDV and meteorological tower measurements.

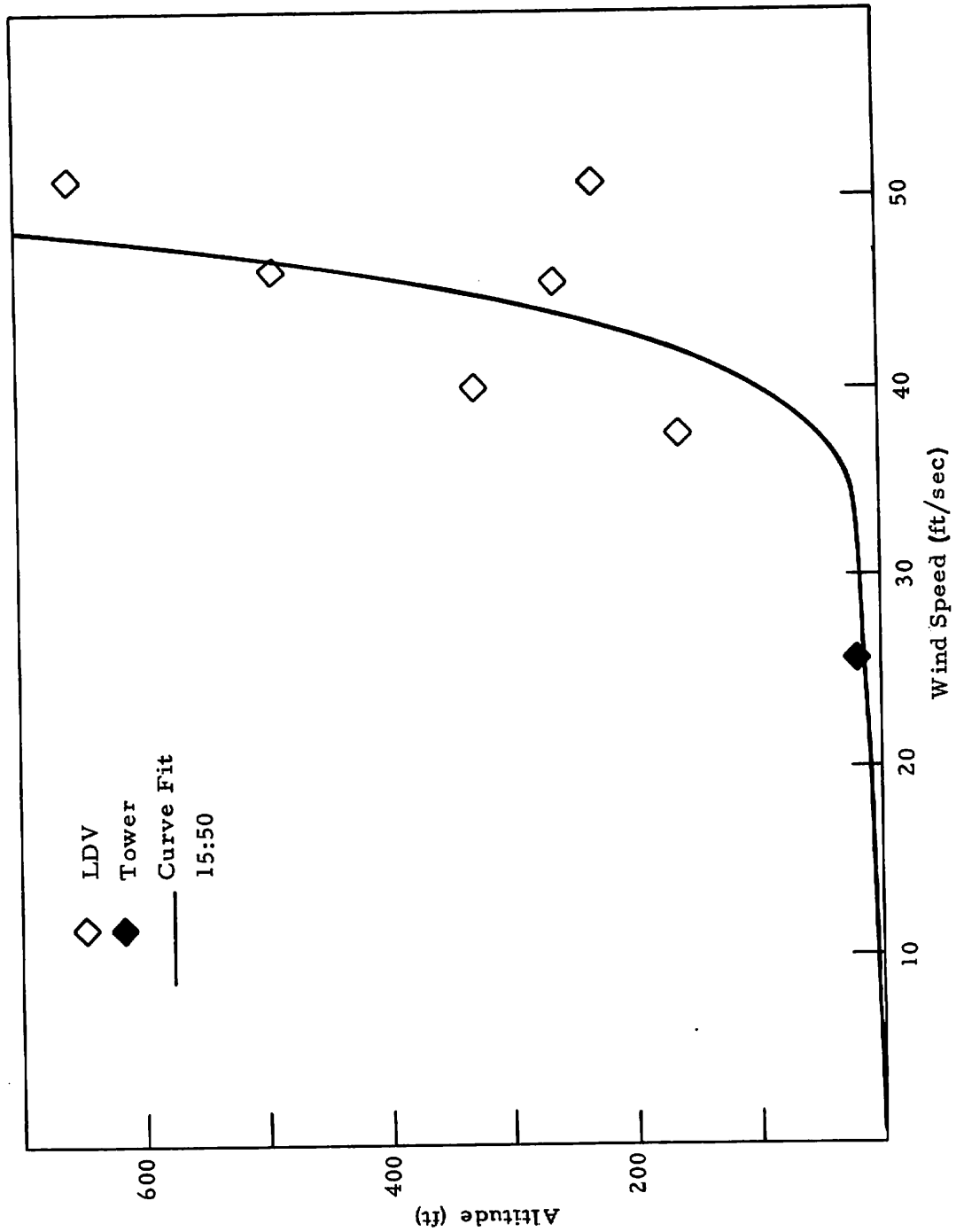


Fig. 6-1 - Wind Profile, JFK Runway 31R (10/30/75)

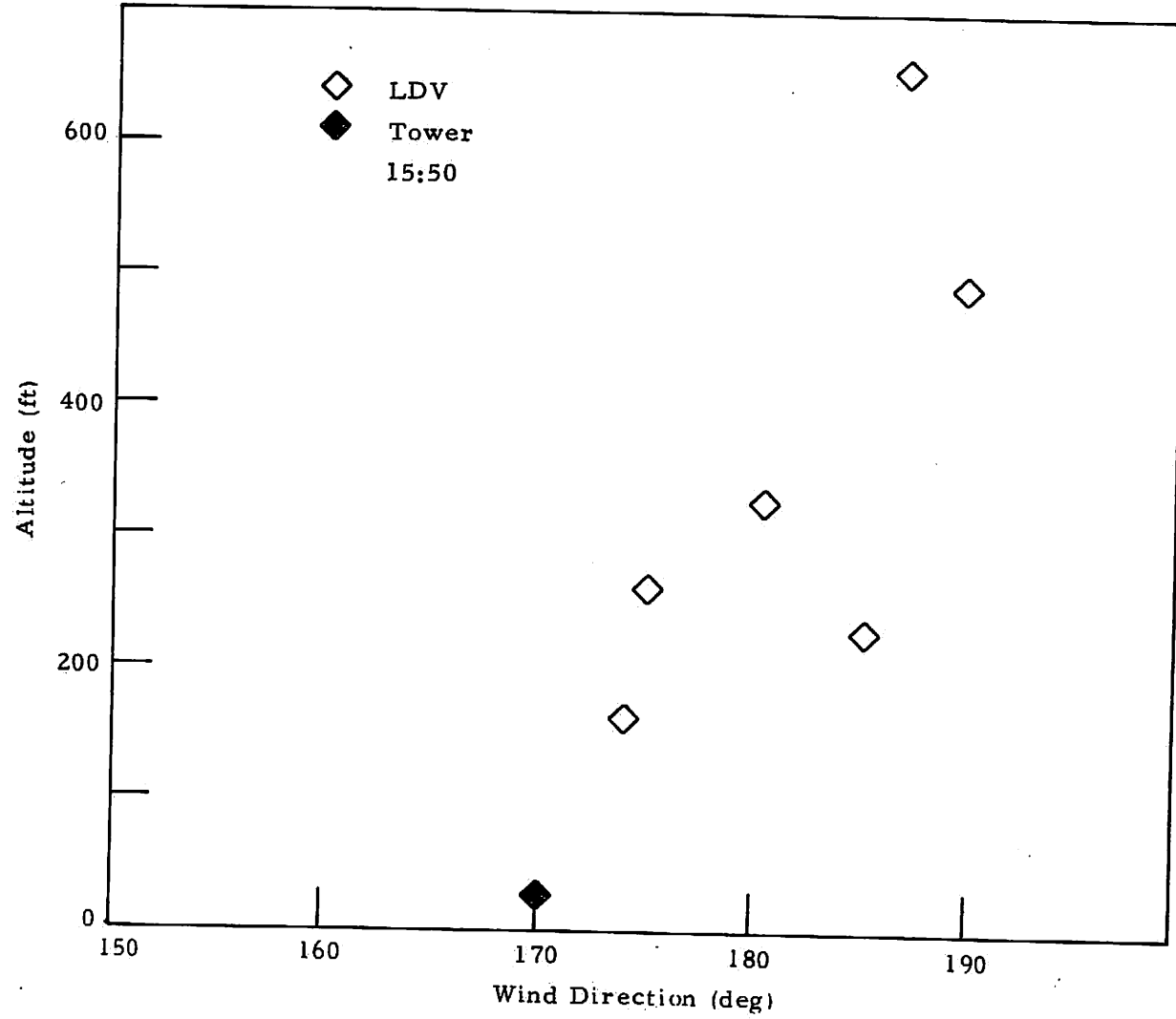


Fig.6-1 - (Continued)

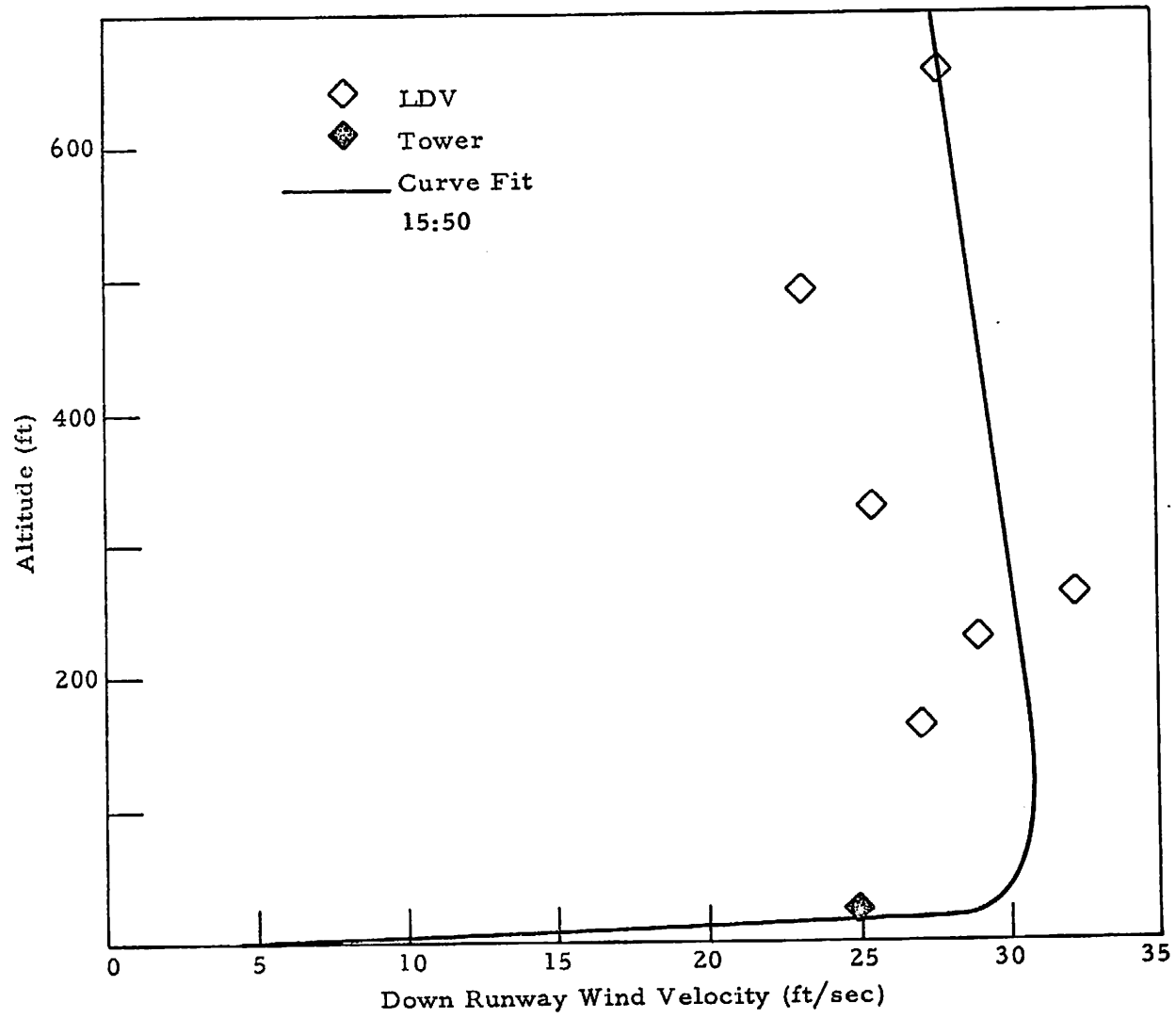


Fig.6-1 - (Continued)

9-9

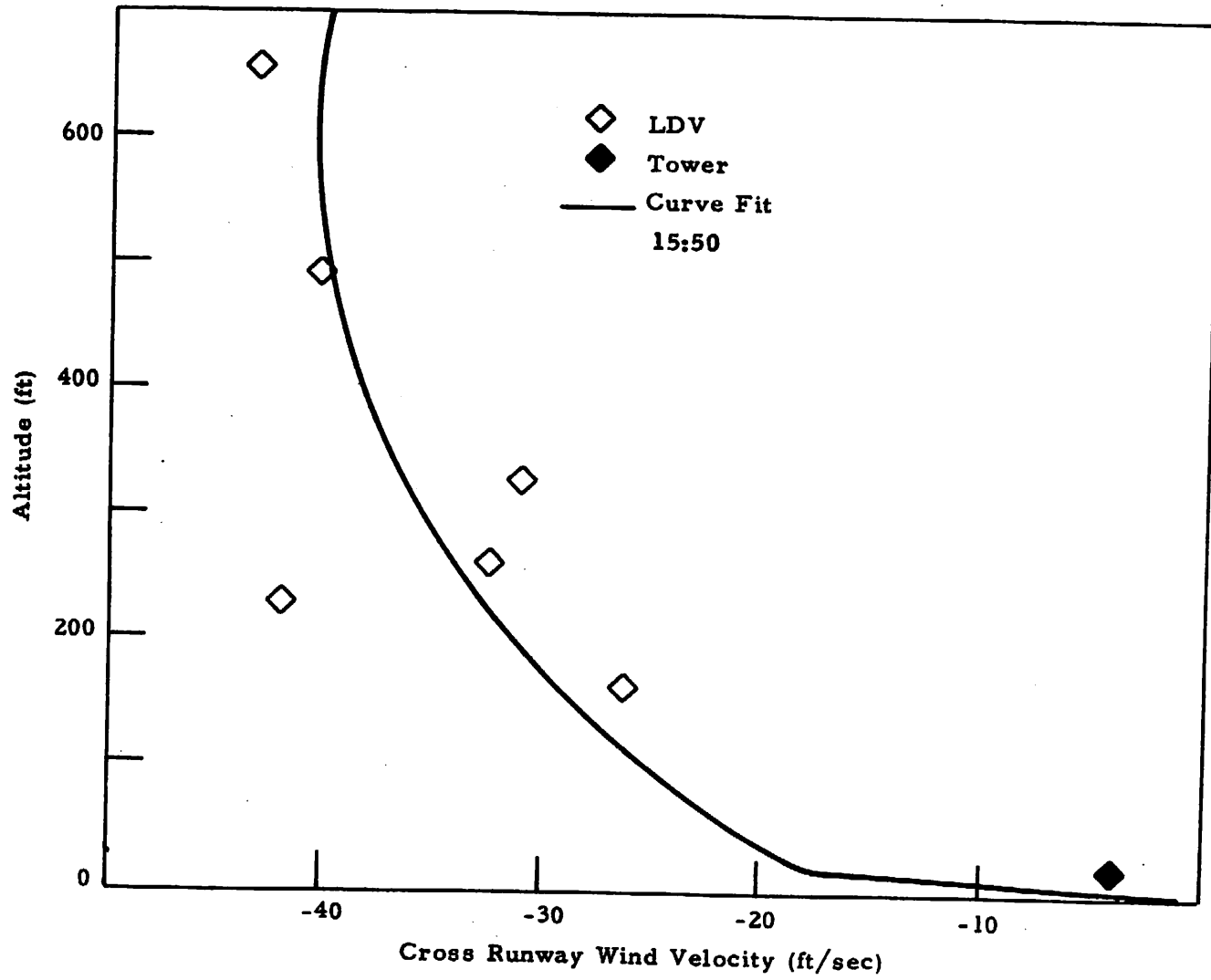


Fig.6-1 - (Concluded)

6-7

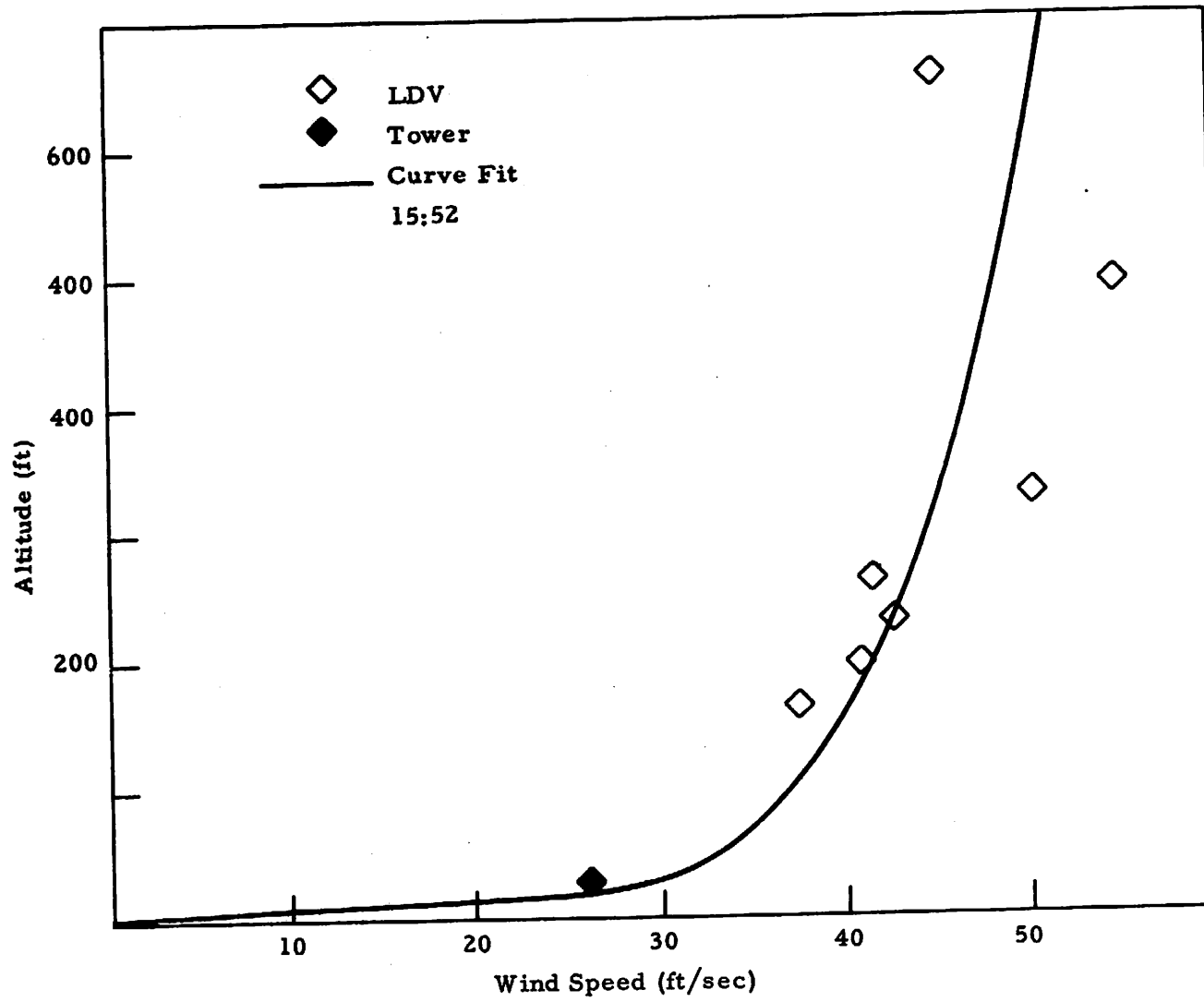


Fig. 6-2 - Wind Profile, JFK Runway 31R (10/30/75)

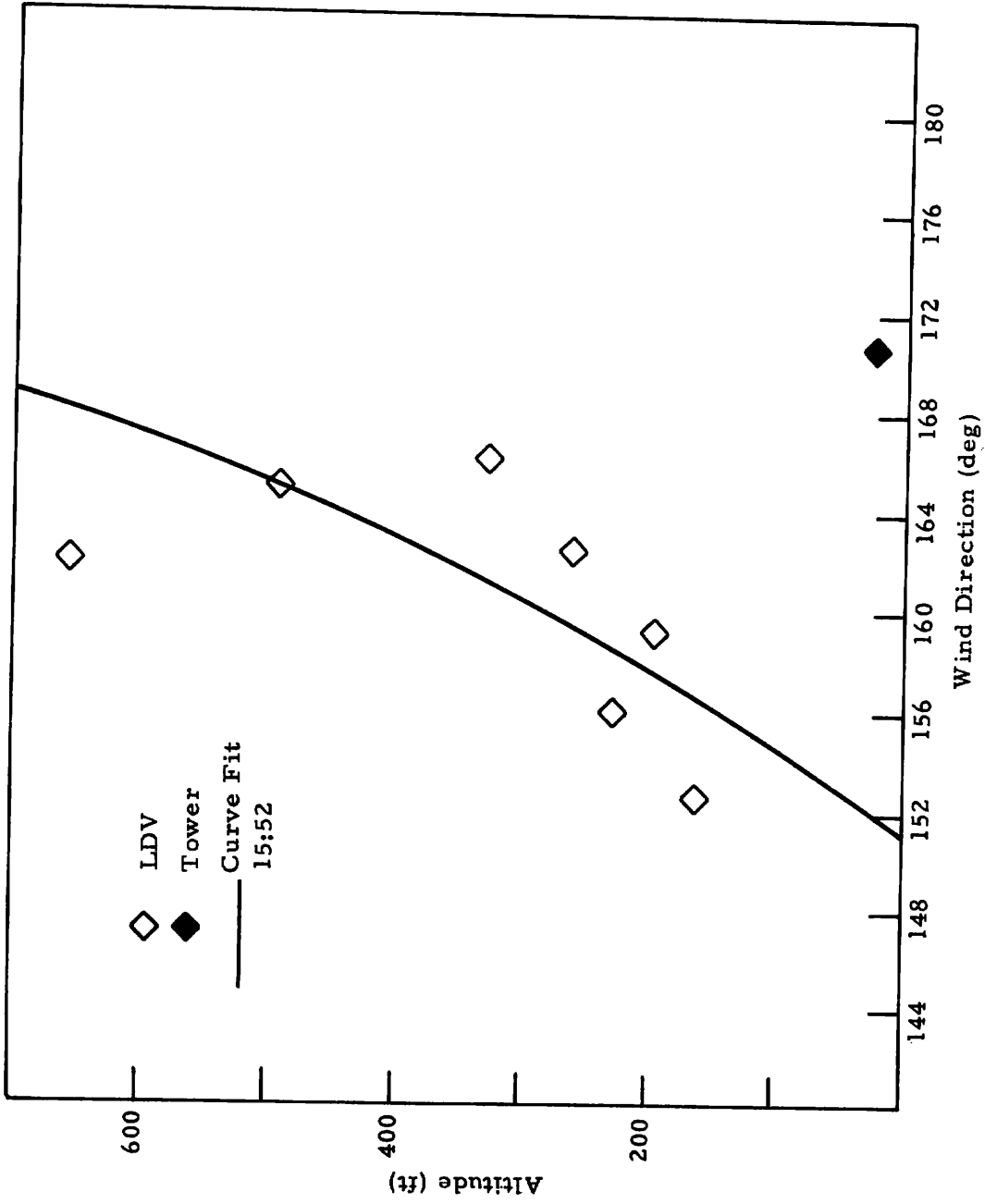


Fig. 6-2 - (Continued)

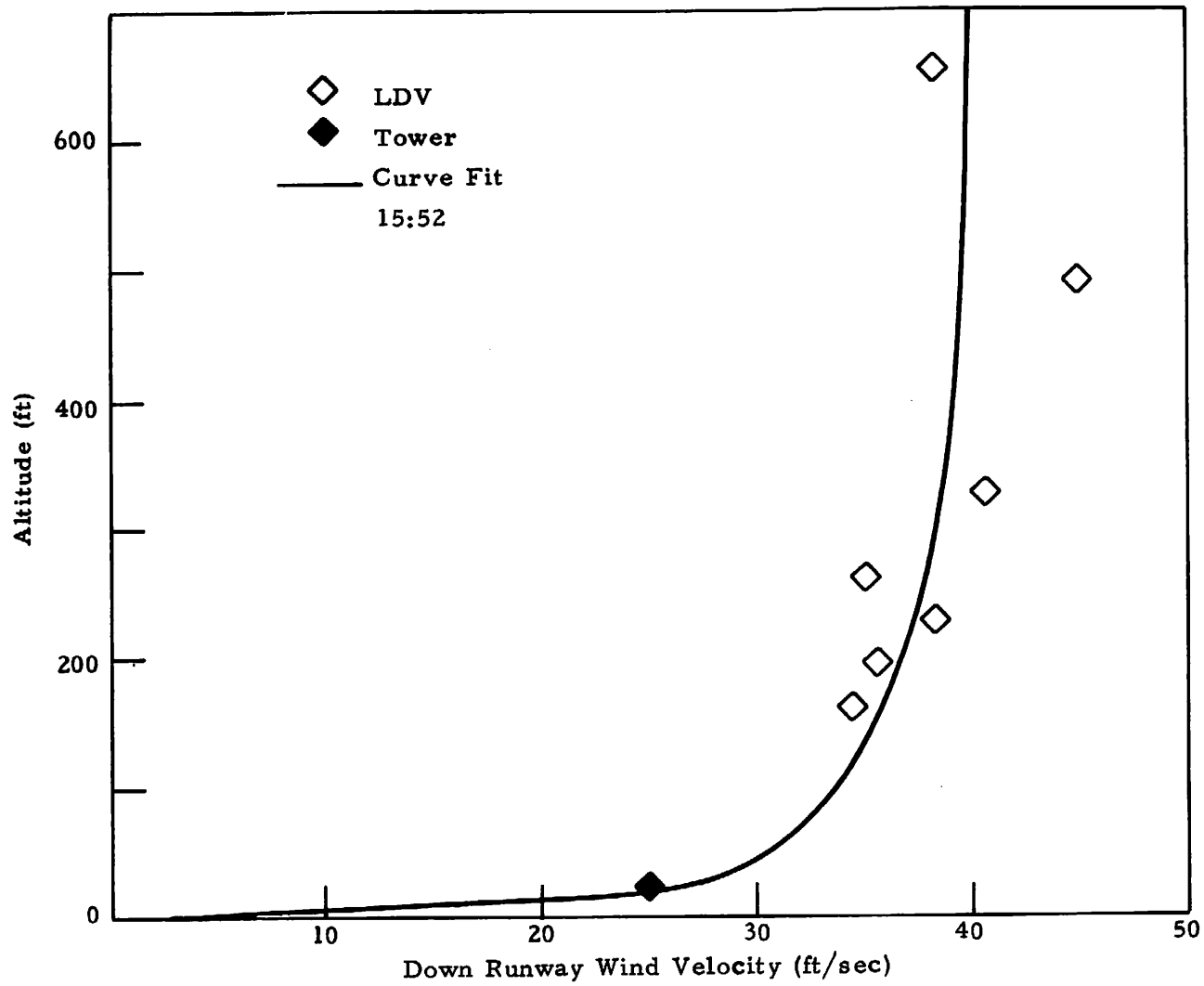


Fig. 6-2 - (Continued)

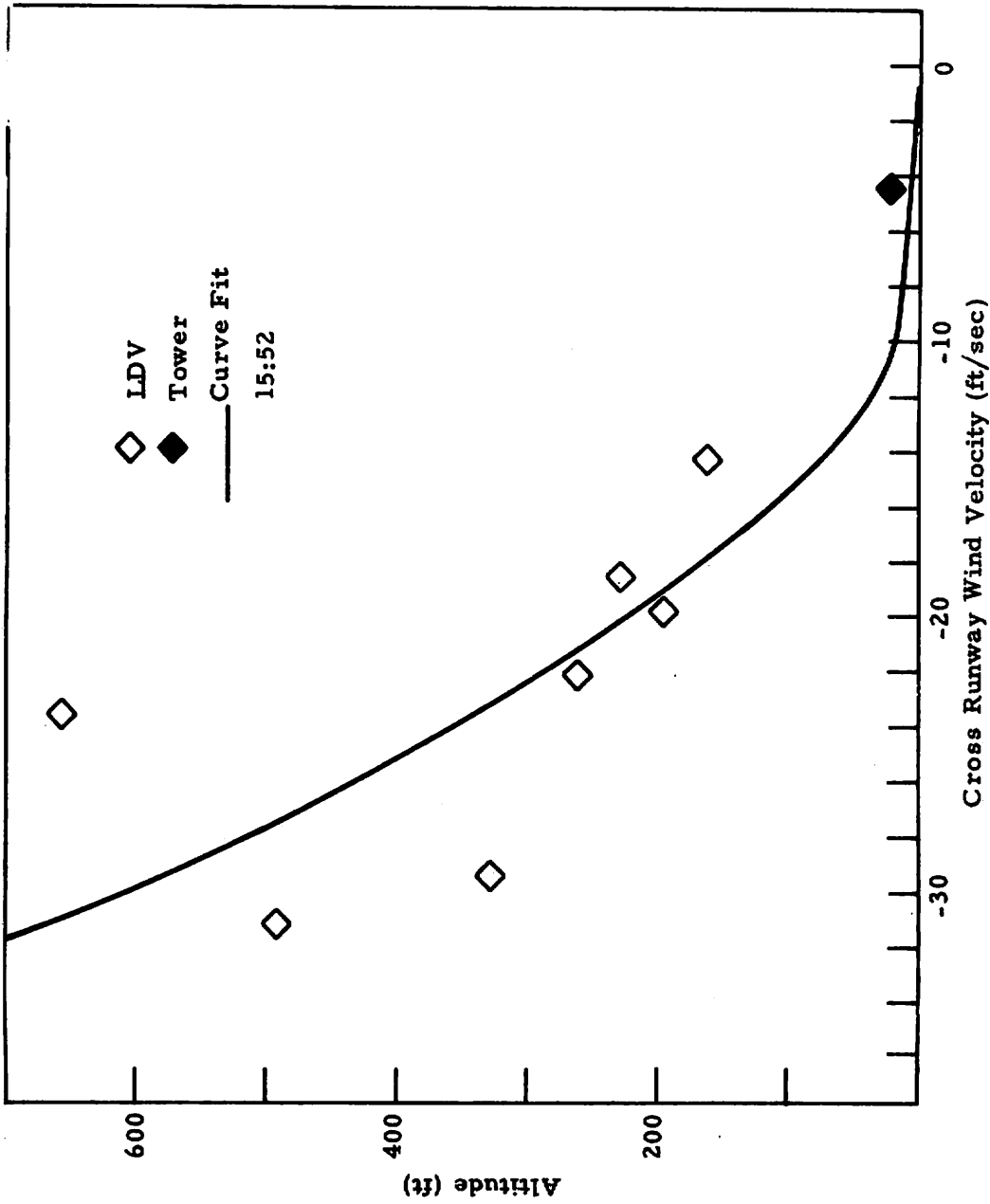


Fig. 6-2 - (Concluded)

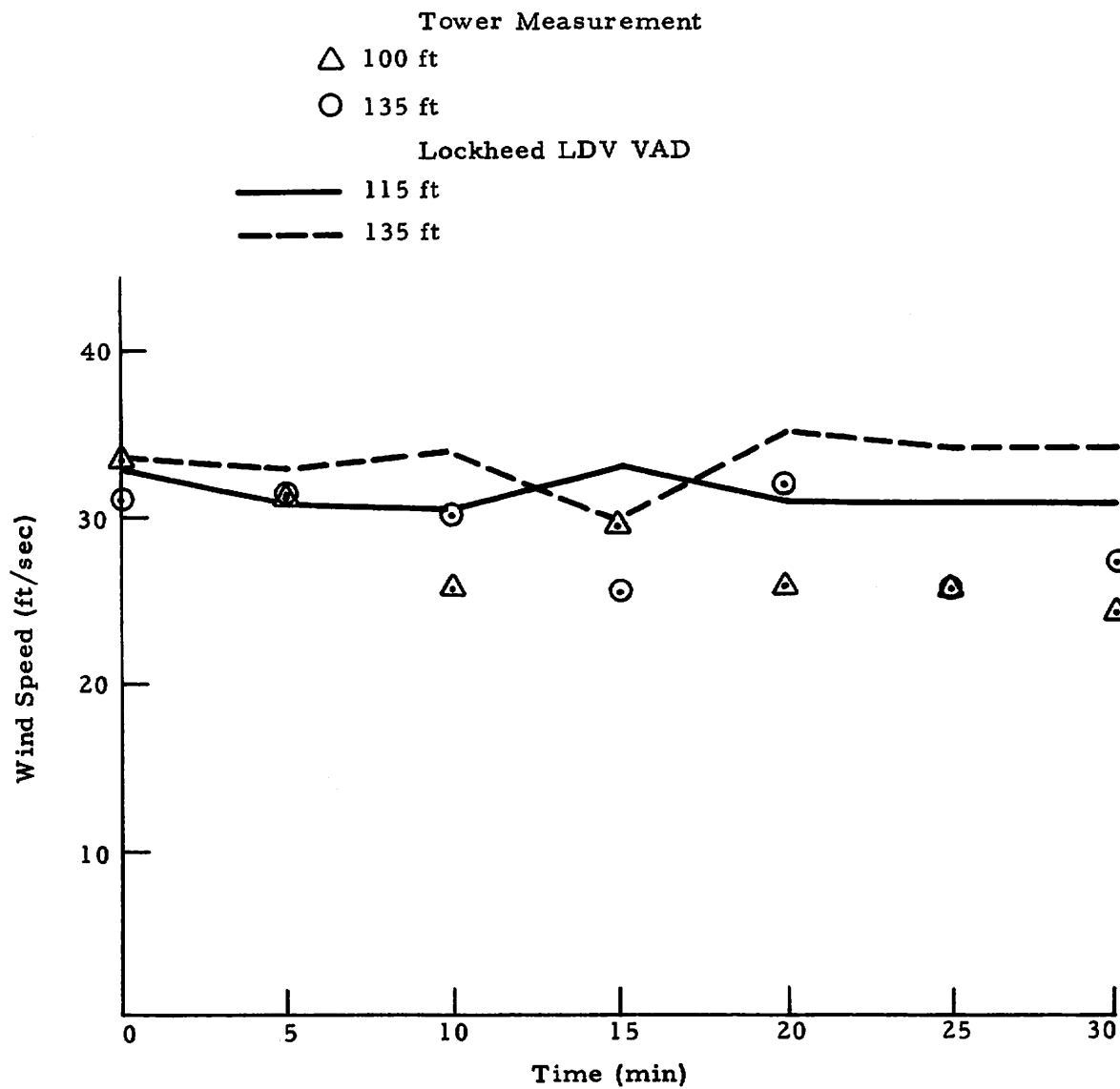


Fig.6-3 - Comparison of Meteorological Tower Wind Speed Measurements with Lockheed-Huntsville LDV at JFK on 11/5/75 14:06-14:36

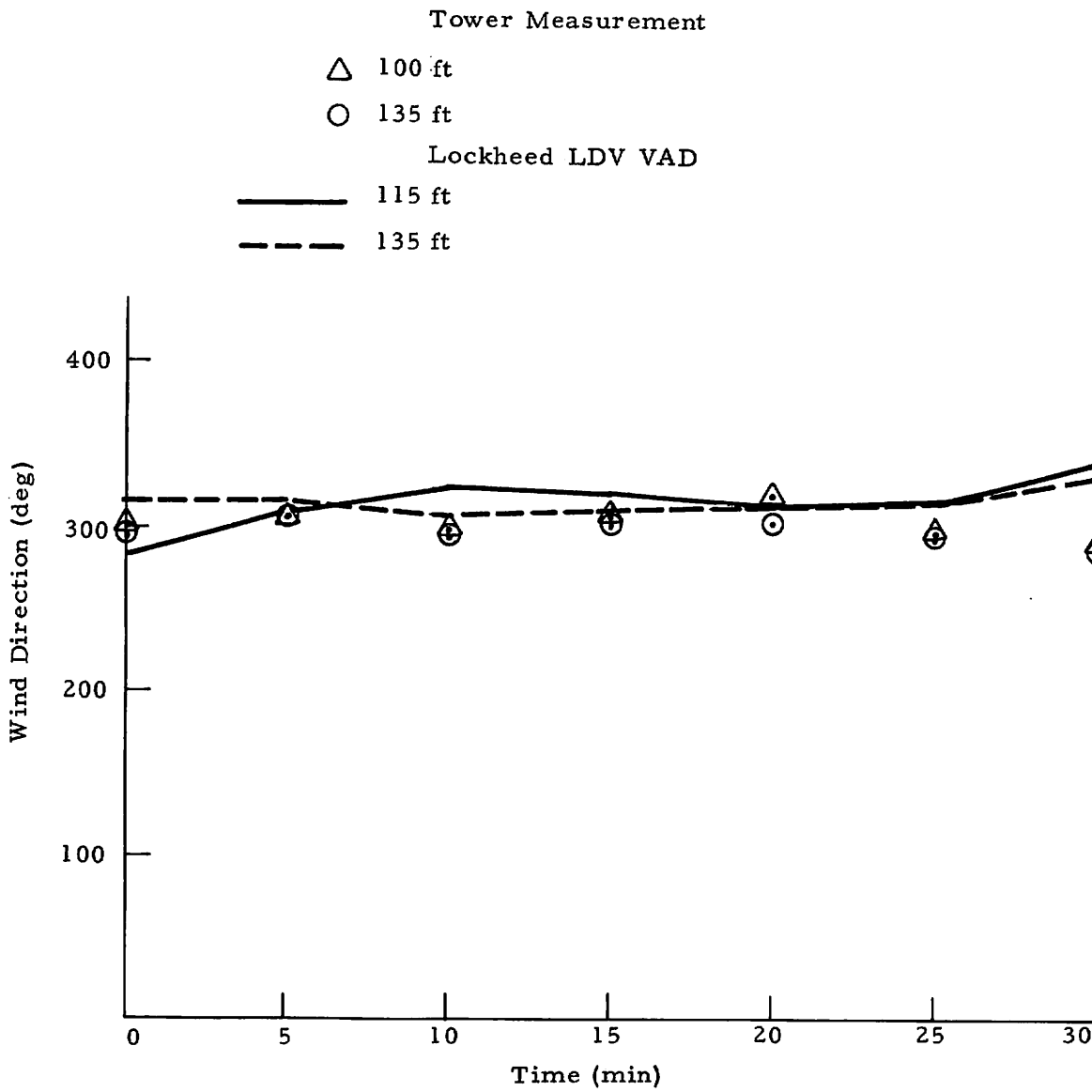


Fig.6-4 - Comparison of Meteorological Tower Wind Direction Measurements with Lockheed-Huntsville LDV at JFK on 11/5/75 14:06 - 14:36

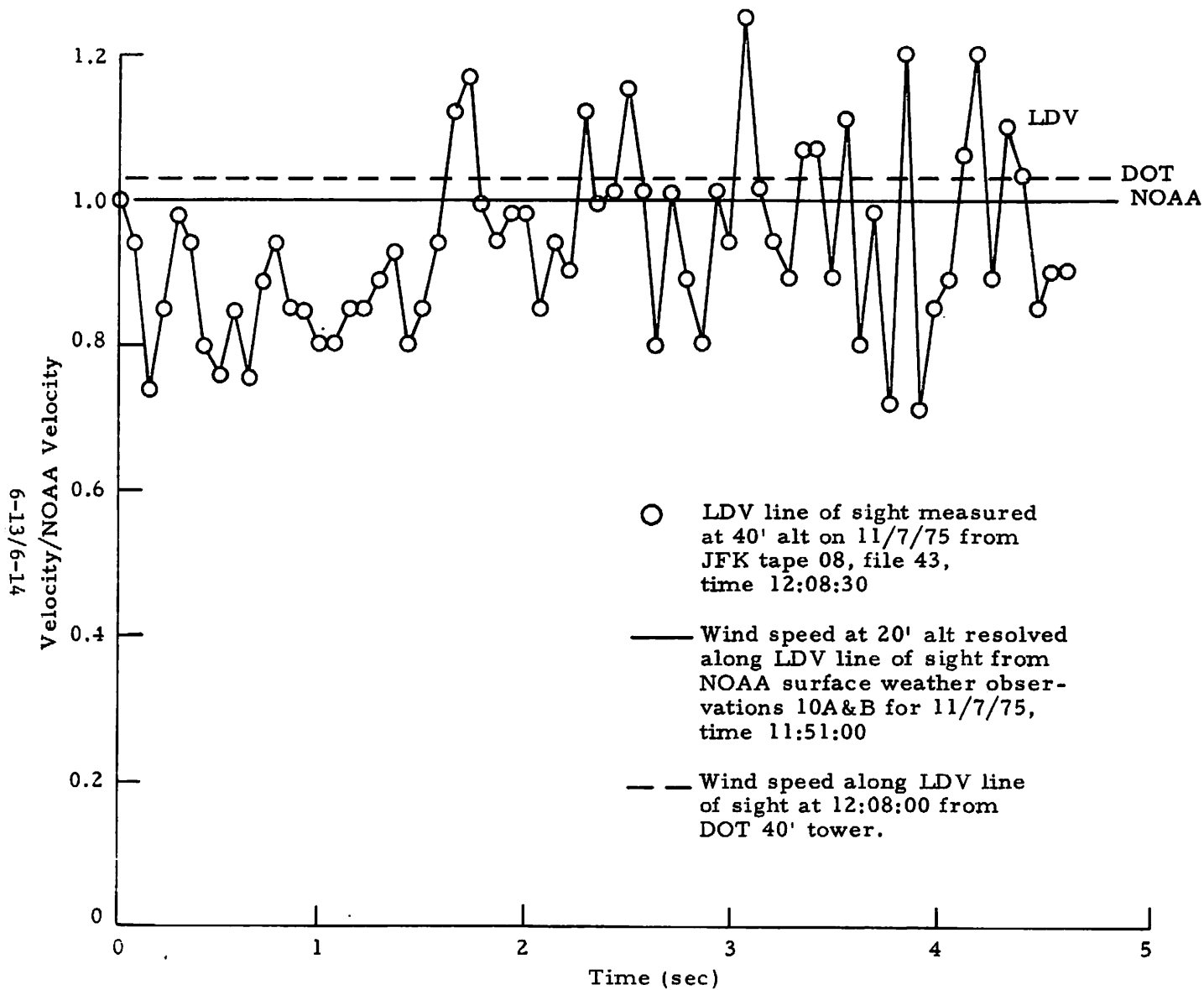


Fig. 6-5 - Comparison of LDV Line of Sight and Corresponding Meteorological Tower Wind Speed Measurements

## 7. CONCLUSIONS

The operational capability of the Lockheed-Huntsville mobile laser Doppler velocimeter system for the measurement of winds and wake vortices at terminal areas has been demonstrated. Wake vortex measurements have been obtained under a range of operating conditions and the existence of wake vortices in the approach corridor was monitored successfully during the field tests. A useful data base of wake vortex trajectories were collected.

Analysis of the performance of the LDV suggested that the following modifications could further improve the remote sensing capabilities of the system:

1. Incorporate actual rather than commanded elevation angle signal into the scanner and double buffer the onboard computer to eliminate anomalies in the data acquisition.
2. Increase the data acquisition rate and resolution of the system by integrating a filter bank into the signal processor.
3. Explore different scan configurations and different vortex discrimination concepts to improve the definition of the vortex tracks.

The results of the research program obtained a valuable data of wake vortex trajectories, demonstrated the basic reliability of the LDV system, and suggested techniques for refining the capability of the LDV remote sensing system.

## 8. REFERENCES

1. Little, C. G., V. E. Derr, R. H. Kleen, R. S. Lawrence, R. M. Lhermitte, J. C. Owens and G. D. Thayer, "Remote Sensing of Wind Profiles in the Boundary Layer," ESSA Technical Report ERL 168-WPL-12, June 1970.
2. Lawrence, T. R., M. C. Krause, L. K. Morrison and C. E. Craven, "A Study of Laser Doppler Velocimeter Atmospheric Wind Interrogation Systems - Final Report," LMSC-HREC TR D306888, Lockheed Missiles & Space Company, Huntsville, Ala., October 1973.
3. Huffaker, Robert M., H. B. Jeffreys, E. A. Weaver, J. W. Bilbro, G. D. Craig, R. W. George, E. H. Gleason, P. J. Massero, E. J. Reinbolt and J. E. Shirley, "Development of a Laser Doppler System for the Detection, Tracking, and Measurement of Aircraft Wake Vortices," FAA-RD-74-213, March 1975.
4. Bilbro, J. W., H. B. Jeffreys, E. A. Weaver, R. M. Huffaker, G. D. Craig, R. W. George and P. J. Marrero, "Laser Doppler Velocimeter Wake Vortex Tests," NASA TM X-64988, March 1976.
5. Lhermitte, R. M., and D. Atlas, "Precipitation Motion by Pulse Doppler Radar," Proc. 9th Weather Radar Conference, Boston, 1961, pp. 343-346.
6. Brashears, M. R., and W. R. Eberle, "Verification of Wind Measurement with Mobile Laser Doppler Wind Measurement System," LMSC-HREC TR D497071, November 1976.
7. Ciffone, D. L., "Correlation for Estimating Vortex Rotational Velocity Downstream Dependence," J. Aircraft, Vol. 11, No. 11, November 1974, pp. 716-717.